Investigating the Role of Exosomes in MYCN Tumourigenesis and Neuroblastoma

A THESIS SUBMITTED FOR THE DEGREE OF DOCTOR OF PHILOSOPHY

BY

ALEXIA TSAKANELI

October 2019

Department of Life Sciences, College of Health & Life Sciences

Brunel University London

Declaration

I hereby declare that the research presented in this thesis is my own work, except where otherwise specified, and has not been submitted for any other degree.

Alexia Tsakaneli

For my parents,

to whom I am eternally grateful.

Acknowledgments

Firstly, I would like to thank Neuroblastoma UK for funding me and my research throughout my PhD and making it possible for me to be a part of Brunel University London.

I would like to extend my deepest gratitude to my supervisor Prof. Arturo Sala. From the day of my interview to this day, he has always been mentoring me and helping me evolve and become a better scientist. Thank you for pushing me, giving me the freedom to express my ideas and helping me reach my goals during and after my PhD.

My supervisory team, Dr Evgeny Makarov and especially Prof. Paola Vagnarelli, thank you for supporting and advising me through this journey.

I would also like to thank everybody that helped me through the process of data collection. Our collaborator Prof. Giuseppe Palmisano for the mass spectrometry data, Brunel University's ETC facility for the electron microscopy data, the BIT-Gaslini Biobank in Genoa for providing me with the plasma samples and finally, Prof. Louis Chesler and Dr Evon Poon from the Institute of Cancer Research for the TH-MYCN mice tumour sections.

I would not be able to complete this PhD without my two amazing parents, Christos and Chrisoula, who so unconditionally love and support me. To thank them for everything will simply never be enough. I live every day of my life trying to meet the high standards they have inspired to me.

My amazing boyfriend (now husband) Kimon was the first one to realise how much patience and effort you need in order to go through a PhD. He was patient and strong for both of us and without him I would have been a different person. Making you proud of me is the fuel that drives me forward. Thank you for making me a better version of myself! Sorry for losing the "Mrs"!

Finally, I would like to thank the first person I met on my first day in Brunel. Raquel, thank you for being there for the ups and the downs. Thank you for the understanding and the standing by me when I reached my lows. I could write a whole other thesis on the effects you had on me. Thank you for everything! You brightened my days when no one else could and you made this building a happy place for me. Raquel, thank you for the coffee…

Abstract

Amplification of the proto-oncogene *MYCN* is a key molecular aberration in high-risk neuroblastoma and predictive of poor outcome in this childhood malignancy. We investigated the role of MYCN in regulating the protein cargo of exosomes, vesicles secreted by cells that can be internalised by recipient cells with functional consequences. Using a switchable MYCN system, we found that MYCN regulates a set of proteins in the exosomes secreted by neuroblastoma cells. Exosomes secreted by MYCN-expressing cells are enriched in the oncogenic glycolytic enzymes pyruvate kinase M2 and hexokinase II, promoting the Warburg effect in cells incorporating the extracellular vesicles. Exosomes produced by MYCN expressing cells induced glycolysis, proliferation, phosphorylation of histone H3 on threonine 11 and c-MYC expression in target cells. Mechanistically, we linked the cancer promoting activity of extracellular vesicles to the oncogenic glycolytic kinase pyruvate kinase M2 that was enriched in exosomes secreted by MYCN expressing neuroblastoma cells. Importantly, the glycolytic enzymes were selectively detected in exosomes circulating in the blood stream of neuroblastoma patients. In addition, exosomes secreted by MYCN positive neuroblastoma cells carry the histidine kinases NME1 and NME2, two kinases that have been correlated with oncogenic activity in neuroblastoma. Overall, we suggest that neuroblastoma cells might spread oncogenic signals to remote locations by MYCN-regulated proteins incorporated in extracellular vesicles.

Publications

Tsakaneli A., et al. (2019). *MYCN regulates neuroblastoma metabolism, proliferation and gene expression through vesicular transfer of glycolytic kinases*. Submitted.

Conferences

September 2017: Childhood Cancer 2017, Children with Cancer UK, Newcastle, UK, **Poster presentation**

December 2017: 3rd CHLS PGR Student Conference, Brunel University London, Uxbridge, UK, **Oral presentation**

- 2nd prize: Highly commented oral presentation

February 2018: Key targets and new therapeutic approaches for Neuroblastoma: From the bench to the bedside 2018, University of Chieti – Pescara, Chieti, Italy, **Oral presentation**

May 2018: Building Bridges for Neuroblastoma Research 2018, Advances in Neuroblastoma, Research Association (ANRA), San Francisco, California, U.S.A., **Poster presentation**

July 2018: Research Student Conference (Poster) 2018, Brunel University London, Uxbridge, UK, **Poster presentation**

December 2018: 4th CHLS PGR Student Conference, Brunel University London, Uxbridge, UK, **Oral presentation**

- 1st prize: Best oral presentation

April 2019: 33rd Genes and Cancer Conference, Cambridge University, Cambridge, UK, **Poster presentation**

- Selected for Flash Talk

April 2019: 5th Neuroblastoma Research Symposium, Neuroblastoma UK, Cambridge, UK, **Poster presentation**

- Prize for the best poster presentation in the 'MYCN' category
- Prize for the best poster presentation in the 'Public Vote' category

December2019: 5th CHLS Conference for Doctoral Researchers, Brunel University London, Uxbridge, UK, **Poster presentation**

- Highly commented presentation

Table of contents

I. List of figures

II. List of tables

III. Abbreviations

Abs	Absorbance
ADP	Adenosine diphosphate
AHSCT	Autologous hematopoietic stem-cell transplantation
ALK	Anaplastic lymphoma kinase
APC	Adenomatous polyposis coli
APS	Ammonium persulfate
ATP	Adenosine triphosphate
AURKA	Aurora kinase A
BARD1	BRCA1-associated RING domain protein 1
BCA	Bicinchoninic acid
bHLHZ	Basic helix-loop-helix zipper
BMP	Bone morphogenic protein
BRCA1	Breast cancer type 1 susceptibility proteins
BRCA2	Breast cancer type 2 susceptibility proteins
BRIP1	BRCA1-interacting protein 1
BSA	Bovine serum albumin
CAR	Chimeric antigen receptor
CASC15	Cancer susceptibility 15
CCE	Cancer cell derived exosome
CDK	Cyclin-dependent kinase
cDNA	Complementary DNA
CGH	Comparative genome hybridization
ChIP	Chromatin immunoprecipitation
CHK1	Checkpoint kinase 1
CHK1	Checkpoint kinase 2
CNV	Copy number variations
CO_2	Carbon dioxide
Cryo-EM	Cryo-electron microscopy
DAB	3,3'-Diaminobenzidine

DDX4	DEAD-box helicase 4
DMEM	Dulbecco's modified Eagle medium
DMSO	Dimethyl sulfoxide
DNA	Deoxyribonucleic acid
dNTP	Deoxyribonucleotide triphosphate
DUSP12	Dual specificity protein phosphatase 12
ECL	Enhanced chemiluminescence
ECM	Extracellular matrix
EDTA	Ethylenediaminetetraacetic acid
eEF2	Eukaryotic elongation factor 2
EM	Electron microscopy
EMT	Epithelial-mesenchymal transition
ESC	Embryonic stem cell
ESCRT	Endosomal sorting complexes required for transport
EV	Extracellular vesicle
EZH2	Enhancer of zeste homolog 2
FACS	Fluorescence-activated cell sorting
FAK	Focal adhesion kinase
FBS	Fetal bovine serum
FISH	Fluorescence *in situ* hybridization
FITC	Fluorescein isothiocyanate
GD2	Disialoganglioside
GM-CSF	Granulocyte-macrophage colony stimulating factor
GN	Ganglioneuroma
GNB	Ganglioneuroblastoma
GPC2	Glypican-2
GSK3β	Glycogen synthase kinase 3β
GWAS	Genome wide association studies
HACE1	HECT domain and ankyrin repeat containing E3 ubiquitin protein ligase 1
HDAC	Histone deacetylase
HIF-1	Hypoxia-inducible factor 1

HRP	Horseradish peroxidase
HSD17B12	Hydroxysteroid (17β) dehydrogenase 12
IDRF	Image-defined risk factors
IF	Immunofluorescence
IHC	Immunohistochemistry
IL	Interleukine
ILV	Intraluminal vesicle
INRG	International Neuroblastoma Risk Group
INSS	International Neuroblastoma Staging System
iPSC	Induced pluripotent stem cell
KIF18	Kinasin-like protein 18
K-PTA	Potassium phosphotungstate
LAMP	Lysosomal-associated membrane proteins
LDH	Lactate dehydrogenase
LIN28B	Lin-28 homolog B
LMO1	Rhombotin-1
M.O.M.	Mouse on mouse
MAPK	Mitogen-activated protein kinase
MHC	Major histocompatibility complex
MMP20	Matrix metalloproteinase-20
mRNA	Messenger RNA
MVB	Multivesicular body
MVE	Multivesicular endosome
NaCl	Sodium chloride
NB	Neuroblastoma
NBPF17P	Neuroblastoma breakpoint family member 17
NEFL	Neurofilament light polypeptide
NF1	Neurofibromin 1
NGF	Nerve growth factor
NP-40	Nonident P40
NPM	Nucleophosmin

NTA	Nanoparticle tracking analysis
o/n	Overnight
PAGE	Polyacrylamide gel electrophoresis
PALB2	Partner and localizer of BRCA2
PBS	Phosphate buffered saline
PCR	Polymerase chain reaction
PDE6G	Retinal rod rhodopsin-sensitive cGMP 3',5'-cyclic phosphodiesterase subunit gamma
PES	Polyethersulfone
PFA	Paraformaldehyde
PFKP	Phosphofructokinase protein
PHOX2B	Paired mesoderm homeobox protein 2B
PI3K	Phosphatidylinositol 3-kinase
PKM	Pyruvate kinase M
PNT	Peripheral neuroblastic tumours
PSG	Primary sympathetic ganglia
PTPN11	Protein tyrosine phosphatase non-receptor type 11
qPCR	Quantitative PCR
RNA	Ribonucleic acid
Rpm	Rounds per minute
RSRC1	Arginine and serine rich coiled-coil 1
RT	Reverse transcriptase
SCHB	Succinate dehydrogenase
SDS	Sodium dodecyl sulfate
SEM	Standard error of the mean
SEQC	Sequencing quality control consortium
Ser	Serine
siRNA	Small interfering RNA
SKP2	S-phase kinase associated protein 2
SWI/SNF	SWItch/Sucrose non-fermentable
TBS	Tris buffered saline

TC	Tissue culture
TCR	T cell receptor
TEM	Transmission electron microscopy
Thr	Threonine
TP53	Tumour protein p53
TRRAP	Transformation/Transcription domain associated protein
VEGF	Vascular endothelial growth factor

1. General introduction

1.1. Neuroblastoma

1.1.1. The origin of neuroblastoma

In 1910, James Wright described a group of tumours with cells that associated with fibrils in a way that resembled neuroblasts. He called these tumours neurocytomas or neuroblastomas and described twelve cases, nine out of which were in children (Wright, 1910). Today we know that neuroblastoma is the most common extra cranial solid tumour in childhood and it accounts for 15% of all childhood oncology deaths (Gherardi, et al., 2013). It is a malignancy that arises from cells of the neural crest as they develop and differentiate in order to form the sympathetic nervous tissue (De Bernardi, et al., 2008).

As it originates from any neural crest element in the developing sympathetic nervous system, it has the potential to result in tumours in the adrenal glands and sympathetic ganglia. Neuroblastoma is a member of the peripheral neuroblastic tumours (PNTs), a group of tumours that accounts for 7-10% of all tumours in children (De Bernardi, et al., 2008). The prevalence of neuroblastoma is about one case in 7,000 live births and the median age of diagnosis for the patients is about 18 months with almost half of the cases being diagnosed by the first year of age (Brodeur & Maris, 2002).

The neural crest consists of a transient collection of multipotent embryonic progenitors in the developing ectoderm and it arises from the neural tube after tube closure. It is the origin of a large number of different cell types including melanocytes, craniofacial chondrocytes and osteocytes, smooth muscle myocytes and peripheral nervous system neurons (Huber, 2006). Neural crest cell specification occurs via an epithelial to mesenchymal transition. This process allows cells to lose their polarity and reduce their adhesive properties in order to delaminate and migrate from the neural tube. These neuroblast progenitors migrate to a region immediately lateral to the notochord and the dorsal aorta under the influence of the transcription factor MYCN, bone morphogenetic proteins (BMPs), DNA methylation and histone modifications (Fig. 1.1). This complex series of epigenetic and transcriptional regulation determines whether the neural progenitor cells that migrate to the dorsal aorta will undergo specifications as the primary sympathetic ganglia before divergence into neural

cells of the mature sympathetic ganglia or chromaffin cells of the adrenal medulla. The cells of the dorsal aorta that differentiate into sympathoadrenal progenitor cells will eventually give rise to cells of the peripheral nervous system, including sympathetic ganglia and the adrenal gland, which are the main sites of neuroblastoma development (Matthay, et al., 2016).

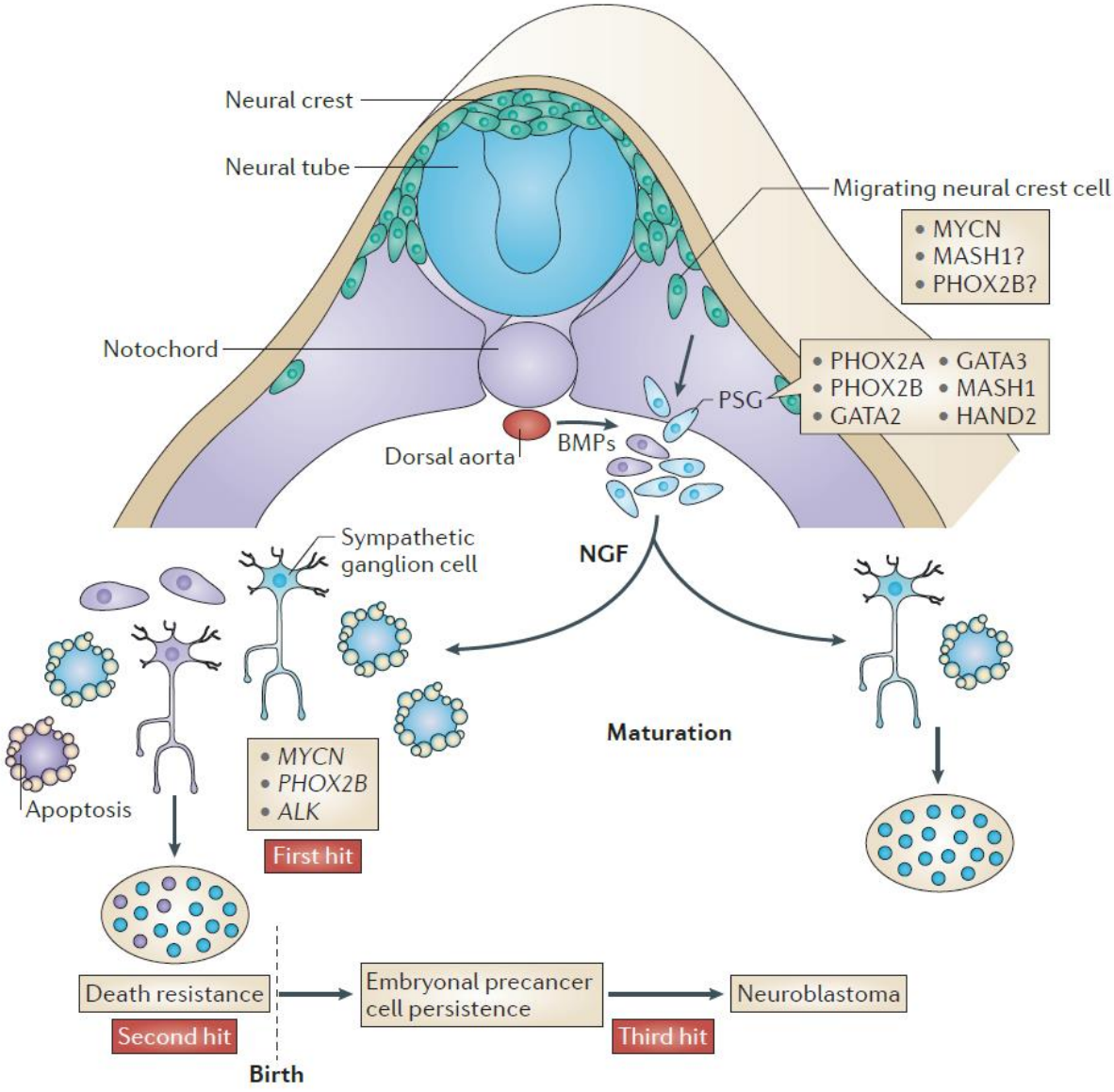

Figure 1.1: The origin of neuroblastoma cells. MYCN and Bone morphogenic proteins (BMPs) regulate the migration of neuroblast progenitors from the neural crest. Depending on the access to nerve growth factor (NGF), the primary sympathetic ganglia (PSG) (blue) will mature into terminal ganglion cells or they will undergo apoptosis. The population of cells that survive the absence of trophic factors will remain as neuroblast pre-cancer cells (purple) and potentially transform into neuroblastoma cells in early childhood (Marshall, et al., 2014).

1.1.2. Mechanisms, genetics and pathophysiology of neuroblastoma

Genetic predisposition for neuroblastoma

In 1972, neuroblastoma was proposed to have a genetic predisposition for its development that follows an autosomal-dominant pattern of inheritance and has a similar genetic basis with retinoblastoma. Knudson's two-hit hypothesis estimates that up to 22% of all neuroblastoma could be the result of germline mutation (Knudson Jr & Strong, 1972). However, unlike retinoblastoma, cases of familial neuroblastoma are extremely rare, with only 1-2% of the patients positive.

In 2008, germline gain of function mutation experiments identified *ALK* gene, encoding for anaplastic lymphoma kinase (ALK) as the main predisposing factor for familial neuroblastoma (Mossë, et al., 2008; George, et al., 2008). ALK belongs to the insulin receptor superfamily and can act as an oncogene. Therefore, ALK can promote the transformation of mammalian cells upon activation (Mossë, et al., 2008). Post translationally, it can be phosphorylated and trigger multiple signalling pathways. Interestingly, due to their similar locations on 2p, *ALK* and *MYCN* can be co-amplified. *ALK* is expressed only in neural tissues and is overexpressed in advanced neuroblastoma and in Schwannian stroma-poor tumours, where it triggers more than one metabolic pathways upon phosphorylation (Longo, et al., 2007).

In addition to *ALK*, high risk neuroblastoma has been highly associated with the polymorphic alleles within the *LIN28B* locus that encodes the paralogous RNA-binding protein lin-28 homologue B (Diskin, et al., 2012). LIN28A and LIN28B control neural crest cell commitment by regulating the let-7 microRNA family during embryogenesis (Rybak, et al., 2008). Moreover, when the expression of *LIN28B* is altered in neuroblastoma cells, MYCN is overexpressed, while mice that are misexpressing *LIN28B* develop neuroblastoma with high levels of MYCN (Molenaar, et al., 2012).

The majority of syndromic neuroblastoma cases, in which neuroblastoma co-segregates with central congenital hypoventilation syndrome and/or Hirschsprung disease are predisposed by the gene that encodes the paired mesoderm homeobox protein 2B (PHOX2B), which is a master regulator of neural crest development (Trochet, et al., 2004). Finally, genome-wide association studies revealed that the formation of neuroblastoma can be influenced by

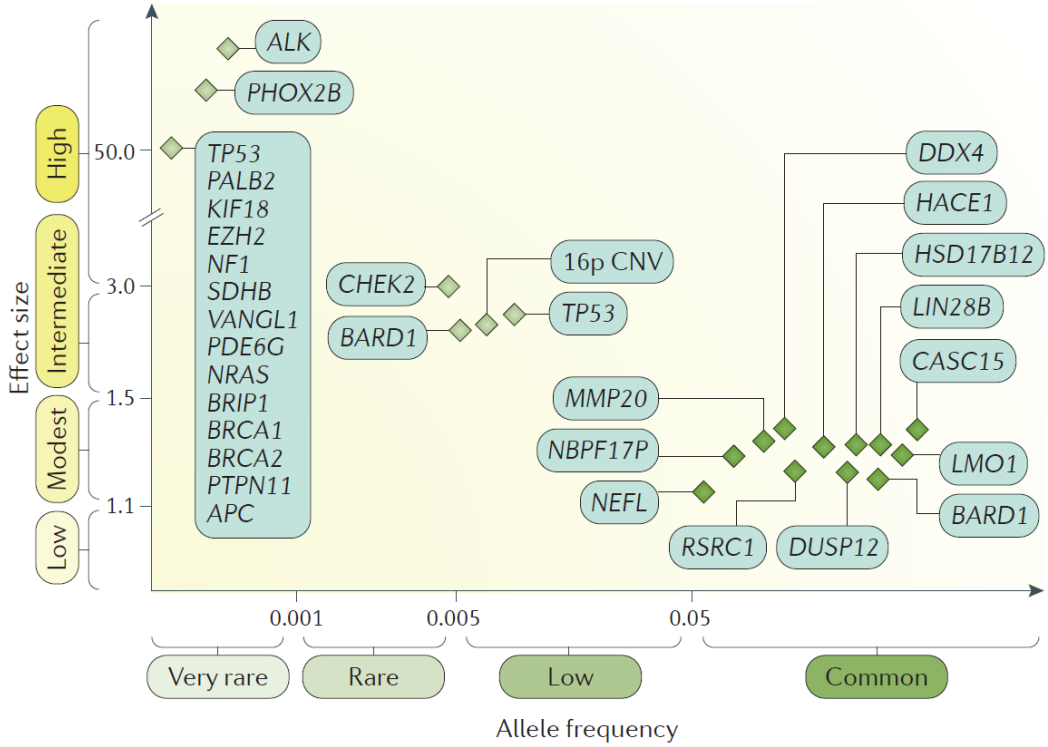

Figure 1.2: Genes implicated in genetic predisposition of neuroblastoma. Common polymorphic alleles have been identified with genome-wide association studies (GWAS) in neuroblastoma. Mutations of the *ALK* and *PHOX2B* genes are the found in cases of familial neuroblastoma. More common damaging mutations, such as TP53, NRAS and BRCA2 have also been identified as potential factors that predispose to neuroblastoma. Also, polymorphisms that are commonly found, but individually have a small effect on tumour initiation (BARD1, LMO1) may have a cooperative action for the initiation of neuroblastoma tumours. Genes with very rare polymorphic alleles: Anaplastic lymphoma kinase (ALK), Paired like homeobox 2B (PHOX2B), Tumour protein p53 (TP53), Partner and localizer of BRCA2 (PALB2), Kinasin-like protein 18 (KIF18), Enhancer of zeste homolog 2 (EZH2), Neurofibromin 1 (NF1), Succinate dehydrogenase (SCHB), Strabismus-related protein VANGL1, Retinal rod rhodopsin-sensitive cGMP 3',5'-cyclic phosphodiesterase subunit gamma (PDE6G), N-ras oncogene (NRAS), BRCA1-interacting protein 1 (BRIP1), Breast cancer type 1 and 2 susceptibility proteins (BRCA1,2), Protein tyrosine phosphatase non-receptor type 11 (PTPN11), Adenomatous polyposis coli (APC). Genes with rare or low polymorphic alleles: Checkpoint kinase 2 (CHEK2), BRCA1-associated RING domain protein 1 (BARD1), 16 p copy number variations (16p CNV), TP53, Matrix metalloproteinase-20 (MMP20), Neuroblastoma breakpoint family member 17 (NBPF17P), Neurofilament light polypeptide (NEFL). Genes common polymorphic alleles: Arginine and serine rich coiled-coil 1 (RSRC1), Dual specificity protein phosphatase 12 (DUSP12), DEAD-box helicase 4 (DDX4), HECT domain and ankyrin repeat containing E3 ubiquitin protein ligase 1 (HACE1), Hydroxysteroid (17β) dehydrogenase 12 (HSD17B12), Lin-28 homolog B (LIN28B), Cancer susceptibility 15 (CASC15), Rhombotin-1 (LMO1), BARD1 (Matthay, et al., 2016).

common polymorphic alleles and to date, there have been identified twelve highly significant and validated genetic associations with neuroblastoma (Manolio, et al., 2009). In addition to *ALK* and *PHOX2B*, *TP53*, *NRAS* and *BRCA2* can predispose to neuroblastoma when they have damaging mutations in the germline. Cooperative effects of common polymorphisms, such as *BARD1* or *LMO1* have been linked to sporadic neuroblastoma tumourigenesis, even though individually they have a relatively small effect on tumour initiation (Fig. 1.2).

Nevertheless, most neuroblastomas occur spontaneously, and the patients do not show any predisposition for the disease. The development of sporadic neuroblastoma comes as a result of alterations in many genetic features, such as ploidy status, oncogene amplification and allelic loss.

MYCN amplification in neuroblastoma

The family of the MYC transcription factors has three members: c-MYC, a protein expressed in a plethora of normal tissues and the most deregulated proto-oncogene in human cancer, L-MYC, a protein induced in a group of lung cancers, and MYCN, the product of a gene whose expression is restricted spatiotemporally in order to regulate the development of the nervous system during embryogenesis and its increased expression has been described in paediatric tumours (Sala, 2015).

Almost 25% of neuroblastoma cases present the amplification of *MYCN*. The overexpression of this transcription factor serves as a diagnostic marker of poor prognosis in neuroblastoma (Fig. 1.3) (Brodeur, et al., 1984). The significance of *MYCN* amplification in neuroblastoma was soon established, as it was shown that mice with targeted overexpression of *MYCN* in the neural crest via the rat tyrosine hydroxylase (TH) promoter developed neuroblastoma (Weiss, et al., 1997).

MYCN is a master regulator of transcription with cyclin-dependent kinase 4 (CDK4) (Gogolin, et al., 2013), serine/threonine protein kinase cell cycle checkpoint kinase 1 (CHK1) (Cole, et al., 2011), inhibitor of DNA-binding 2 (ID2) (Iavarone, et al., 1994; Lasorella, et al., 1996), minichromosome maintenance protein (MCM) (Koppen, et al., 2007), Myb-related protein B (MYBL2) (Raschellà, et al., 1999; Hossain, et al., 2008; Gualdrini, et al., 2010) and S phase kinase-associated protein 2 (SKP2) (Bell, et al., 2007; Muth, et al., 2010) among its transcription targets that can promote cell cycle progression. In addition, MYCN can promote

differentiation by transcriptionally regulating cyclin-dependent kinase-like 5 (CDKL5) (Valli, et al., 2012) and tissue transglutaminase (TG2) (Liu, et al., 2007; Valli, et al., 2012). Because the range of genes that can be activated by MYCN is so wide, it is extremely difficult to define a simple downstream pathway of activation upon *MYCN* amplification. It is clear though, that MYCN can promote cancer progression and repress genes that promote cell differentiation (Huang & Weiss, 2013).

MYCN controls many pathways and biological processes that act in favour of neuroblastoma. For example, it can enhance invasive and metastatic behaviour, as it downregulates proteins of the family of integrins. More specifically, by downregulating integrins α1 and β1, MYCN promotes the detachment of the extracellular matrix allowing the cells to migrate and invade other tissues (Tanaka & Fukuzawa, 2008). Almost half the cases of neuroblastoma are metastatic. The most frequent metastatic locations are the bone marrow (70%), bones (55%), lymph nodes (30%), liver (30%) and brain (18%) (Goodman, et al., 1997). MYCN is also implicated in the regulation of integrins by promoting the transcription of focal adhesion kinase (FAK), that is shown to regulate integrins and enhance migration and metastasis in tumour cells (Beierle, et al., 2007).

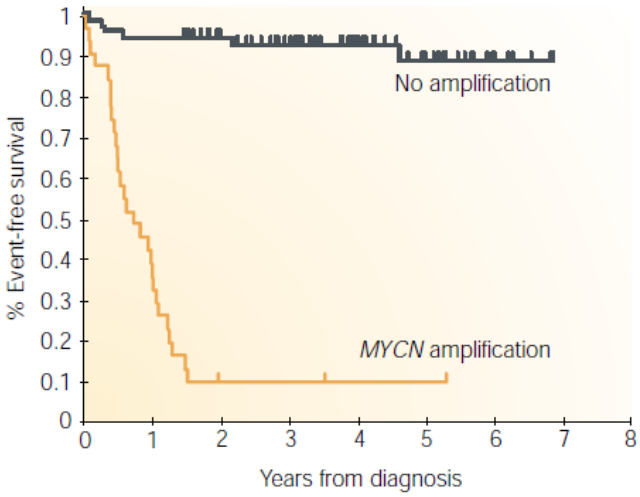

Figure 1.3: Kaplan-Meier survival curve of infants with metastatic neuroblastoma based on *MYCN* status (Brodeur, 2003).

Moreover, *MYCN* amplification and increased dissemination have been correlated with high vascularity in neuroblastoma which is indicative of poor outcome. In 1999, a study revealed

that conditioned media from neuroblastoma cell lines that overexpress *MYCN* leads to the loss of inhibitors of endothelial growth (Fotsis, et al., 1999).

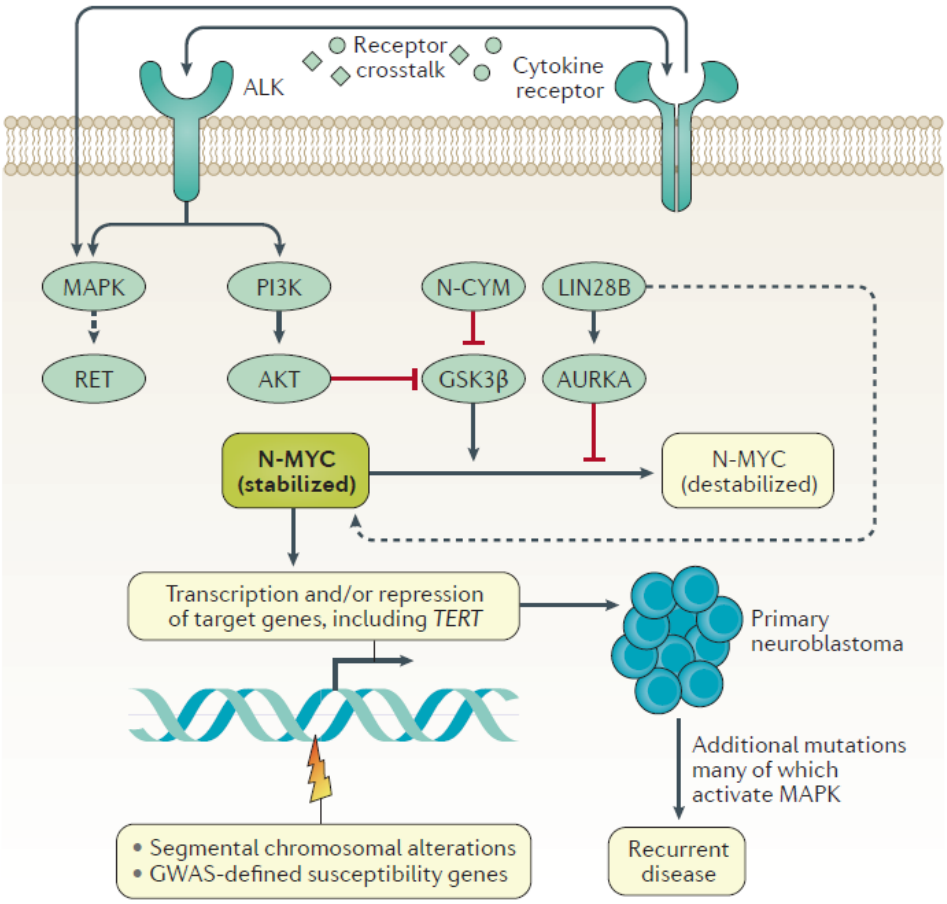

Figure 1.4: Mechanisms of initiation of *MYCN* amplified neuroblastoma. In aggressive, high-risk neurobalstoma cells with *MYCN* amplification, many pathways can affect the stability of the protein. Some of the key molecules implicated in the stabilisation of MYCN are ALK, PI3K, LIN28B, Mitogen-activated protein kinase (MAPK), glycogen synthase kinase 3β (GSK3β) and Aurora kinase A (AURKA). The understanding of the pathways that sustain MYCN in neuroblastoma is important for providing insight of the mechanisms leading to aggressive neuroblatoma tumours as well as helping us characterise potentially drugable targets in *MYCN*-amplified neuroblastoma. (Matthay, et al., 2016).

In addition, it is likely that MYCN can alter the characteristics of self-renewal and multipotency of the neural crest cells that give rise to neuroblastoma, as it can substitute for MYC in the

reprogramming of fibroblasts into induced pluripotent stem cells (iPS) (Nakagawa, et al., 2010).

Finally, one of the most studied tumourigenic effects of MYCN is its ability to promote proliferation and cell cycle progression. MYCN can affect the cell cycle by upregulating CHK1, which regulates S phase and G2/M checkpoints (Cole, et al., 2011). This mechanism has been suggested as a way through which *MYCN* amplified neuroblastoma escapes standard chemotherapy.

The complex role of Myc in the regulation of gene expression is further discussed in chapter 1.2.

Cytogenetics of neuroblastoma

Flow cytometric analysis used to determine the total DNA content of neuroblastoma cells and not specific chromosomal rearrangements showed that DNA content is significantly correlated with tumour stage, with tumours of a more advanced stage having a higher frequency of diploidy (Look, et al., 1984). Although the determination of ploidy status content of neuroblastoma cells from infants can be predictive of the outcome for the patient, ploidy does not apply as a prognostic factor for patients who are older than 2 years of age (Look, et al., 1991). In addition to stage determination, DNA ploidy has been shown to be a factor of prognosis for the response to chemotherapy, with tumours of advanced stage showing resistance to treatment and poor survival probability (Gansler, et al., 1986; Cohn, et al., 1990).

The amplification of *MYCN* on the 2p24 locus is associated predominately with advanced stages of the disease, poor outcome, rapid tumour progression and poor prognosis, as explained above. Remarkably, amplification of at least six, *MYCN* nonsyntenic regions has been shown in neuroblastoma cells and primary tumours. The *MYCN* locus at 2p24 is co-amplified with DNA from chromosome 2p22 and 2p13, the *MDM2* gene on 12q13 and the *MYCL* gene at 1p32 (Brodeur, et al., 1997).

Sporadic neuroblastoma seems to be dependent on the gain or loss of alleles and changes in tumour cell ploidy. Indeed, the karyotype of tumour cells can have prognostic value, since patients with lower stages of the disease are often hyperdiploid or near triploid (Kaneko, et

al., 1987). To supplement the data provided by the cytometric analyses, comparative genome hybridization (CGH) and fluorescence *in situ* hybridization (FISH) have been employed in order to screen neuroblastoma cells genome-wide and determine the biological significance of chromosomal gains and losses in neuroblastoma. Firstly, it was confirmed that triploid tumours show favourable prognosis for the patients and the imbalance in the number of chromosomes is not paired with abnormalities in the chromosomal structures. Secondly, the gain of chromosome 17 was found to be the most frequently observed abnormality, with the gain of the whole chromosome 17 in low stage tumours and the gain of 17q in high stage tumours (Vandesompele, et al., 2001). Additional studies have suggested the strong prognostic potential of 17q gain for patients at high risk for neuroblastoma progression (Bown, et al., 1999; Lastowska, et al., 1997; Bown, et al., 2001).

Analysis of the cytogenetic characteristics of neuroblastoma tumours and neuroblastoma cell lines identified the short arm of chromosome 1 (1p) to be deleted in most of the cases (Brodeur, et al., 1977). Allelic loss of 1p has a negative prognostic impact especially in diploid tumours (Kaneko, et al., 1987). In addition to chromosomal imbalances involving chromosome 1, 15% of neuroblastomas have been reported to be characterised by allelic loss of 11q (Mertens, et al., 1997). Chromosome 11 seems to play a tumour supressing role in neuroblastoma, as introduction of the chromosome in the neuroblastoma cell line NPG leads to cell differentiation (Bader, et al., 1991).

Finally, in addition to the genetic alterations that lead to the inactivation of tumour suppressor genes, epigenetic mechanisms also contribute to the regulation of the gene expression of tumour supressing genes in neuroblastoma. A screening of a set of neuroblastoma cell lines identified the gene encoding for caspase 8 as either deleted or silenced by methylation, and therefore as one of the most important tumour supressing genes in neuroblastoma (Teitz, et al., 2000). Another gene possibly acting as a tumour suppressor in neuroblastoma is a RAS association domain family protein (*RASSF1A*), that in neuroblastoma and other malignancies is methylated on the promoter and therefore epigenetically silenced (Dammann, et al., 2000; Astuti, et al., 2001).

Overall, it is clear that neuroblastoma is a disease with a very large biological diversity and high molecular and clinical complexity. Therefore, the understanding of the molecular

pathways that regulate the behaviour of neuroblastoma cells and coordinate their complex behaviours is of tremendous importance for the advancement of the strategies against the disease.

1.1.3. Epidemiology of neuroblastoma

Although neuroblastoma is a rare malignancy in the general population, it is the most frequent solid tumour in children under the age of 5. According to the RARECAREnet project, in the period from 2000 to 2007 the annual incidence of neuroblastoma was 6 cases per million in European children between the ages 0-14 years (Gatta, et al., 2014), with the occurrence being 13% more frequent in boys (Spix, et al., 2006).

The early age of diagnosis supports the hypothesis that neuroblastoma could be the outcome of certain prenatal exposures and factors that could interfere with the foetal neuronal development. The fact that neuroblastoma cases are overall rare forms a challenge for epidemiological studies. Therefore, there is no clear documentation about the environmental factors that could be implicated in the development of neuroblastoma. However, there are reports suggesting that exposure to certain environmental factors has been associated stronger with the development of the disease. Among others, maternal drug use (Bluhm, et al., 2006), the use of hair dyes during pregnancy (McCall, et al., 2005), maternal alcohol consumption during pregnancy (Olshan, et al., 1999), maternal tobacco use (Heck, et al., 2009), exposure to non-volatile and volatile hydrocarbons, especially diesel fuels (De Roos, et al., 2001), use of oral contraceptives or other sex hormones in early pregnancy (Schüz, et al., 2001), fertility hormones (Michalek, et al., 1996) and consumption of codeine containing medication during pregnancy or lactation (Cook, et al., 2004) show evidence of association with neuroblastoma.

1.1.4. Diagnosis, staging and prognosis

Acute effects of neuroblastoma include pain, neurological symptoms, such as blindness, spinal cord compression syndrome or opsoclonus myoclonus syndrome, frequent hospitalization, nausea, mucositis, veno-occlusive disease, electrolyte imbalance, growth

delay, social isolation and risk of toxic health (Matthay, et al., 2016). A combination of diagnostic tools is applied in the diagnosis of neuroblastoma including laboratory tests, radiographic imaging and pathology of the tumour. Accurate diagnosis and staging can be accomplished with computed tomography (CT) or magnetic resonance imaging (MRI) of the site of the primary tumour, histological examination of the primary tumour and any possible metastases, bone marrow aspirate and biopsy at 2 different sites to test the tissue for bone marrow infiltration, meta-iodo-benzyl-guanidine (I-MIBG) scintigraphy, CT of the bones that come out positive on MIBG scan in children younger than 1 year of age, measurement of catecholamine metabolites and additional evaluation of the levels of ferritin, serum lactate dehydrogenase (LDH) and neuron-specific enolase (NSE) (Luksch, et al., 2016).

Based on the study of local and distant extension of the disease and on the possibility of tumour resection for non-metastatic cases, the International Neuroblastoma Staging System (INSS) has been developed for the staging of the disease (Table 1.1).

MYCN status and the age of the patient are used in combination with the stage of the tumour in order to define prognosis and design the treatment. These factors define two distinct groups of the disease; neuroblastoma which arises in the first months of life and *MYCN* amplified tumours or metastatic tumours and age >18 months of diagnosis (De Bernardi, et al., 2008). Patients that belong in the first group usually show spontaneous regression or have very high survival rates under minimal treatment. On the other hand, patients that fit in the second group are prognosed with unfavourable outcome. Cases of neuroblastoma in adolescents and adults are rare. More often, in adult cases, neuroblastoma occurs in the absence of metastatic events and is not accompanied by *MYCN* amplification (Mossé, et al., 2014).

The risk in neuroblastoma is classified as low, intermediate, or high with the group of patients that do not respond to therapy being characterised as “ultra-high”. The International Neuroblastoma Risk Group (INRG) Staging System was designed to provide a universal pre-treatment risk groups system (Table 1.2) and enable different clinical trials conducted internationally (Cohn, et al., 2009).

Table 1.1: International Neuroblastoma Staging System (INSS) (Park, et al., 2008)

Stage	Characteristics
Stage 1	Localised tumour with complete gross excision, with or without microscopic residual disease; representative ipsilateral lymph nodes negative for tumour microscopically (nodes attached to and removed with the primary tumour may be positive).
Stage 2A	Localised tumour with incomplete gross excision; representative ipsilateral non-adherent lymph nodes negative for tumour microscopically.
Stage 2B	Localised tumour with or without complete gross excision, with ipsilateral non-adherent lymph nodes positive for tumour. Enlarged contralateral lymph nodes must be negative microscopically.
Stage 3	Unresectable unilateral tumour, infiltrating across the midline,* with or without regional lymph node involvement; or localised unilateral tumour with contralateral regional lymph node involvement; or midline tumour with bilateral extension by infiltration or lymph node involvement.
Stage 4	Any primary tumour with dissemination to distant lymph nodes, bone, bone marrow, liver and/or other organs (except as defined for Stage 4S).
Stage 4S	Localised primary tumour (as defined for Stage 1, 2A or 2B), with dissemination limited to liver, skin, and/or bone marrow (limited to infants <1 year of age).

Table 1.2: International Neuroblastoma Risk Group Staging System (INRGSS)

Risk group for treatment	INRG stage	IDRFs in primary tumour	Distant metastases	Age (months)	Histological category	Grade of differentia-tion	*MYCN* status	Genomic profile	Ploidy
Very-low	L1	Absent	Absent	Any	GNB nodular, NB	Any	-	Any	Any
Very-low	L1 or L2	Any	Absent	Any	GN, GNB intermixed	Any	-	Any	Any
Low	L2	Present	Absent	<18	GNB nodular, NB	Any	-	Favourable	Any
Low	L2	Present	Absent	≥18	GNB nodular, NB	Differentiating	-	Favourable	Any
Low	MS	Any	Present	<12	Any	Any	-	Favourable	Any
Intermediate	L2	Present	Absent	<18	GNB nodular, NB	Any	-	Unfavourable	Any
Intermediate	L2	Present	Absent	≥18	GNB nodular, NB	Differentiating	-	Unfavourable	Any
Intermediate	L2	Present	Absent	≥18	GNB nodular, NB	Poorly differentiated, undifferentiated	-	Any	Any
Intermediate	M	Any	Present	<18	Any	Any	-	Any	Hyper-diploid
Intermediate	M	Any	Present	<12	Any	Any	-	Unfavourable and/or diploid	
Intermediate	MS	Any	Present	12-18	Any	Any	-	Favourable	Any
Intermediate	MS	Any	Present	<12	Any	Any	-	Unfavourable	Any
High	L1	Absent	Absent	Any	GNB nodular, NB	Any	+	Any	Any
High	L2	Present	Absent	≥18	GNB nodular, NB	Poorly differentiated, undifferentiated	+	Any	Any
High	M	Any	Present	12-18	Any	Any	-	Unfavourable and/or diploid	
High	M	Any	Present	<18	Any	Any	+	Any	Any
High	M	Any	Present	≥18	Any	Any	Any	Any	Any
High	MS	Any	Present	12-18	Any	Any	-	Unfavourable	Any
High	MS	Any	Present	<18	Any	Any	+	Any	Any

IDRF: image defined risk factors, GNB: ganglioneuroblastoma, NB: neuroblastoma, GN: ganglioneuroma

1.1.5. Management and treatment

There are several types of treatment that are applied against neuroblastoma and are determined based on the distinct risk strata (Table 1.2). Induction chemotherapy (commonly carboplatin, cisplatin, cyclophosphamide, doxorubicin, vincristine and topotecan) is used for patients that achieve a very good remission by the INRG criteria, while local control with surgical resection of primary tumours is challenging for high-risk patients even after chemoreduction. For this group of patients the approach followed is treatment with myeloablative therapy with autologous hematopoietic stem-cell transplantation (AHSCT) (Fig. 1.5). For patients with relapsed neuroblastoma, the prognosis is 1-3 years without a treatment. For these patients, the most common approach is the use of topotecan with cyclophosphamide, irinotecan with temozolomide or topotecan with temozolomide (Matthay, et al., 2016).

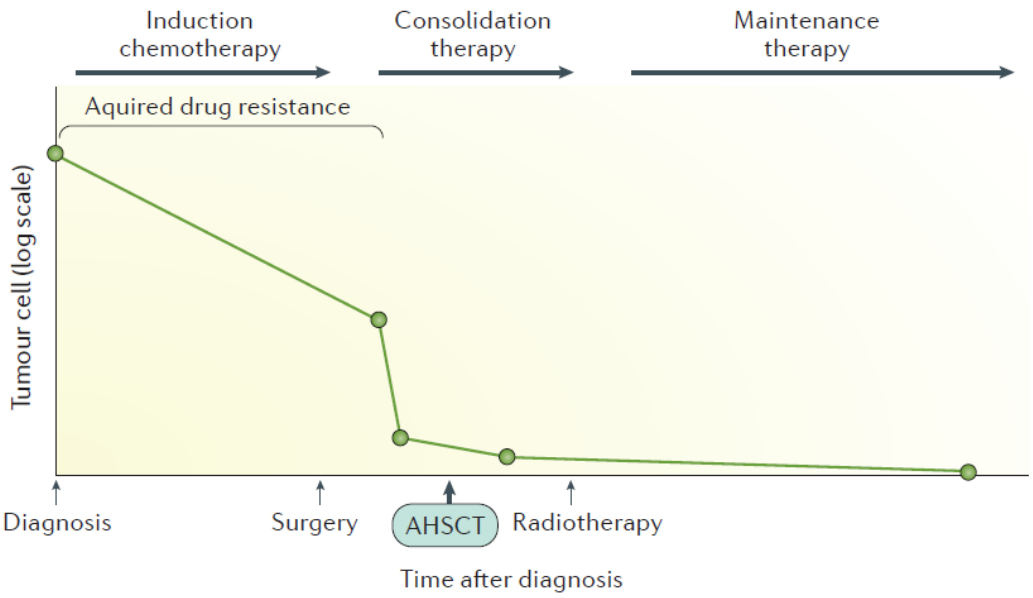

Figure 1.5: Overall treatment approach for neuroblastoma (Matthay, et al., 2016).

As mentioned before, *MYCN* amplification is one of the factors that define high-risk neuroblastoma. Since MYCN can drive so many pathways that either initiate or act in favour of neuroblastoma, targeting MYCN could provide a therapeutic strategy against the disease. In addition to MYC and MYCN's redundancy, targeting of either MYC or MYCN is challenging due to their composition of two extended alpha-helices that do not leave obvious surfaces for small molecule binding (Huang & Weiss, 2013). The therapeutic strategies that could

tackle *MYCN* amplified neuroblastoma include the use of BRET-bromodomain inhibitors to block MYCN-dependent transcription, inhibition of histone deacetylases (HDACs), the use of antagonizing proteins that are involved in the stabilization of MYCN protein, the suppression of MDM2, which acts by stabilizing MYCN mRNA and disrupts p53-mediated apoptosis and the use of factors that can induce neuronal differentiation (Huang & Weiss, 2013).

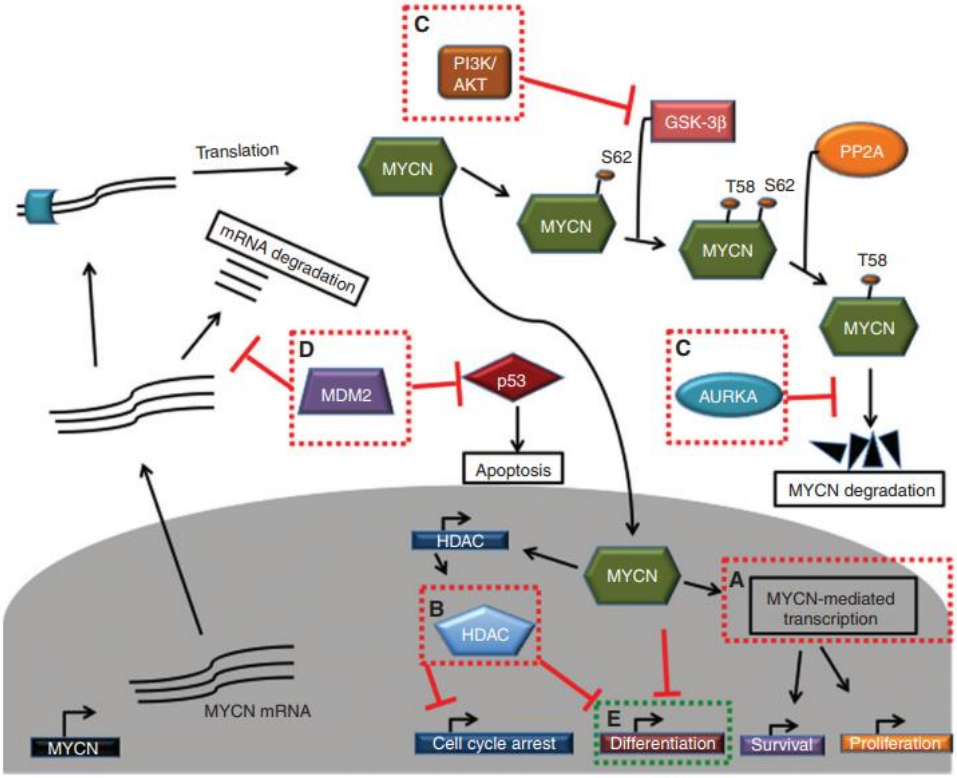

Figure 1.6: Therapeutic strategies to target MYCN in neuroblastoma. Indirect ways to target MYCN in *MYCN* amplified neuroblastoma include the use of BET-bromodomain inhibitors that block MYCN-dependent gene transcription, inhibitors of proteins that stabilise MYCN protein, such as AURKA, PI3K and MDM2 inhibitors or inducers of cell differentiation and regulators of cell cycle, such as histone deacetylases (HDACs) inhibitors (Huang & Weiss, 2013).

A novel and promising approach for cancer treatment is the use of chimeric antigen receptor (CAR) T cells. This method takes advantage of the fact that CARs drive the $CD8^+$ T cells that approach the tumour microenvironment to recognize tumour associated antigens presented on the membranes of cancer cells. When the T cell receptor (TCR) of a CAR T cell recognizes its antigen, a major histocompatibility complex (MHC)-independent mechanism of

cytotoxicity is triggered. The use of CAR T cells has been reported to be successful in haematological malignancies, however solid tumours like neuroblastoma seem to be more complicated, probably due to their complex tumour microenvironment that leads to resistance in many of the available therapeutic approaches (Newick, et al., 2017). In high-risk neuroblastoma patients, the combination of anti-disialoganglioside (GD2) monoclonal antibodies with inteleukin 2 (IL-2) and granulocyte-macrophage colony stimulating factor (GM-CSF) has been used. Although the GD2 immune-therapy showed improved outcomes in the randomized phase 3 clinical trial, it was quite toxic, due to the expression of GD2 on nocireceptor-containing peripheral nerves (Yu, et al., 2010).

In 2017, glypican-2 (GPC2) was identified as an oncoprotein and prominent candidate for immunotherapeutic target in high-risk neuroblastoma (Bosse, et al., 2017; Li, et al., 2017). GPC2 is highly expressed on the cell membrane of most neuroblastoma cells, while being low in normal tissues in childhood (Bosse, et al., 2017). The expression specificity of this protein makes it a really promising target for the development of new CAR T cell-based therapies for neuroblastoma.

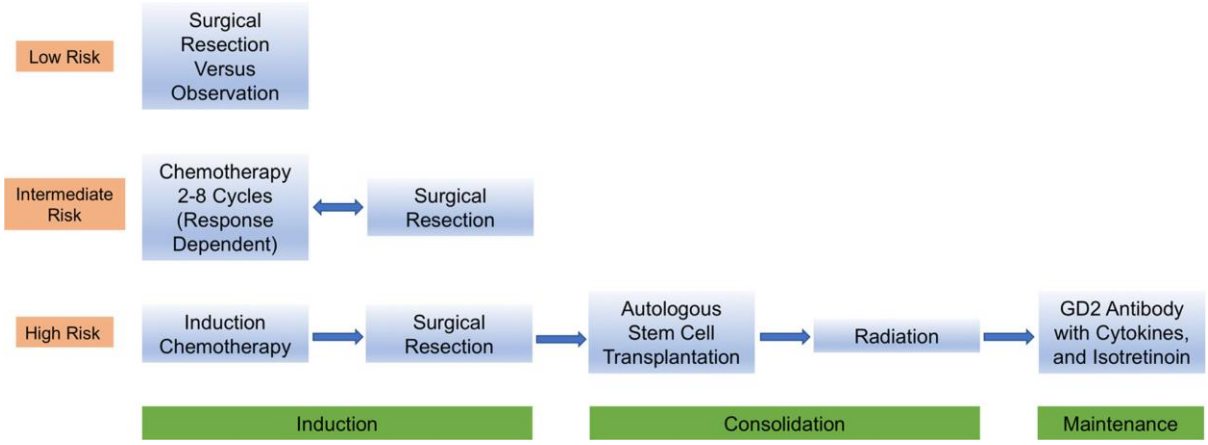

Figure 1.7: Neuroblastoma treatment approach based on risk classification (Tolbert & Matthay, 2018).

In conclusion, immunotherapy with antibodies targeting GD2 has been a breakthrough in the therapeutic approaches for neuroblastoma. However, the need for effective therapies for the patients with high-risk neuroblastoma remains. Data from studies using CAR T cells designed to target neuroblastoma cells seem very promising and importantly, these studies reveal information about the complexity of immunotherapy in neuroblastoma and the role of the

tumour microenvironment of the aggressive tumours. If targeted immunotherapy and personalised medicine are combined with therapeutic strategies that can tackle the ability of tumours like neuroblastoma to escape the mechanisms of the immune system, we may develop therapies in the future that overcome the initial tumour escape and successfully target these tumours.

1.2. The world of MYC

1.2.1. The members of the *MYC* family are proto-oncogenes that regulate gene expression

The MYC family of transcription factors in humans has three evolutionary conserved members: c-MYC, L-MYC and N-MYC (MYCN). It is one of the most well studied protein families and MYC's activity has been shown to be crucial for a plethora of biological processes both in normal and cancer cells (Eilers & Eisenman, 2008). Normal organism development depends on MYC expression. This is evident as in embryonic stages MYC genes reach their highest levels of expression, while they are downregulated in mature differentiated mammalian cells (Zimmerman, et al., 1986). In addition, genetic knock-out of c-MYC is lethal in early embryonic stages, partially due to defects in vasculogenesis and angiogenesis (Baudino, et al., 2002).

MYC is a basic helix-loop-helix zipper (bHLHZ) protein that can heterodimerise with the small bHLHZ protein Max and bind to the CACGTG sequence of E-boxes on DNA (Fig. 1.9). The binding of E-boxes by the MYC/Max heterodimer has been associated with gene activation. In normal cells, MYC responds to developmental or mitogenic signals and regulates among others proliferation, metabolism, cell differentiation and apoptosis (Eisenman, 2001). At the same time, MYC can also promote transcriptional repression. For example, it can regulate the transcriptional repression of $p15^{INK4b}$ by binding and inhibiting the transcriptional activator Miz-1 (Staller, et al., 2001). In addition, it can inhibit the expression of the tumour suppressor gene encoding for clusterin (CLU) by interacting with the histone methyl transferase and polycomb protein EZH2 to induce bivalent epigenetic changes in the 5'-flanking region of the *CLU* gene (Corvetta, et al., 2013).

Although MYC is exhaustedly studied, the description of the role of MYC in gene activation and repression is difficult to approach, as the vast repertoire of MYC's transcriptional targets consists of a very large list of genes that includes genes transcribed by RNA polymerase II , but also RNA polymerases I (Arabi, et al., 2005; Grandori, et al., 2005) and III (Gomez-Roman, et al., 2003), targeting genes encoding ribosomal RNAs involved in translation and growth, as well as miRNAs (Fig. 1.9) (Lin, et al., 2009; Lotterman, et al., 2008).

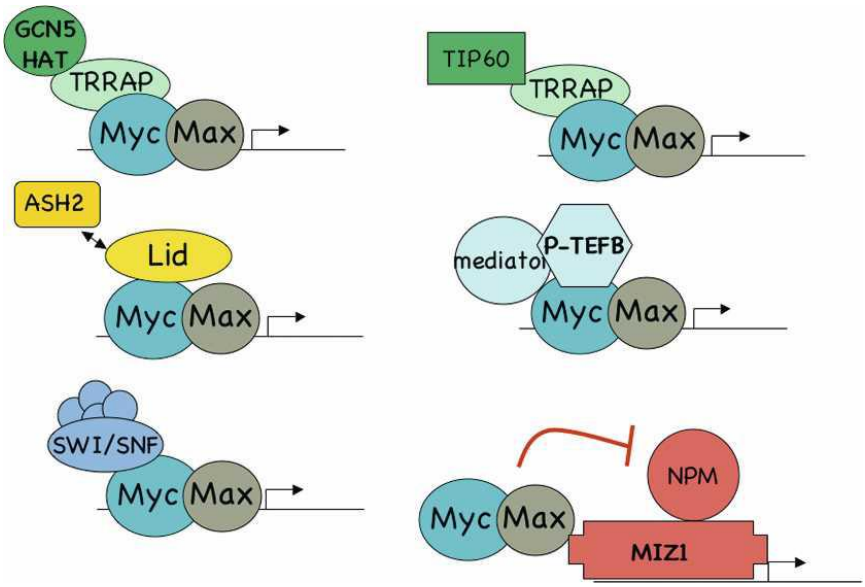

Figure 1.8: Transcriptional complexes associated with MYC. The MYC/Max heterodimer associates with different complexes in order to induce gene transcription. It can form complexes with histone acetyltrasferases, such as GCN5, HAT and TIP60 that together with Transformation/Transcription domain associated protein (TRRAP) activate gene expression. Also, it interacts with the histone methyltransferase complex subunit ASH2 and the positive transcription elongation factor (P-TEFb) that recruits Mediator for transcription to start. Finally, MYC/Max can interact with the SWItch/Sucrose non-fermentable (SWI/SNF) nucleosome remodeling complex or inhibit Nucleophosmin (NPM) and therefore regulate the transcription of target genes (Eilers & Eisenman, 2008).

The broad effects of MYC on gene expression gives rise to the question of which of those effects are direct or indirect. To address that, several studies used chromatin immunoprecipitation (ChIP) to characterise the genomic locations bound by MYC/Max (Li, et al., 2003; Fernandez, et al., 2003; Zeller, et al., 2006; Chen, et al., 2007). Strikingly, these studies show that the MYC/Max heterodimer binds 10%-15% of genomic loci in mammals. These genomic loci are mostly correlated with gene expression, however a number of sites identified with these screenings is not directly coupled to transcription. The fact that MYC/Max is found to bind these sites can be a reflection of cell specificity in a developmental context (Lawlor, et al., 2006), indicate the regulation of genomic loci encoding miRNAs (O'Donnell, et al., 2005; Chang, et al., 2008; Schulte, et al., 2008) and/or RNA polymerase III transcripts (Gomez-Roman, et al., 2003) or even non-productive binding by MYC.

The binding of MYC/Max on DNA is regulated by the chromatin context and epigenetic signatures on the DNA, such as CpG methylation, that inhibits the binding of MYC to some sites (Perini, et al., 2005; Guccione, et al., 2006), as well as methylation of H3K4 and H3K79 (Guccione, et al., 2006).

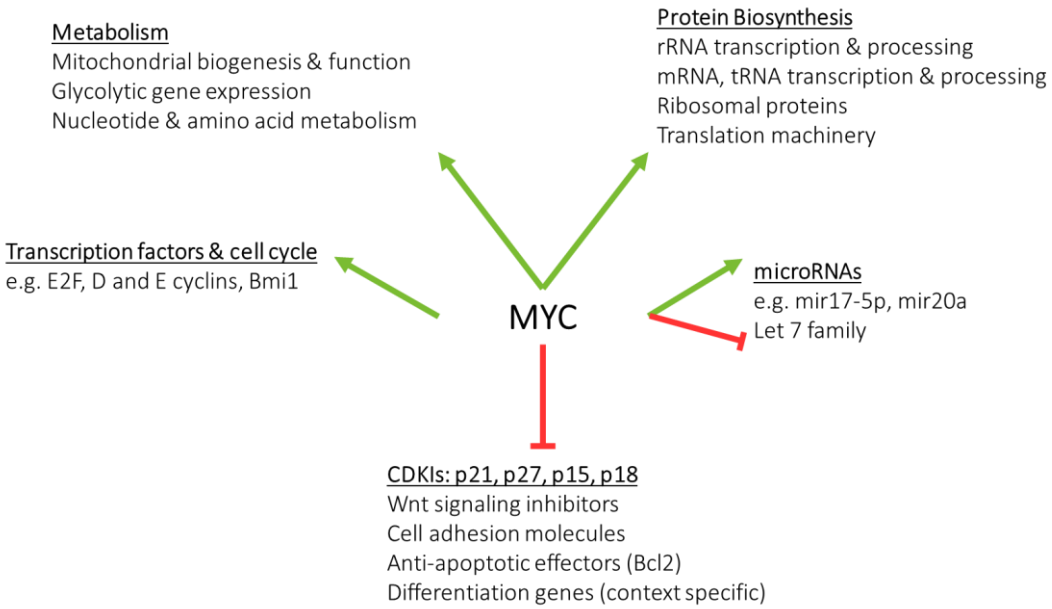

Figure 1.9: Functional categories of genes regulated by augmented MYC expression (Adapted from Eilers & Eisenman, 2008).

Another mechanism to antagonise MYC/Max binding to DNA involves the Mxd (formerly known as Mad) family of proteins. Mxd proteins are transcriptional repressors that contain bHLHZ domains that can heterodimerise with Max and bind to E-boxes, thus antagonising with MYC for the availability of binding sites and causing transcriptional repression (Grinberg, et al., 2004). The MYC/Max/Mxd interplay and the ability of Mxd proteins to regulate the access of MYC to DNA is crucial in mammal cells, as it regulates among others development, growth and cell size of T lymphocytes (Iritani, et al., 2002), terminal differentiation of granulocytes (McArthur, et al., 2002) and tumour cell proliferation (Adhikary, et al., 2005).

Finally, a critical step in the regulation of the dynamics of MYC's DNA binding is the balance for MYC's degradation. MYC protein levels can be regulated by proteasome-mediated

degradation induced by the ubiquitin ligases FBW7 (Welcker, et al., 2004; Yada, et al., 2004) and SKP2 (Kim, et al., 2003; Von Der Lehr, et al., 2003) or HectH9/Huwe1, in case of MYCN, a process taking place during cell differentiation (Zhao, et al., 2008).

1.2.2. MYC's role in stemness and tumourigenesis

The paramount importance of MYC's expression in stem cells is suggested by the facts that MYC can bind to a large number of genomic loci in embryonic stem cells (ESCs) (Kim, et al., 2008) and importantly, together with Sox2, Klf4 and Oct4, it belongs to the group of transcription factors that are capable of inducing the reprogramming of differentiated adult cells to pluripotent cells (Nakagawa, et al., 2008). Furthermore, MYC regulates miRNAs involved in self-renewal and differentiation repression (Lin, et al., 2009). Intriguingly, using a gene module map to systematically relate transcriptional programs in ESCs, adult tissue stem cells, and human cancers it has been shown that c-MYC alone is sufficient to induce an ESC-like program in both normal and cancer cells (Wong, et al., 2008). Collectively, these data suggest a putative role of MYC in the genesis of a pool of cells with oncogenic potential or the cancer stem cells (Soucek & Evan, 2010).

Since MYC activity is essential for normal cell proliferation, the activation of MYC's oncogenic signalling must be triggered by the dysregulation of its expression. The presence of MYC in cells and the consequent complex biological outcome is not always straightforward. The complexity of the role of MYC in the regulation of its downstream pathways can be highlighted by the fact that different levels of MYC expression can lead to different biological outcomes for the cell. It has been shown that when dysregulated MYC is expressed at low levels *in vivo*, ectopic proliferation of somatic cells and oncogenesis are observed, while, when MYC is massively overexpressed, apoptotic and ARF/p53 intrinsic tumor surveillance pathways are activated (Murphy, et al., 2008).

1.2.3. MYC regulates the tumour microenvironment

Besides its role in regulating the transcriptional program of the cells that endogenously express it, MYC also has the ability to coordinate the communication of the tumour with its

microenvironment (Sodir, et al., 2011). In the process of tumour growth, there are several phases in which the tumour's microenvironment can be of critical importance.

Firstly, the support of a growing tumour requires vascular remodelling. MYC seems to regulate the vasculature of growing tumours, as genetic knockout of *c-myc* interferes with the VEGF signalling and leads to defects in vasculogenesis which are lethal in mice embryos (Baudino, et al., 2002), while overexpression of MYC in a human B-cell line increases the expression of VEGF (Mezquita, et al., 2005). In addition, MYC negatively regulates the inhibitor of neovascularisation, thrombospodin-1 as shown *in vivo* in the MYC-transformed Rat-1A fibroblast (Ngo, et al., 2000) and cecal wall engrafted p53-null mouse colonocytes engineered to overexpress activated K-Ras and MYC (Dews, et al., 2006). Thus, it is becoming clear that MYC plays a dramatic role in the regulation of factors that determine neo-angiogenesis *in vivo.*

Secondly, support of tumour growth can be provided by the tumour's adjacent endothelial and immune cells. Again, MYC seems to regulate this crosstalk, as it has been shown that in a mouse model of pancreatic β cells tumourigenesis, in which the expression of MYC can be reversibly switchable, Myc activation is followed by the release of factors in the β cells' extracellular space that led to induced proliferation of the nearby endothelial cells and the formation of vessels (Shchors, et al., 2006). Moreover, in the same system, MYC's expression caused the recruitment of various inflammatory cells towards the tumour, including mast cells, the cells that are required for tumour growth and expansion (Soucek, et al., 2007). In addition, MYC regulates the alternative macrophage polarization by inducing a subset of genes associated with alternative activation (Pello, et al., 2012).

Finally, there is evidence supporting the bidirectional relationship of MYC with the microenvironment of tumours. In a mouse model for MYC-induced tumourigenesis in hematopoietic cells, the presence of $CD4^+$ T cells engineered to express thrombospodin-1 leads to complete tumour regression (Rakhra, et al., 2010).

1.2.4. MYC-driven tumourigenesis is linked to super-enhancer elements

The term 'super-enhancer' is used to describe genomic sequences with the potential to bind unusually high levels of transcriptional co-activators, such as Mediator, the multiprotein complex that interacts with RNA polymerase II in eukaryotes for transcription to emerge. Super-enhancers can activate transcription of a gene from a distance greater than that of enhancers and they do so independently of their orientation on DNA (Whyte, et al., 2013; Hnisz, et al., 2013; Lovén, et al., 2013).

Besides their physiological roles in gene expression, super-enhancers are acquired by cancer cells where they play a crucial role for the high-level expression of genes that control cell growth and proliferation. One of those genes is *MYC* (Hnisz, et al., 2013; Lovén, et al., 2013).

It has been shown that in neuroblastoma cells with genomic amplification of *MYCN*, super-enhancers are employed in order to induce the activation of the cells' transcriptional program. This is facilitated by cyclin-dependent kinase 7 (CDK7), one of the enzymes regulating the transcription cycle of RNA polymerase II (Chipumuro, et al., 2014). In essence, Chipumuro *et al.* show that super-enhancers regulate the high-level expression of *MYCN* in neuroblastoma. MYCN then binds to promoter and enhancer loci of transcriptionally active genes, including its own promoter, and induces global transcription. Importantly, the involvement of CDK7 sensitises the *MYCN* amplified cells to CDK7 inhibitors, such as THZ1 (Fig. 1.10).

The transcriptional program regulated by the activity on the sites of super-enhancer elements has major repercussions for the cells. In their super-enhancer-defining papers, Whyte *et al* and Hnisz *et al* suggest that the transcription factor networks associated with super-enhancer elements are critical for the determination of lineage identity (Whyte, et al., 2013; Hnisz, et al., 2013). Therefore, it seems possible that super-enhancers may also regulate intratumoural heterogeneity. Indeed, a recent study using ChIP-seq analysis of isogenic pairs of neuroblastoma cells expressing either mesenchymal or adrenergic phenotypes showed that there are two distinctive super-enhancer networks that control lineage commitment and therefore probably control neuroblastoma intratumoural heterogeneity of mesenchymal- or adrenergic-like cells (van Groningen, et al., 2017). Tumour heterogeneity in neuroblastoma is of particular importance, as it can determine the response in treatment. Post-treatment

samples are enriched in the mesenchymal cells, which suggests a possible chemotherapy selection for the mesenchymal cells compared to the adrenergic (van Groningen, et al., 2017; Boeva, et al., 2017). Importantly, the two sub-populations are not static and adrenergic cells have the ability to trans-differentiate into mesenchymal cells in a NOTCH-dependent way that induces a switch from adrenergic to mesenchymal super-enhancers via the remodelling of H3K27 acetylation landscape (van Groningen, et al., 2019).

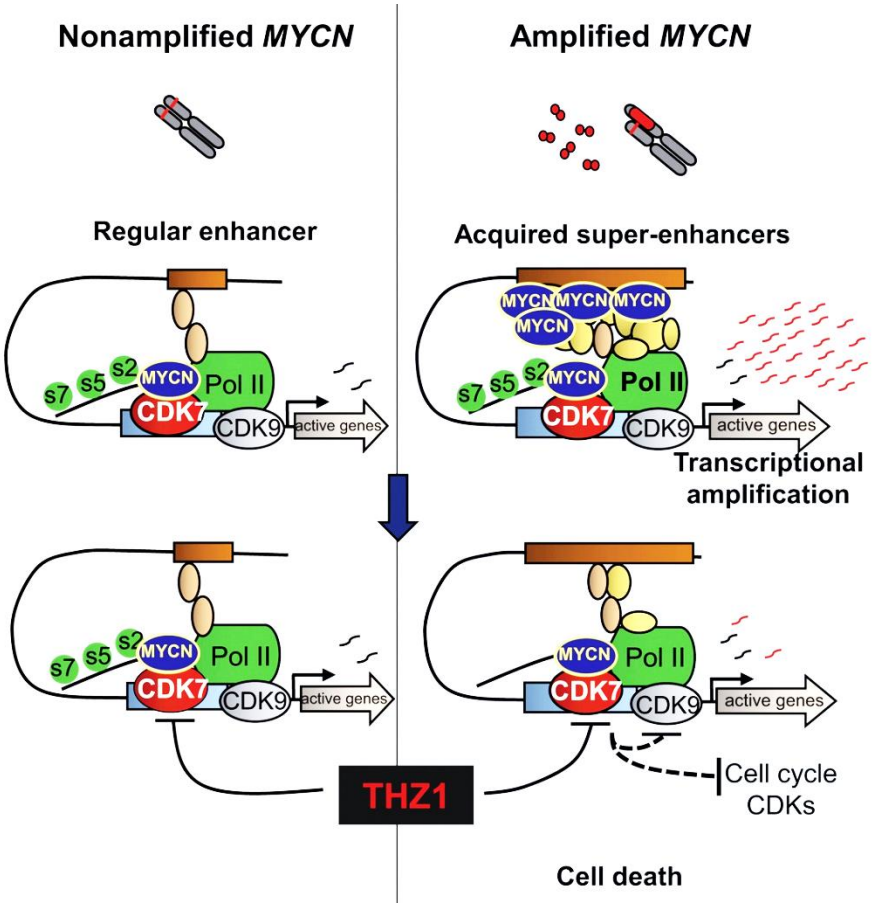

Figure 1.10: CDK7-regulated transcription in *MYCN* amplified neuroblastoma cells is facilitated by super-enhancer DNA elements (Chipumuro, et al., 2014).

These studies shed light on the intricate and sophisticated mechanisms that govern the effects of oncogenes like MYC on cellular fate and behaviour. Altogether and considering all the aspects of development governed by genomic instability, vascularisation, metabolism and inflammation as wells as the endogenous and extracellular effects downstream of MYC dysregulation, MYC 'ticks' the boxes of the hallmarks of cancer (Hanahan & Weinberg, 2011) and seems to be behind it all, something that makes it an extraordinary gene.

1.3. Extracellular vesicles

1.3.1. The discovery of exosomes and extracellular vesicles

The dense structure of solid tumours such as neuroblastoma can create an extremely inhospitable microenvironment for the cells. The tumour cells have to grow within an environment full of obstacles for the essential intercommunication between the tumour cells and their microenvironment. Therefore, the tumour cells have to develop mechanisms to achieve this intercellular communication in order for them to survive and grow. In addition, the presence of multiple cell types within a tumour requires a high-level coordination and regulation of the molecular mechanisms that mediate intercellular communication. One of the mechanisms that can meet the needs of this demanding microenvironment is the cellular communication mediated by extracellular vesicles (EVs).

The secretion of EVs seems to be a well-established mechanism of cell communication and conserved among different species through the evolutionary processes. The release of vesicles towards the extracellular space has been observed from prokaryotic cells to eukaryotes, including amoebae, *Caenorhabditis elegans* and parasites of mammals (Raposo & Stoorvogel, 2013). The biological significance of the release of such vesicles *in vivo* seems to be quite high, as they have been isolated from different body fluids such as milk (Admyre, et al., 2006), sperm (Ronquist & Brody, 1985) and urine (Pisitkun, et al., 2004). The nomenclature of these EVs is unclear, as many different names have been used in the literature. Based on the origin and physical characteristics of the vesicles, they have been characterized as micro- or nano- vesicles (size characterization), prostasomes and oncosomes (based on the tissue from which they originated) or in general ectosomes, exosomes or exovesicles (as they are present outside the cell). In addition, exosomes were originally described as microvesicles secreted by neoplastic cell lines vesicles with size ranging from 40 to 1,000 nm that have the potential to carry 5'-nucleotidase activity (Trams, et al., 1981). Nonetheless, the terms ectosome, shedding vesicle, microparticle and microvesicle are now used to describe 150-1,000 nm vesicles that are released by budding from the cell's plasma membrane (Colombo, et al., 2014). The interest in the biology and the potential of secreted vesicles has created a non-stop growing field of study. As new information is revealed, the nomenclature of extracellular vesicles is becoming more precise, even though difficulties are

presented due to the overlapping size range, morphology and molecular composition of the different EVs.

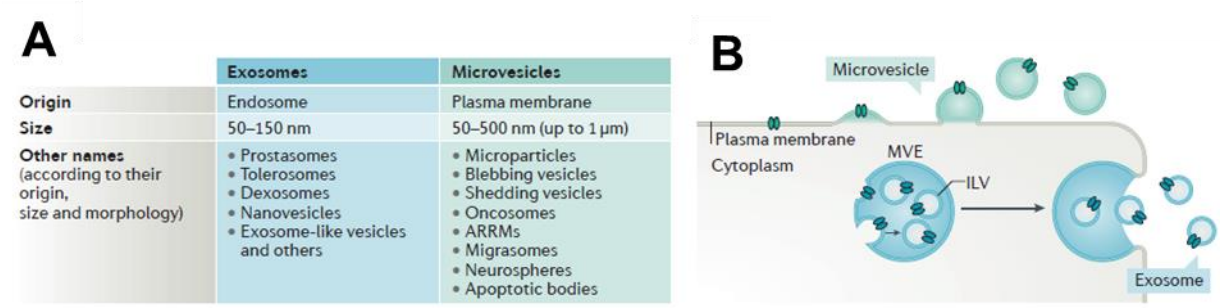

Figure 1.11: The main categories of extracellular vesicles. A. EVs have been categorised based on their size, origin, morphology and molecular content. **B.** Depending on whether EVs are formed by budding of the plasma membrane or as intraluminal vesicles (ILVs) in the lumen of multivesicular endosomes (MVEs) they are called microvesicles or exosomes, respectively (van Niel, et al., 2018).

Although they were initially thought to be products of cell death and debris and were formerly called “platelet dust”, EVs were later described as a more complex mechanism to perform intercellular communication, as they were shown to be vesicles enclosed by a lipid bilayer membrane that avoid lysosomal degradation and, instead, they have the ability to be released, target recipient cells and fuse with their plasma membrane to transfer their content (Harding, et al., 1983; Pan, et al., 1985).

Almost 40 years ago, several groups described EVs found in plasma, within tissues and in various body fluids. Initially, these membrane-enclosed vesicles were thought to be products of plasma membrane budding. However, 20 years later than these initial observations, Johnstone (Pan, et al., 1985) and Stahl’s (Harding, et al., 1983) groups suggested a different mechanism for the secretion of these vesicles. They showed that multivesicular bodies (MVBs) can be formed by inward budding inside an intracellular endosome. The MVBs can then fuse with the plasma membrane and the internal vesicles can be released. These small (30-100 nm) EVs of endosomal origin are from then on referred as exosomes (Fig. 1.11).

The original system of the maturation of reticulocytes

The process through which the reticulocytes mature into erythrocytes can be monitored by the loss of transferrin receptor (TfR) found on the plasma membrane. The mechanism of TfR

release into the extracellular space was described by Stahl and Johnstone. They used gold particles that bound transferrin (Harding, et al., 1983) or antibodies against TfR (Pan, et al., 1985) and with electron microscopy (EM) they observed the trafficking of the receptor from the moment of its endocytosis to the release outside of the cell. They observed that most of the receptor molecules were associated with small internal bodies inside the multivesicular endosome (MVE). These internal bodies of approximately 50 nm of diameter were then released upon fusion of the endosomes with the plasma membrane of the reticulocyte.

The immune system provides a study model for the function of extracellular vesicles

After the initial observation on the system of the maturation of reticulocytes, exosomes were thought to be a way that the cells use in order to discard unwanted molecules towards the extracellular space. However, in the late 90s, studies with Epstein-Barr virus (EBV)-transformed B cell lines (Raposo, et al., 1996) and tumour peptide-pulsed dendritic cell-derived exosomes (Zitvogel, et al., 1998) described potential roles of exosomes as mediators of immune responses and putative immunotherapeutic agents. That was the first time that exosomes were referred as biologically active entities that could mediate intercellular communication.

1.3.2. Definition of exosomes and general properties

Methods of EVs isolation from cell culture media

The protocol used for the original purification of reticulocyte exosomes was developed based on the isolation of exosomes with differential centrifugation. As later described (Théry, et al., 2006), this protocol includes several centrifugation steps and aims to the elimination of different factors that could contaminate the final preparation. Exosomes and small vesicles are precipitated by ultracentrifugation at 100,000 x g. Floating cells, cell debris, apoptotic bodies and larger vesicles are sedimented in previous steps of centrifugation at lower speeds (200-10,000 x g).

As at the speed of 100,000 x g small vesicles precipitate, this technique only allows the enrichment of the preparations in small extracellular vesicles including exosomes. However, it does not include a proper purification step. For that purpose, some protocols suggest the

use of sucrose gradient, as membrane enclosed vesicles can be separated from protein aggregates due to their ability to float. Lipid vesicles and, therefore, exosomes as well, float on sucrose gradient with densities from 1.13 g ml^{-1} to 1.19 g ml^{-1} (Raposo, et al., 1996). The combination of ultracentrifugation through a D_2O/Sucrose cushion with a step of filtration/concentration through a 500 kDa membrane has been proposed for the purification of EVs of clinical grade for therapeutic use (Lamparski, et al., 2002).

Because of the large number of studies that are coming out about EVs, several companies developed commercially available methods for EVs isolation without the step of ultracentrifugation. Most of them are polymer-based precipitation techniques or they use antibody-coated beads to immunocapture the vesicles.

As each different technique offers different advantages to the isolation process, it is difficult to claim which one is better than the other and most often, scientists tent to combine more than one methods in order to have the desired result. In 2013, the International Society of Extracellular Vesicles published a first position paper for the standardized procedure of biological fluids collection and EVs isolation (Witwer, et al., 2013).

Morphological features and physical properties

Given the 200 nm resolution limit of classical optical microscopes, optical microscopy cannot be used to visualize small EVs. Therefore, transmission EM (TEM) has been mostly used in order to characterise their morphology and structure. When analysed by whole-mount EM, they display a “cup”-like shape, which is an artifact of the fixation step (Raposo, et al., 1996). When observed by cryo-EM they appear round-shaped as it is expected (Fig. 1.12) (Raposo & Stoorvogel, 2013). Recently, atomic force microscopy, a variant of scanning EM, is used to evaluate the size and structure of EVs using mechanical probes (Sharma, et al., 2011).

A fast and low cost way to measure size distribution and concentration of nanoparticles is the Nanoparticle tracking analysis (NTA) (Dragovic, et al., 2011). This method measures the Brownian motion of particles in suspension providing accurate quantification of microparticle number and size it can analyse large numbers of particles quite fast and easy, but it cannot separate measurements between small vesicles and protein aggregates.

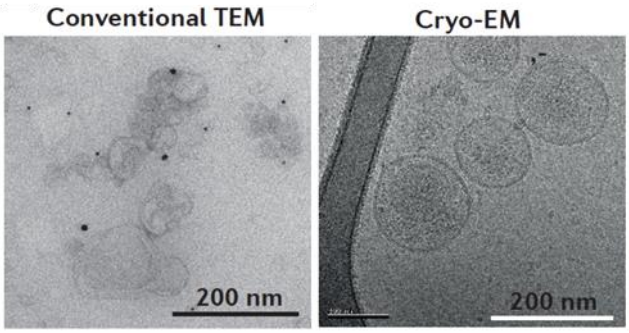

Figure 1.12: Observation of EVs with TEM and cryo-EM (van Niel, et al., 2018).

A most recent, cutting-edge technology applied on the study of EVs biology is the use of imaging flow cytometry. While flow cytometry is commonly used, it suffers from low sensitivity and accuracy. For the first time, the Amnis ImageStreamX Mk II imaging flow cytometer has been used for the analysis of microvesicles in 2014 and it afforded accurate analysis of fluorescent calibration beads ranging from 1 mm to 20 nm (Headland, et al., 2014). This tool is developing to be one of the most powerful applications in the field, as it does not only analyse the size and morphology of the vesicles of the sample, but it can also be used in combination with antibody staining to reveal the pattern of protein molecules transferred within the EVs.

The information that we gain while taking advantage of the above techniques gets us closer towards understanding the physical properties of EVs. We can now separate the different classes of microparticles based on size, on their lipid composition that allows them to float in sucrose gradients, their geometry and composition that is correlated with their behaviour under light scatter etc.

Exosomal content and biochemical properties of EVs

After avoiding degradation from the lysosomal system, exosomes are released in the extracellular space as biologically active entities that can be uptaken by neighbouring cells and get involved in various biological processes.

As the knowledge that we gain about the content of exosomes grows, it becomes clearer that exosomes of different origin share some similarities (Fig. 1.13). The bilipidic layer structure,

the size, the density and a large number of proteins are common among the mammalian exosomes. The similarities of the content of different exosomes provide information about the families of molecules which are potentially involved in the formation of the vesicles within the MVBs, their release in the extracellular space and their ability to be uptaken by neighbouring cells.

Lipids

The lipid composition of exosomes is not completely clear yet. Reticulocyte-derived exosomes are similar in composition with the plasma membrane of the cells (Johnstone, et al., 1987). B cell derived exosomes has been shown to contain lyso-bis-phosphatidic acid, a lipid that is also present in the late endocytic compartments (Denzer, et al., 2000). Compared with the total cell membrane, secreted vesicles are enriched in sphingomyelin, phosphatidylserine, cholesterol and saturated fatty acids (Laulagnier, et al., 2004; Llorente, et al., 2013; Wubbolts, et al., 2003).

Nucleic acids

A revolution in the field was the discovery that mRNA and microRNAs are being carried within the exosomes (Valadi, et al., 2017). Nucleic acids can be transferred through exosomes and, when they do, they influence gene expression in the recipient cells. The presence of exosome derived mRNAs and microRNAs is reported in tumour cell and stem cell derived vesicles (Gajos-Michniewicz, et al., 2014; Valadi, et al., 2017). It is also published that glioblastoma and blood cell derived EVs contain microRNAs. Lately, studies that are taking advantage of the use of next-generation sequencing tools reveal that EVs contain an extended range of genetic material, including non-coding RNA (Nolte-'t Hoen, et al., 2012). There is not yet experimental evidence on the mechanism through which selective mRNAs are enclosed within exosomes of specific cell types, but recently, a bioinformatics analysis of specifically exported RNA sequences revealed a putative RNA export sequence (Batagov, et al., 2011).

Proteins

Many studies have focused on unravelling the protein content of exosomes. Western blot, fluorescence-activated cell sorting (FACS) analysis of exosome coated beads, trypsin digestion and mass spectrometry have been used in order to identify the proteins transferred within exosomes in the extracellular space. Consistent with their endosomal origin, exosomes do not

contain proteins from the nucleus, mitochondria and endoplasmic reticulum, but mostly proteins of the cell cytosol or the plasma membrane (Mears, et al., 2004). Both ubiquitous and cell specific proteins might be targeted selectively in exosomes. The first, are probably the most abundant proteins involved in exosome biogenesis and include cytosolic proteins, such as tubulin, actin and actin-binding proteins, annexins, proteins of the RAB family, which are involved in intracellular membrane fusions and transport and proteins involved in the biogenesis of MVBs, such as Alix and TSG101 (Théry, et al., 2001). Most exosomes also contain MHC class I molecules (Wolfers, et al., 2001) and heat shock proteins, such as Hsp70 and Hsp90 (Théry, et al., 2001). The most commonly found protein family in exosomes is the family of tetraspanins. Specifically, tetraspaninins CD9, CD63, CD81 and CD82 seem to be one of the most enriched groups in exosomes (Kleijmeer, et al., 1998). Due to their abundancy and frequent expression in exosomes of different cell types, tetraspanins, Alix, flotillin, TSG101 and Rab5b are used as molecular marker to confirm the presence of exosomes experimentally (Vlassov, et al., 2012).

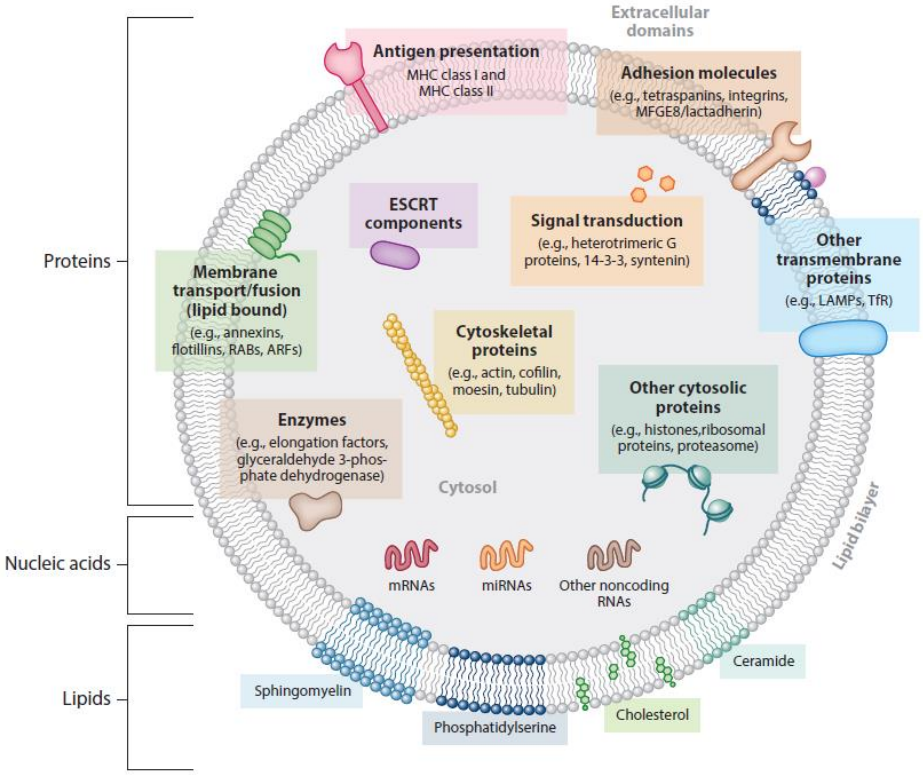

Figure 1.13: General molecular composition of EVs. Exosomes are enclosed by a lipid bilayer and can transfer proteins and nucleic acids from the donor cells in the recipient cells that they target (Colombo, et al., 2014).

1.3.3. The biogenesis of exosomes

The origin of exosomes and the formation of MVBs

Exosomes are formed in the endosomal network, when endocytic vesicles fuse in the plasma membrane to form early endosomes. These early endosomes are then acidified in order to mature into late endosomes. During this process, intraluminal vesicles (ILVs) are accumulated in their lumen forming the multivesicular bodies or MVBs. The MVBs are going to fuse with the lysosome in order to get hydrolysed and their content degraded. However, MVBs that are bearing the tetraspanin CD63, lysosomal-associated membrane proteins LAMP1 and LAMP2 and other molecules avoid lysosomal degradation and form, instead, the late endosomes. Late endosomes can fuse with the plasma membrane and release their content towards the extracellular space. These secreted ILVs are now referred as exosomes (Jaiswal, et al., 2002).

Mechanisms of exosome biogenesis

The endosomal sorting complex required for transport (ESCRT) is a complex composed of approximately thirty proteins organised in four complexes (ESCRT -0, -I, - II and -III). It is until now the best described mechanism for the formation of MVBs and ILVs and it is conserved from yeast to mammals (Hanson & Cashikar, 2012). The recruitment of ESCRT -I and -II is induced by the content of ILVs and early endosomes.

Although the formation of MVBs seems to be ESCRT driven, there has been some evidence that other, ESCRT-independent mechanisms might be involved, since the concomitant inactivation of four proteins of the four ESCRT complexes does not disrupt the formation of the MVBs. CD63 accumulates in the ILVs in the absence of ESCRT and is required for their sorting (Stuffers, et al., 2009). In addition, ESCRT-independent formation of ILVs by inward budding is shown to be induced by two lipid metabolism enzymes that can generate lipids in the limiting membrane of MVBs: neutral sphingomyelinase (nSMase) (Trajkovic, et al., 2008) and phospholipase D2 (Ghossoub, et al., 2014). Therefore, the accumulation of specific proteins within the MVBs may alter the pathway through which the exosomes originate.

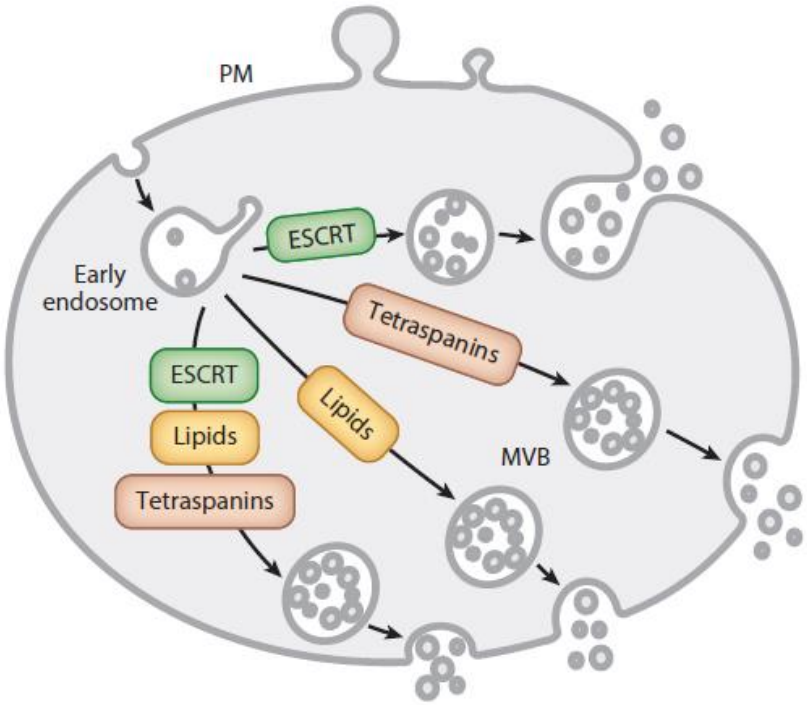

Figure 1.14: Molecular pathways that lead to EV biogenesis (Colombo, et al., 2014)

1.3.4. The secretion of exosomes and their extracellular fate

At the end of the endosomal maturation, MVBs and the enclosed ILVs are situated close to the nucleus. The ILVs are secreted towards the extracellular space, after the MVBs fuse with the plasma membrane. The process of exosome release is accomplished either by the outward exosome and microvesicle budding pathway or by regulated, inducible release that involves several components of the endocytic machinery, including the Rab GTPases, cytoskeleton regulatory proteins, heparanase and SNAREs (Roma-Rodrigues, et al., 2014).

The role of Rab GTPases in exosome secretion

Intracellular vesicular trafficking includes vesicle budding, vesicle and organelle mobility through cytoskeleton interaction and docking of vesicles to target compartment with consequent membrane fusion. These processes are regulated by the Rab family of small GTPases (Kowal, et al., 2014). Their implication in exosome biology was soon identified, as they were among the proteins found in the first proteomic screening of exosomes from dendritic cells (Théry, et al., 2001). Specifically, they were shown to be part of the secretion

machinery, as inhibition of RAB11 in the erythroleukemia cells K562 decreased secretion of TfR and HSC70- bearing exosomes (Savina, et al., 2002), while inhibition of RAB35 impaired PLP-bearing exosome secretion in oli-neu cells (Hsu, et al., 2010). Importantly, in an shRNA-based screen in HeLa cells, inhibition of RAB27A and RAB27B resulted in the most efficient decreased secretion of CD63, CD81 and MHC class II bearing exosomes (Ostrowski, et al., 2010).

The Rab proteins are suggested to regulate exosome secretion by helping the MVBs dock to the plasma membrane. This step is required in order for the two membrane compounds to fuse and for the exosome secretion to be allowed (Fig. 1.15). The main hypothesis for the role of these proteins suggests that RAB11 and RAB35 associate to recycling and early sorting endosomes and RAB27A/B to late endosomal and secretory compartments (Stenmark, 2009).

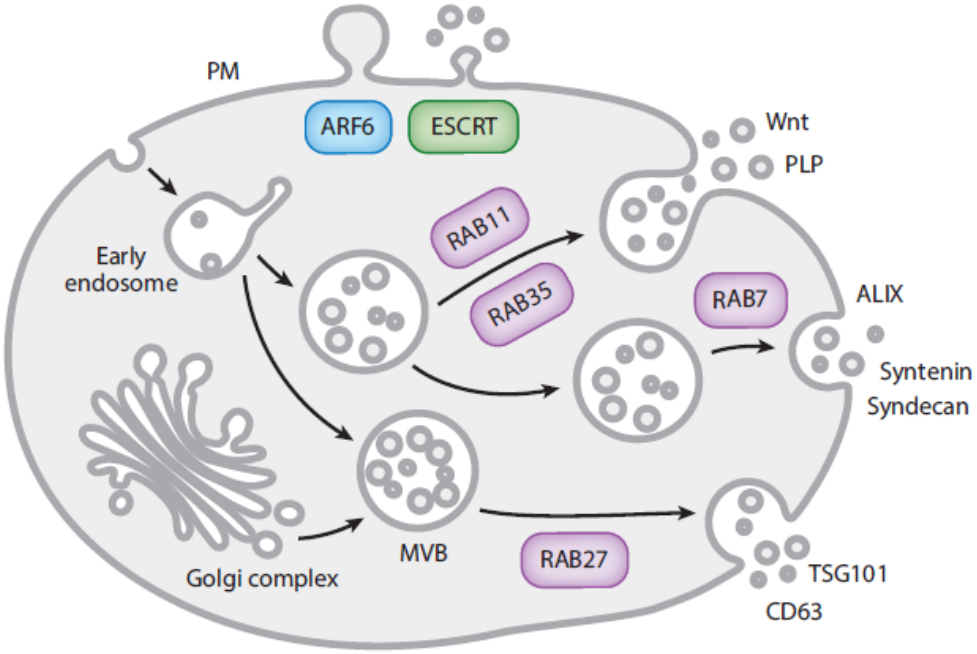

Figure 1.15: Molecular machineries implicated in EV secretion. RAB1, RAB35, RAB7 and RAB27 have been shown to drive exosome secretion at different steps of the endocytic pathway (Colombo, et al., 2014).

Other molecules implicated in exosome secretion

After the initial docking of the membranes of the intracellular compartments, the fusion of the lipid bilayers is performed by the soluble NSF-attachment protein receptor (SNARE)

complexes (Zylbersztejn & Galli, 2011). When SNARE proteins form complexes with SNAPs between two membranes, they mediate membrane fusion between two organelles. The complexes of plasma membrane localised SNAP-23 and lysosomal vesicle-associated membrane protein-8 (VAMP8) in mastocytes (Puri & Roche, 2008) or VAMP7 in epithelial cells (Rao, et al., 2004) and neurotrophils (Logan, et al., 2004) are involved in Ca^{2+} - regulated fusion of secretory lysosomes with the plasma membrane.

To date, it seems that the different SNARE complexes that have been studied mediate the fusion of different MVBs subpopulations within a single cell type and among different cell types. That means that impaired expression of one SNARE protein would alter the secretion of a specific exosome subpopulation and not EV secretion in general (Colombo, et al., 2014).

Uptake of the exosomes by recipient cells and the fate of the exosomes after their release

In order for the EVs to have biological significance and alter the intercellular communication of the cells of their microenvironment, they have to be uptaken by recipient cells upon secretion. Although it is not yet clear how exosomes interact and fuse with target cells, there are three putative mechanisms that are suggested at the moment: (a) fusion of the exosomes with the cellular membrane and release of the exosomal content into the cytoplasm; (b) exosome uptake by endocytosis; (c) receptor regulated uptake depending on the proteins that are presented on the membrane of the recipient cell and their ability to bind exosomes or exosomal proteins (Gajos-Michniewicz, et al., 2014).

There is a large number of studies that describe the interaction of specific receptors on both EVs and the plasma membrane as the first step of the binding of EVs to the cell surface and they include several classical ligand/receptor pairs. For example, DCs that express LFA-1 on their surface can capture ICAM-1 bearing DC-EVs (Segura, et al., 2005). Also, tumour cells capture tumour EVs that contain heparin sulfate proteoglycans (Christianson, et al., 2013) and erythrocyte EVs are captured by macrophages due to the expression of galectin-5 on their surface (Barrès, et al., 2010).

1.3.5. The exosomes as part of the tumour microenvironment and their role in cancer

Normal cells can be transformed to cancer cells following events that can establish major modifications. These modifications can be dictated by the accumulation of mutations and the altered expression of known oncogenes or tumour suppressor genes that lead to uncontrolled growth (Marshall, et al., 2014). In order for a tumour to grow, the initial evasion of growth and apoptotic control should be followed by angiogenesis and metastasis. So, beyond the cell level, the microenvironment of a tumour cell has to follow the major metabolic and gene expression changes that the tumour dictates for its support. The adaptation of the microenvironment can be driven by the interaction with the genetically unstable malignant cells that are constantly releasing EVs with altered protein and nucleic acid cargo. Tumour and stromal cells interact via cell-cell interactions mediated by gap junction channels, paracrine mechanisms and EVs. Interestingly, exosomes do not only mediate intercellular communication within the approximate distance of a solid tumour, but also between tumours and distant cells, as they have the ability to trigger the secretion of growth factors, cytokines, angiopoietic factors and ultimately induce proliferation and favour metastatic events (Zhang & Grizzle, 2014).

More and more studies are focused on the importance of exosomes in cancer biology, since there is growing evidence of the presence of these vesicles in biological fluids of cancer patients and interestingly, the content of cancer cell derived exosomes (CCEs) is increased as the tumour progresses and they provide both anti- and pro- tumourigenic effects (Bang & Thum, 2012). The uptake of CCEs by neighbouring cells seem to be able to regulate and sustain the intratumour heterogeneity, which can result in the alteration of the phenotype of normal cells of the microenvironment of colorectal, lung and prostate cancer cells (Taylor & Gercel-Taylor, 2013).

In addition, exosomes may be regulators of the inter- and intra- communication of cancer cells with immune cells and therefore, they can be implicated in the immunological responses within the tumour microenvironment. The microenvironment of an early tumour is quite similar to an open wound. The immune response at the site involves innate immune and adaptive immune cells and it is the balance of the activation level that will ultimately dictate

whether tumour inflammatory response or anti-tumour immunity will be the reaction of the immune modulators (Grivennikov, et al., 2010). This balance can be regulated by exosomes, as it has been shown that the release of exosomes by several tumours, including pleural malignant mesothelioma and prostate cancer cells, can result in the inhibition of the proliferative response of lymphocytes and natural killer cells (Clayton, 2012). In the same context, exosomes can influence the rate of angiogenesis in the site of a tumour, as they can stimulate the JAK-STAT pathway or deliver angiogenic miRNAs (Gajos-Michniewicz, et al., 2014). Also, EVs released by glioblastoma cells in hypoxic tumour contain angiogenic stimulatory molecules, such as IL-8 and PDGF (Kucharzewska, et al., 2013).

Finally, a significant step of the tumour progression in which exosomes are implicated is tumour cell dissemination and metastasis. More specifically, exosomes seem to interfere with the process of epithelial-to-mesenchymal transition (EMT). In prostate cancer cells released exosomes, proteins that are involved in the formation and pathways of epithelial adherens junctions and cytoskeleton remodelling are found and they are suggested to increase the invasiveness of the tumour (Ramteke, et al., 2015). Moreover, metastatic cells from bladder carcinoma cell lines release exosomes with increased levels of vimentin, casein kinase II and annexin A2 compared to non metastatic cells lines of the same origin, suggesting the role of exosomes in cellular movement and intercellular signalling (Jeppesen, et al., 2014). An interesting observation comes from exosomes secreted by melanoma cells. A study shows that these exosomes are preferentially uptaken by sentinel lymph nodes that in turn recruit free melanoma cells (Hood, et al., 2011). This observation could describe a new role for CCEs, as it shows that exosomes can act by preparing the premetastatic niche at a new anatomical location for the invasion of the cancer cells. Consistent with the above, another study shows that melanoma secreted exosomes enhance vascular leakiness at the premetastatic sites and increase metastatic events of bone marrow cells via the MET receptor kinase (Peinado, et al., 2012).

In conclusion, it becomes clear that CCEs can have a major impact on the metastasis process and can be implicated in several different steps that will finally increase the malignancy of a tumour (Fig. 1.16).

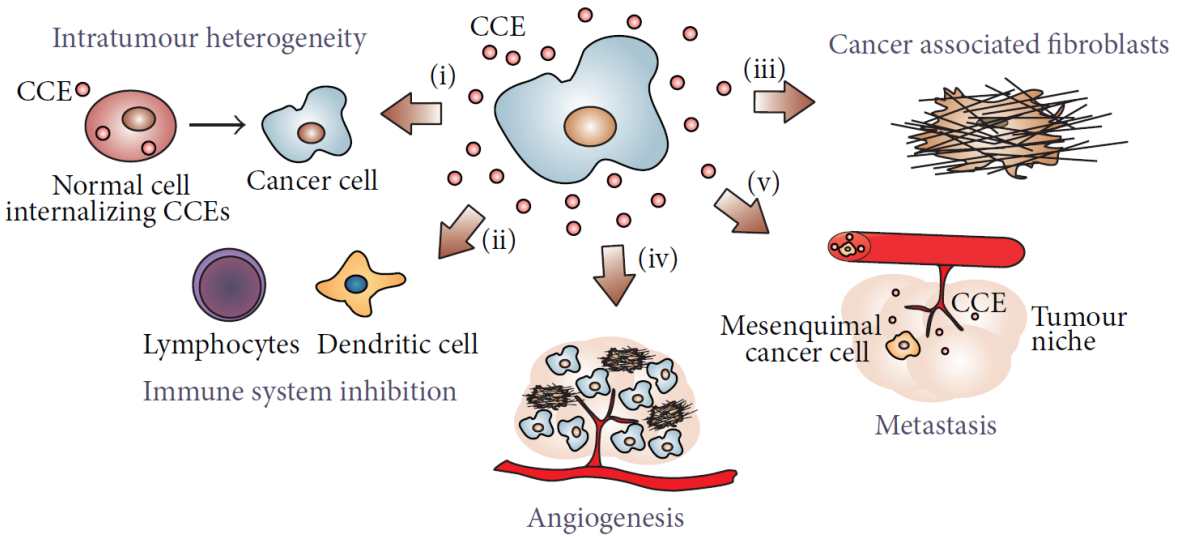

Figure 1.16: The pathways and processes affected by CCEs in the tumour microenvironment. i) CCEs that are released in the tumour microenvironment can target normal cells and modify their phenotype leading to intratumour heterogeneity; ii) the internalisation of CCEs can regulate the anti-tumoural immune response by downregulating the proliferative response of lymphocytes; iii) CCEs can stimulate the differentiation of fibroblasts into cancer associated fibroblasts; iv) CCEs can upregulate the angiogenic process to support the tumour; and v) CCEs can regulate epithelial to mesenchymal transition (EMT) and potentially act in distant locations to prepare he metastatic dissemination (Roma-Rodrigues, et al., 2014).

Extracellular vesicles and cancer

The study of exosomes gained again interest and many groups studied them by isolating them from cell culture supernatants. The secretion of exosomes *in vitro* is based on the presence of MVBs and MVB components in the preparations of extracellular vesicles. There have been references of exosome secretion by epithelial cells (Van Niel, et al., 2001), neurons (Fauré, et al., 2006), Schwann cells (Fevrier, et al., 2004) and tumour cells (Wolfers, et al., 2001). Interestingly, the role of exosomes on tumour biology seems to be quite complicated with multiple levels of coordination, as it is shown that EVs have the potential to transfer tumour antigens to DCs for the efficient induction of anti-tumour immune responses (Wolfers, et al., 2001). Furthermore, exosomes play a role in the metastatic dissemination of tumour cells. They can alter the behaviour of bone marrow progenitor cells and promote their migration to new metastatic sites (Peinado, et al., 2012) and increase the local mobility of tumour cells by communicating with the neighbouring fibroblasts (Luga, et al., 2012). It becomes, therefore,

clearer that exosomes are important regulators of the homeostasis of tumours and tumour microenvironment.

Exosomes in neuroblastoma

In neuroblastoma, exosomes are secreted from the cancer cells, and, although the number of studies focusing on neuroblastoma derived exosomes and their potential roles is increasing, there are still many questions unanswered.

There are a few studies focusing on the protein cargo of exosomes secreted from neuroblastoma cells lines and their oncogenic potential (Marimpietri, et al., 2013; Keerthikumar, et al., 2015; Colletti, et al., 2017). In a 2019 paper, Fonseka *et al.* compare the protein cargo of exosomes secreted by MYCN positive and negative cell lines and they suggest that proteins involved in cell communication and signal transduction are enriched in the exosomes secreted from cells with *MYCN* amplification. They also show that when the MYCN negative neuroblastoma cells SH-SY5Y are treated with exosomes from the *MYCN* amplified cells SK-N-BE2 they observe an increase in their migration and colony formation potential and also increased resistance to doxorubicin induced apoptosis (Fonseka, et al., 2019). However, there is not yet a direct link between specific proteins that could mediate the pro-tumourigenic effects of neuroblastoma secreted exosomes. Also, it is not clear if MYCN can alter this behavior by regulating the molecules that are loaded in the exosomes secreted from neuroblastoma cells.

1.4. Aim of the study

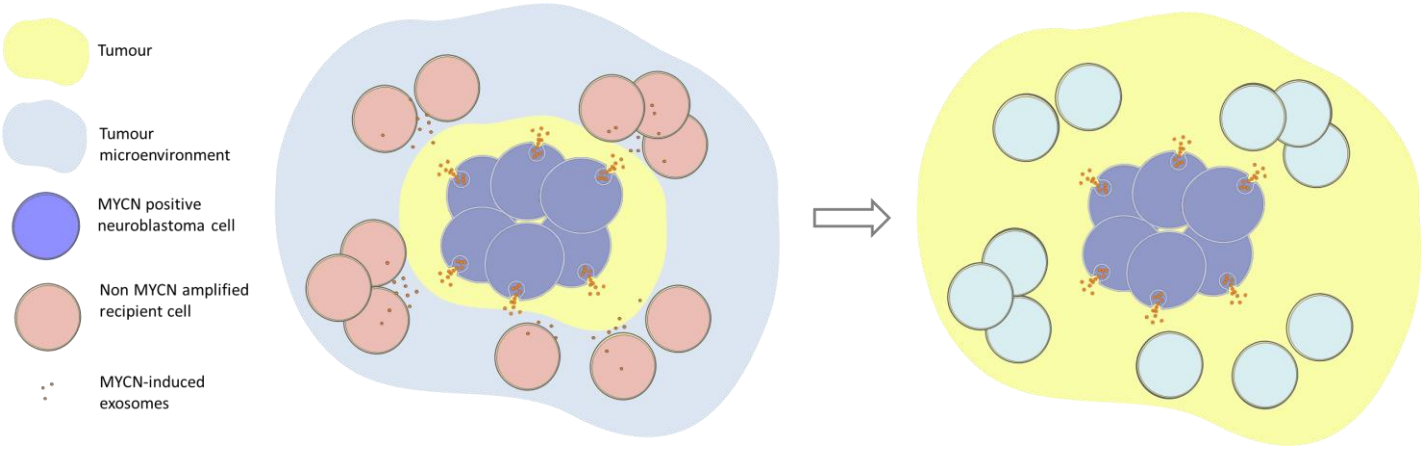

Figure 1.17: Working hypothesis. The MYCN positive neuroblastoma cells within a neuroblastoma tumour secrete exosomes. The protein cargo of the secreted exosomes depends on the MYCN expression background. When the exosomes secreted by MYCN positive neuroblastoma cells are uptaken by cells of the tumour microenvironment, they release their content. The behaviour of the recipient cells is then altered in order to support tumour growth.

The purpose of this investigation is to verify whether proteins contained in exosomes secreted by neuroblastoma cells in a MYCN-dependent manner contribute to tumourigenesis and cancer progression. More specifically, we will:

a. Validate preliminary mass spectrometry data by assessing the presence of MYCN-inducible exosomal proteins in the supernatant of neuroblastoma cell lines.

b. Purify exosomes from MYCN expressing and non-expressing neuroblastoma cells and deliver them to recipient cells in order to investigate whether they affect directly or indirectly their behaviour.

In conclusion, this study aims to determine the role of MYCN in the secretion of physiologically functional exosomes containing proteins that could cause the “conditioning” of recipient cells in the tumour microenvironment. The profiling of exosomes secreted by MYCN positive neuroblastoma cells could lead to the identification of useful biomarkers and new opportunities to uncover vulnerabilities in MYC addicted tumours, such as neuroblastoma.

2. Materials and methods

2.1. Reagents, chemicals, equipment and recipes used for the experiments

Table 2.1: Equipment needed to carry out the experiments

Piece of equipment	**Supplier**
Optima™ XPN 80K - Preparative Ultracentrifuge	Beckman Coulter Life Sciences
Type 70.1 Ti Rotor, Fixed Angle, 12 x 13.5 mL, 70,000 rpm, 450,000 x g	Beckman Coulter Life Sciences
Type 70 Ti Rotor, Fixed Angle, 8 x 39 mL, 70,000 rpm, 504,000 x g	Beckman Coulter Life Sciences
Bottle, with Cap Assembly, Polycarbonate, 26.3 mL, 25 x 89 mm, 1 x 3-1/2 in	Beckman Coulter Life Sciences
Bottle, with Cap Assembly, Polycarbonate, 10.4 mL, 16 x 76 mm	Beckman Coulter Life Sciences
Heraeus™ Megafuge™ 16	Thermo Scientific
ImageStream®X Mk II Imaging Flow Cytometer	Amnis Corporation
Versatile Upright Microscope for Materials Analysis Leica DM4000 M	Leica Microsystems
Microplate reader	BIO-RAD
NanoSight LM10	Malvern Panalytical
Q125 Sonicator	QSONICA Sonicators
X-ray film processor CURIX 60	AGFA Healthcare
Filtropur V50 0.2 μm filter units	Sarstedt
Amersham™ Hyperfilm™ ECL	GE Heathcare
0.4 μm pores PET TC inserts	Sarstedt

Table 2.2: Reagents and chemicals

Reagents and chemicals	Supplier	Cat. number
Acrylamide	National diagnostics	EC-890
Ammonium persulfate (APS)	Fisher Scientific	BP179-25
Avidin, NeutrAvidin HRP conjugate	Molecular Probes	A2664
Bicinchoninic acid (BCA) protein assay kit	Pierce	23225
Bovine serum albumin (BSA)	Sigma Aldrich	A9647-50G
Bromophenol Blue	Fisher Scientific	BP115-25
Casein	Sigma Aldrich	C7078
CellTiter 96® AQueous One Solution Cell Proliferation Assay (MTS)	Promega	G3582
Citric acid	Sigma Aldrich	251275
cOmplete™, Mini, EDTA-free Protease Inhibitor Cocktail	Roche	4693159001
Dimethyl sulfoxide (DMSO)	Fisher Scientific	BP231-100
DMEM, high glucose	GIBCO, Life Technologies	11584486
DNase I, RNase-free	Thermo Scientific	EN0521
Doxycycline hyclate	Sigma Aldrich	D9891
DPX mountant for histology	Sigma Aldrich	O6522
Enhanced chemilumescent Western blotting substrate (ECL)	Pierce	32106
Ethanol	Fisher Chemical	E/0500DF/08
Ethylenediaminetetraacetic Acid (EDTA)	Fisher Scientific	BP166-500
ExoEASY Maxi kit	QIAGEN	76064
Fetal Bovine Serum (FBS)	GIBCO, Life Technologies	11573397
GenElute™ Mammalian Total RNA Miniprep Kit	Sigma Aldrich	RTN70
Geneticin selective antibiotic (G418)	GIBCO, Life Technologies	11811031
Glutaraldehyde	Sigma Aldrich	G5882
Glycerol	Fisher Scientific	BP229-1
Glycine	Fisher Scientific	G-P460/53

Reagents and chemicals	Supplier	Cat. number
Glycolysis cell-based assay kit	Cayman Chemical	600450
Hematoxylin	Sigma Aldrich	H3136
HistoChoice clearing agent	Sigma Aldrich	H2779
Hydrochloric acid (HCl)	Alfa Aesar	87617
Hydrogen peroxide	Fisher Bioreagents	BP2633-500
Hygromycin B	Invitrogen	10453982
Isopropanol	Fisher Bioreagents	BP2618
jetPRIME	Polyplus Transfection	114-01
Latex beads, polystyrene, 0.1 µm mean particle size	Sigma Aldrich	LB1-1ML
Latex beads, sulfate-modified polystyrene, fluorescent orange	Sigma Aldrich	L1528-1ML
Magnesium sulfate	Sigma Aldrich	M2643
Methanol	Fisher Scientific	M/3950/17
N,N,N',N'-Tetramethylethylenediamine (TEMED)	Sigma Aldrich	T9281
NP-40	Alfa Aesar	J60766.AP
Paraformaldehyde	Fisher Chemical	P/0840/53
Penicillin/Streptomycin (Pen/Strep)	GIBCO, Life Technologies	12090216
Phosphatase inhibitor Cocktail	Sigma	P5726
Phosphate Buffered Saline (PBS)	HyClone	SH30256.01
PKH67 Green Fluorescent Cell Linker Kit	Sigma Aldrich	MINI67
Ponceau S	Fisher Scientific	BP103-10
PowerUp™ SYBR™ Green Master Mix	Applied Biosystems	A25742
Sodium bicarbonate	Sigma Aldrich	S5761
Sodium chloride (NaCl)	Fisher Scientific	BP358-1
Sodium deoxycholate	Sigma Aldrich	D6750-25G
Sodium dodecyl sulfate (SDS)	Fisher Scientific	BP166-500
SuperScript™ II Reverse Transcriptase	Invitrogen	18064014
Tris base	Fisher Scientific	BP152-1

Reagents and chemicals	Supplier	Cat. number
Trisodium citrate dihydrate	Sigma Aldrich	S1804
Triton X-100	Fisher Scientific	T/3753/44
Trypan blue	Life Technologies	T10282
Trypsin-EDTA (0.25%)	GIBCO, Life Technologies	25200072
Tween 20	Fisher Scientific	BP335-500
Ultra-0.5 Centrifugal Filter Units	EMD Millipore	UFC510024
Urea	Sigma Aldrich	U5378
Vectashield antifade mounting medium with DAPI	Vector Laboratories	H-1200
β-Merkaptoethanol	Sigma Aldrich	M3148

Table 2.3: Recipes of the solutions used in the experimental procedures

Solution	Recipe
Laemmli Buffer 4X:	8% v/v SDS 10% 40% v/v glycerol 240 mM Tris 0.04% w/v bromophenol – blue H_2O
pHis sample buffer 5X:	250 mM Tris-HCl pH8.8 0.02% bromophenol blue 50% glycerol 50 mM EDTA 500 mM DTT 10% SDS
SDS-PAGE running buffer 5X:	25 mM Trizma base 250 mM glycine 10% w/v SDS Adjust to pH 8.3

Solution	Recipe
Transfer buffer stocking solution 10X:	25 mM Tris base 192 mM Glycine
Transfer buffer working solution 1X:	100 mL transfer buffer 10X 200 mL methanol 700 mL deionized H_2O
Tris-buffered saline (TBS) 10X:	20 mM Trizma base 137 mM NaCl Adjust to pH 7.6
10% resolving gel for Tris-glycine SDS-PAGE gel:	For 5 ml: 1.9 ml H_2O 1.7 ml 30% acrylamide mix 1.3 ml 1.5 M Tris (pH 8.8) 0.05 ml 10% SDS 0.05 ml 10% APS 0.002 ml TEMED
5% stacking gel for Tris-glycine SDS-PAGE gel:	For 1ml: 0.68 ml H_2O 0.17 ml 30% acrylamide mix 0.13 ml 1.5 M Tris (pH 8.8) 0.01 ml 10% SDS 0.01 ml 10% APS 0.001 ml TEMED
RIPA buffer 1X:	50 mM Tris – HCl pH 7.6 150 mM NaCl

Solution	Recipe
	1% v/v NP-40 0.5% w/v sodium deoxycholate 0.1% w/v SDS
Citric acid buffer:	14.7 g Tri-sodium citrate 1.125 g citric acid dH_2O up to 1L Adjust to pH 8.0 Dilute 1:5 with dH_2O before use
Scott's tap water:	20 g $MgSO_4$ 2 g $NaHCO_3$ dH_2O up to 1L

2.2. Cell culture

The human neuroblastoma cell lines SH-EP, SK-N-AS, IMR-32 and KELLY were purchased from ATCC. TET21-N were kindly supplied by Prof. Giovanni Perini. The neuroblastoma cells were cultured in Dulbecco's modified Eagle's medium (DMEM) medium in the presence of 10% fetal bovine serum (FBS) and 100 units/ml Penicillin/Streptomycin. The cells were cultured in a 5% CO_2 humidified incubator at 37°C. For the isolation of exosomes from the supernatant, the cells were cultured in exosome depleted medium. The TET21-N cells were cultured under selection for the plasmids of the tet-off system in the presence of 0.2 mg/ml G-418 and 0.15 mg/ml Hygromycin B. For the silencing of MYCN, the cells were cultured in the presence of 0.1-1.0 μg/ml doxycycline.

2.2.1. Harvesting and maintenance of cell lines

The media of cells grown in culture flasks or dishes was removed and the cells were washed briefly one time in sterile phosphate buffered saline (PBS) 1X solution. PBS was removed and 1 ml 0.25% Trypsin-EDTA 1X was added to detach the cells. The culture flasks or dishes were incubated in a 5% CO_2 humidified incubator at 37°C until adherent cells became completely

detached. Complete medium was added to the cells and all cells were collected or seeded in a new flask for the maintenance of the cell line.

2.2.2. Freezing and thawing of cells

The cells were trypsinised and centrifuged at 1,200 rpm for 5 min. The supernatant was discarded and the cell pellet was resuspended in 1 ml cell culture medium. The cell suspension was mixed with 1 ml freezing medium consisting of 50% cell culture medium, 40% FBS and 10% dimethyl sulfoxide (DMSO) and transferred in cryovials. The vials were then transferred into an isopropanol-filled freezing container and stored at -80°C for approximately 24 h before being transferred to the liquid nitrogen storage tanks for long term storage.

When the use of cells was necessary, a cryovial of frozen cells was thawed in a 37°C water bath rapidly. The cells were then transferred to a 15 ml centrifuge tube and centrifuged at 1,200 rpm for 5 min at room temperature (RT) to remove the DMSO. Cells were resuspended in complete culture medium, plated in a suitable culture flask or dish and maintained in a 5% CO_2 humidified incubator at 37°C overnight before fresh medium was replaced on the next day.

2.2.3. Preparation of exosome depleted media

To produce exosome depleted medium, DMEM supplemented with 20% FBS was ultracentrifuged at 100,000 x g for 20 h at 4°C for the precipitation and removal of the exosomes contained in the FBS. The supernatant was collected and sterilised with the use of a vacuum filtration unit with a 0.22 μm polyethersulfone (PES) filter. The sterilised medium was then diluted with equal volume of DMEM supplemented with 200 units/ml Penicillin/Streptomycin. After the dilution, the exosome depleted medium contained 10% FBS and 100 units/ml Penicillin/Streptomycin.

2.3. Isolation of exosomes from cell culture supernatant media

2.3.1. Preparation of conditioned media

For the preparation of the conditioned media used for the exosome isolation, cells were seeded in T175 flasks and cultured until the density reached 60-70% confluence. The cells

were then washed with PBS 1X and each flask was supplemented with exosome depleted media and cultured for 48 h.

2.3.2. Exosome precipitation

The conditioned medium was collected and centrifuged at 3,000 x g for 30 min and 100,000 x g for 70 min. The final pellet was resuspended in PBS 1X and ultracentrifuged again at 100,000 x g for 70 min. The pellet was resuspended in PBS 1X and stored at -80^{o}C.

2.3.3. Exosome quantification

The protein concentration of the isolated exosomes was quantified with the bicinchoninic acid (BCA) assay after the addition of urea at a final concentration of 2.3 M. Urea was used as a chaotropic agent, in order to disrupt the membranes of the exosomes.

2.4. Exosome isolation from plasma samples

Frozen plasma samples from 10 patients with *MYCN* amplified neuroblastoma, 10 patients with *MYCN* non amplified neuroblastoma and 10 non-neuroblastoma patients were provided to us by the BIT Gaslini Biobank, Genoa, Italy.

For the isolation of exosomes from neuroblastoma patients' plasma samples the Qiagen exoEasy maxi kit was used according to manufacturer's instructions. Briefly, 500 μl of plasma were mixed with equal volume of XBP buffer. The sample/XBP mixtures were loaded onto the exoEasy spin column and centrifuged at 500 x g for 1 min. The flow through was discarded. 10 ml XWP buffer were added and the column was centrifuged at 3,000 x g for 5 min to remove residual buffer from the column. The flow through was discarded. The column was transferred in a clean collection tube. 400 μl of XE buffer were added to the membrane, incubated for 1 min and centrifuged at 500 x g for 5 min to collect the eluate. The eluate was re-applied on the column, incubated for 1 min and centrifuged at 5,000 x g for 5 min to collect the eluate and transfer to an appropriate tube. All the buffers used were supplemented with protease inhibitors cocktail.

To concentrate the final eluate, the preparation was loaded onto 100 kDa NMW ultrafiltration units and centrifuged at 14,000 x g for 10min. The filter was then reversed and centrifuged at 2,000 x g for 2 min. The final eluate was stored at -80^{o}C.

2.5. Staining of exosomes with the PKH67 dye

For the staining of exosomes, the PKH67 membrane specific dye was used. The exosome preparations were transferred in the 8.9 ml OptiSeal tubes and balanced with PBS 1X. The preparations were ultracentrifuged in the Ty70.1Ti rotor at 100,000 x g at 4^{o}C for 70 min. The exosome pellet was resuspended in 200 μl Diluent C, which is an iso-osmotic for mammalian cells and contains no detergents or organic solvents, but also lacks physiologic salts and buffers. Separately, 0.8 μl of PKH67 dye were mixed with 200 μl Diluent C. The solutions were mixed and incubated at RT for 4 min. The reaction was stopped with equal volume (400 μl) of bovine serum albumin (BSA) 1% in PBS 1X. The exosomes were ultracentrifuged at 100,000 x g at 4^{o}C for 70 min. The final pellet was resuspended in PBS 1X.

2.6. ImageStream flow cytometry

The samples were acquired on an ImageStream^{X} Mk II imaging cytometer, 60X magnification with low flow rate/high sensitivity without EDF using the INSPIRE software. The instrument and INSPIRE software were set up as follows: channel 01 (bright field) and channel 06 (scattering channel), plus required fluorescence channels. The lasers 488 and 745 were activated for fluorescence and side-scatter, respectively. For simple enumeration of pre-prepared microparticles samples, the acquisition cut-off is set to 10,000. Other parameters, such us diameter and perimeter were determined by addition to the features list, after adjusting the mask in channel 01 to fit tightly around the event.

2.7. Size distribution analysis with nanoparticle tracking analysis (NTA)

The analysis of the size distribution of the particles isolated with our exosome isolation protocol was performed with dynamic light scattering. The principle of this technique is based

on the fact that particles and molecules that are in Brownian motion (a constant random thermal motion) will diffuse at a speed that is directly related to their size, with smaller particles diffusing faster than larger particles. The diffusion speed is measured after illuminating the particles with a laser. In addition, NTA allows the visualisation of the particles in suspension due to a camera mounted on a microscope. Therefore, NTA analysis allows the determination of the particles' size distribution and the quantification of the number of particles that come within the camera's field of view. For the NTA analysis, a certain volume of particles in suspension was delivered with a syringe into the NTA chamber and then analysed under the microscope. The results are recorded in a video file.

2.8. Transmission electron microscopy (TEM)

2.8.1. Fixation of the exosomes

The exosomes that were resuspended in PBS were mixed with equal volume of paraformaldehyde (PFA) 4% so that PFA reached the final concentration of 2%. glutaraldehyde was added to a final concentration of 1%.

2.8.2. Negative staining of exosomes

The fixed exosomes were mixed with 1% potasium phosphotungstate (K-PTA) and a drop of this mixture was placed onto a carbon coated EM grid that has been glow discharged for 20 sec. The mixture was left for 1 min and then removed almost completely with a filter paper.

2.9. Protein isolation and quantification

For the isolation of proteins from whole cell lysates, cells were trypsinised, pelleted with centrifugation at 1,200 rpm for 5 min, washed with PBS 1X and pelleted again. The final pellets were resuspended in RIPA buffer supplemented with phosphatase inhibitors and protease inhibitors cocktail. The cells were vortexed thoroughly, incubated with the buffer on ice for 30 min and then centrifuged at 14,000 rpm at 4^{o}C for 20 min. The supernatant was transferred in a new tube and stored at -80^{o}C. The concentration of the proteins in the protein lysates was determined with the BCA assay. Briefly, 10 μl of protein extracts were added in 200 μl of

BCA Working Reagent, vortexed thoroughly and incubated at 37°C for 30 min. After that, the reaction was shared in 2 wells of a 96-well plate (100 μl in each) and the absorption was assayed in a plate spectrophotometer at the wavelength of 562 nm. The measurements were compared with that of BSA dilutions with defined concentrations re-suspended in BCA Working Reagent with the same ratio to generate a standard curve (Fig. 2.1).

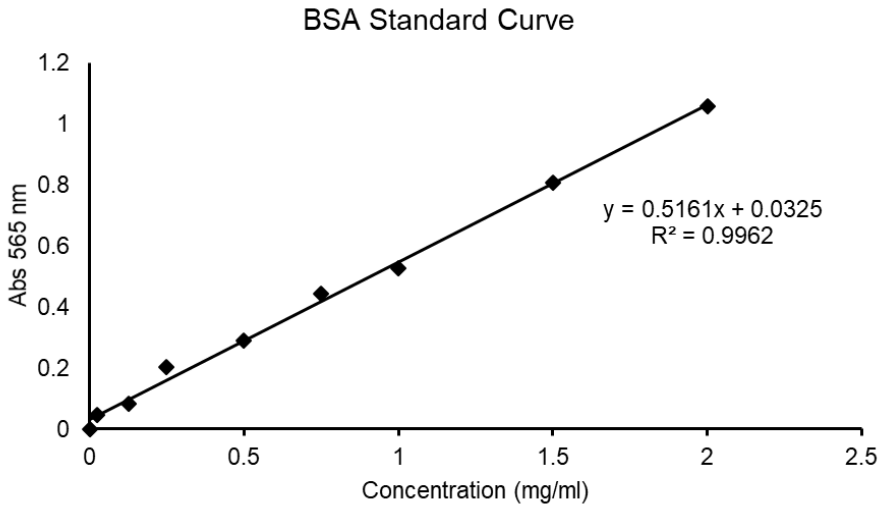

Figure 2.1: BSA standard curve in BCA used for the quantification of protein lysates concentration.

2.10. Western blot analysis

Equal amounts of proteins were separated by electrophoresis in sodium dodecyl sulfate polyacrylamide gels (SDS-PAGE). The proteins that were separated on the gels were transferred on nitrocellulose membranes with wet transfer with 300 mA for 1h at 4°C. The membranes were then blocked with 5% milk in tris-buffered saline (TBS) with 0.1% Tween-20 for 1h at RT. The membranes were probed over night at 4°C with primary antibodies against the proteins of interest. After washing with TBS 0.1% Tween-20 3 times for 5 min at RT, the membranes were incubated with horseradish peroxidase (HRP)-conjugated secondary antibodies for 1h at RT. The membranes were washed with TBS 0.1% Tween-20 3 times for 5 min at RT and incubated with enhanced chemilumenescent (ECL) substrate. The protein bands were visualized after exposure and developing of x-ray films in the dark.

2.10.1. Western blot for phospho-histidine

For phosphohistidine analysis with Western blot, equal number of cells were lysed directly with 2X pHis sample buffer, incubated on ice and sonicated for 20 sec at 35% amplitude to disrupt cells and sheer DNA. The lysates were centrifuged at 10,000 x g for 15 min at 4^{o}C and the supernatants were collected. Fresh lysates were resolved immediately with SDS-PAGE at 4^{o}C in pre-chilled running buffer and with a modified stacking gel, pH 8.8 and 10% resolving gel, pH 8.8. Transfer was carried out at 4^{o}C for 1h at 300mA. The nitrocellulose membranes were blocked in casein blocking buffer containing 0.1% casein in PBS 1X, pH 8.8. The membranes were incubated with primary antibodies against N1 or N3 histidine phosphorylation diluted in casein blocking buffer with 0.1% Tween-20 o/n at 4^{o}C. The membranes were washed with TBS 0.1% Tween-20 pH 8.8 3 times for 15 min each at 4^{o}C. The membranes were then incubated with HRP-conjugated secondary antibodies diluted casein blocking buffer with 0.1% Tween-20 for 1h. The membranes were washed with TBS 0.1% Tween-20 3 times for 5 min at and incubated with ECL substrate. The protein bands were visualized after exposure and developing of films in the dark.

Table 2.4: List of antibodies used for Western blot

Antibody	Host	Dilution	Supplier	Cat. number
anti-Actin	Goat	1:1,000	Santa Cruz	sc-1616
anti-AHCY (SAHH)	Mouse	1:500	Abnova	H00000191-M07A
anti-Aldolase A	Rabbit	1:1,000	Cell Signaling	8060
anti-CD63	Mouse	1:200	Santa Cruz	sc-5275
anti-CD71 (Tranferrin 1)	Rabbit	1:200	Santa Cruz	sc-9099
anti-Clusterin	Rabbit	1:200	Santa Cruz	sc-8354
anti-eEF2	Rabbit	1:1,000	Cell Signaling	2332
anti-Galectin-3BP	Goat	1:1,000	R&D Systems	AF2226
anti-GAPDH	Rabbit	1:1,000	Cell Signaling	5174S
anti-Glypican 1	Rabbit	1:500	Invitrogen	PA5-24972
anti-Goat HRP	Donkey	1:10,000	Santa Cruz	sc-2020
anti-Hexokinase I	Rabbit	1:1,000	Cell Signaling	2024S
anti-Hexokinase II	Rabbit	1:1,000	Cell Signaling	2867S

Antibody	Host	Dilution	Supplier	Cat. number
anti-LHPP	Rabbit	0.4 μg/ml	Novus Biologicals	NBP1-83273
anti-Mouse HRP	Goat	1:10,000	Santa Cruz	sc-2031
anti-MYCN	Mouse	1:200	Santa Cruz	sc-53993
anti-N1-phosphohistidine	Rabbit	0.5 μg/ml	Merck Millipore	MABS1330
anti-N1-phosphohistidine	Rabbit	0.5 μg/ml	Merck Millipore	MABS1341
anti-N3-phosphohistidine	Rabbit	0.5 μg/ml	Merck Millipore	MABS1352
anti-N3-phosphohistidine	Rabbit	0.5 μg/ml	Merck Millipore	MABS1351
anti-NME1/NDKA	Rabbit	1:1,000	New England Biolabs	3345S
anti-NME2	Rabbit	1:1,000	Abcam	ab131329
anti-PFKP	Rabbit	1:1,000	Cell Signaling	8164S
anti-PKM1/2	Rabbit	1:1,000	Cell Signaling	3190S
anti-PKM2	Rabbit	1:1,000	Cell Signaling	4053S
anti-Rabbit HRP	Donkey	1:10,000	Santa Cruz	sc-2313
anti-Rabbit IgG HRP	Goat	1:2,000	Cell Signaling	7074S
anti-Rib. L10a	Mouse	1:500	Santa Cruz	sc-100827

2.11. Kaplan-Meier survival curves

For the generation of the Kaplan-Meier survival curves the R2: Genomics Analysis and Visualization Platform was used (http://r2.amc.nl). The RNA sequencing expression data from the Kocak (Kocak, et al., 2013) and Sequencing Quality Control Consortium (SEQC) (Zhang, et al., 2015) cohorts found on the platform were used to correlate gene expression with event-free survival probability in neuroblastoma patients.

2.12. Cell density

To determine the total number of cells in culture the cells were counted using a Neubauer hemocytometer after trypsinisation. 10 μl of cell suspension were placed under a glass coverslip on the hemocytometer. Using a microscope with a 40X magnification lens the cells

in 16 corner squares were counted until all 4 sets of 16 corners were counted. The cell number per ml of cell suspension was determined as the average of cell count from each of the sets of 16 corner squares multiplied by 10^4.

2.13. MTS proliferation assay

To evaluate the number of viable cells in proliferation, we used a colorimetric method that is based on the bioreduction of MTS into a formazan product that is soluble in tissue culture medium. For the MTS assay, 2,000 SH-EP cells were seeded in each well of a 96-well plate and incubated overnight in a 5% CO_2 humidified incubator at 37°C. Exosomes were added to the cells to a final concentration of 100 μg/ml in a total volume of 100 μl. The cells were treated with the exosomes for 24 and 48 h. 20 μl of MTS/PMS solution were added to the cells and the cells were incubated for 4 h at 37 °C. The absorbance was measured at 490 nm.

2.14. Glycolysis assay

The assay is based on the production of L-lactate that is secreted by glycolytically active cells. In this assay lactate dehydrogenase catalyses the reaction between NAD^+ and lactate yielding pyruvate and NADH. The NADH directly reduces a tetrazolium salt (INT) to a coloured formazan which absorbs between 490 and 520 nm. The quantity of formazan produced is proportional to the lactate in the culture media and is thus an indirect measurement of glycolysis. For the glycolysis assay, 2,000 SH-EP cells were seeded in each well of a 96-well plate and incubated overnight in a 5% CO_2 humidified incubator at 37°C. The glycolytic activity of the cells was measured 24 h after treatment with 100 μg/ml exosomes isolated from TET21-N cells treated with or without doxycycline. After the treatment, the cell culture supernatant was centrifuged at 1,200 rpm for 5 min. In a clear 96-well plate, 90 μl of Assay Buffer were transferred to each well. 10 μl of L-lactate standards or cell supernatants were added to corresponding wells of the new plate. 100 μl of Reaction Solution were added and the reaction was incubated for 30 min at RT with gentle shaking. The absorbance was measured at 490 nm.

2.15. Immunofluorescence (IF)

2.15.1. Treatment of cells and staining

The cells were cultured on coverslips or in microwells. The cells were fixed in 4% PFA for 10 min at RT. After washing with PBS 1X for 3 times, the cells were permeabilised with 0.5% Triton X-100 in PBS 1X for 5 min at RT. After washing with PBS 1X for 3 times, nonspecific sites were blocked with 5% BSA in PBS 1X for 1 h at RT. The cells were incubated with the primary antibody diluted in 3% BSA in PBS 1X o/n at 4^{o}C or for 1 h at 37^{o}C. After washing with PBS 1X for 3 times, the cells were incubated with the secondary antibody diluted in BSA 1% in PBS 1X for 1 h at RT. One drop of Vectashield antifade mounting medium with DAPI was added to each sample. The samples were observed with the Leica DM4000 microscope.

For the study of AKT phosphorylation, SH-EP cells were starved o/n with DMEM 0% FBS for the levels of p-AKT to drop. The next day, the cells were treated with exosomes, fixed and stained as described above.

2.15.2. Quantification of cell fluorescence using the ImageJ software

To quantify the intensity of immunofluorescence in whole cells (cytoplasmic proteins), each cell was gated using the polygon tool of ImageJ. From the “Analyse” menu, “Measure” is selected. The same area gated around the cells is transferred to an area on the background and measured as well.

To quantify the intensity of immunofluorescence in nuclei (nuclear proteins), a mask selecting each nucleus of each image was created in the ImageJ as follows:

The picture with the merge colours (staining and DAPI) was split into the different channels. The nuclei were the selected on the DAPI channel by following the Process → Binary → Make Binary and Process → Binary → Fill Holes commands.

To analyse the particles, the command Analyze → Analyze Particles was followed and the setting were set as 0-Infinity; Circularity 0-1; Show: Overlay Outlines; Add to Manager; In Situ Show.

Then the green (staining) channel was selected and the Image → Overlay → From ROI Manager was selected. The measurements of the intensity were obtained by selecting

"Measure" on the ROI manager. A measurement of a circle with the same size as the nuclei was taken on each picture for the background intensity

The corrected cell florescence was calculated as follows:

Corrected intensity = Mean Fluorescence of the cell – Mean Fluorescence of the background

Table 2.5: List of antibodies used for IF

Antibody	Host	Dilution	Supplier	Cat. number
anti-phospho-AKT (Ser473)	Rabbit	1:25	Cell Signaling	9271
anti-c-MYC	Rabbit	1:800	Cell Signaling	5605
anti-phospho-histone H3 (Thr11)	Rabbit	1:100	Abcam	ab5168
anti-rabbit FITC	Donkey	1:200	Jackson Immunoresearch	711-095-152
anti-rabbit Alexa Fluor 594	Donkey	1:200	Jackson Immunoresearch	711-585-152

2.16. Immunohistochemistry (IHC)

Neuroblastoma tumour sections from the TH-MYCN transgenic mouse model were kindly provided by Prof. Louis Chesler from the Institute of Cancer Research. The sections were PFA fixed and paraffin embedded.

2.16.1. Dewax and rehydration

To dewax and rehydrate the tumour sections, the samples were incubated in HistoChoice clearing agent to remove the wax and then in 100% EtOH, 90% EtOH, 70% EtOH and 50% EtOH. Finally, the sections were incubated in dH_2O twice for 5 min.

2.16.2. Antigen unmasking

The slides were heated submersed in 1X citrate unmasking solution in a microwave until boiling was initiated, followed with 20 min simmering in the microwave and 20 min cooling. The sections were washed twice in dH_2O and the endogenous peroxidase was removed with

incubation in 3% H_2O_2 in dH_2O for 20 min at RT. The sections were washed once in dH_2O and twice in PBS 1X.

2.16.3. Staining for MYCN and c-MYC

The sections were incubated with mouse on mouse (M.O.M.) mouse IgG blocking reagent for 1 h at RT. After the blocking, the sections were washed in PBS 1X and incubated for 5 min in working solution of M.O.M. diluent. The excess of diluent was removed and the sections were incubated with mouse anti-MYCN or anti-c-MYC primary antibodies diluted in blocking buffer 1:10 in PBS 1X o/n at 4°C. The sections were washed in PBS 1X twice for 2 min and then incubated with working solution of M.O.M. biotinylated anti-mouse IgG reagent for 10 min. Finally, the slides were washed twice in PBS 1X for 2 min and incubated with Avidin, NeutrAvidin HRP conjugate diluted 1:1,000 in PBS for 2 h at RT.

2.16.4. Staining for phospho-AKT (Ser473)

The sections were incubated for 20 min with 2.5% normal horse blocking serum. The primary antibody was diluted in 2.5% normal horse serum and applied on the sections for 1 h at RT. The sections were washed for 5 min in PBS 1X and incubated with ImmPRESS reagent for 30 min. The sections were washed in PBS 1X twice for 5 min.

2.16.5. Development using ImmPACT™ DAB Substrate

1 drop of ImmPACT DAB chromogen was diluted in 1 ml of ImmPACT DAB diluent and applied on the sections for 2-10 min until desired colour intensity was developed. The sections were washed for 5 min in dH_2O.

2.16.6. Hematoxylin counter staining

After the DAB visualisation, the sections were incubated in hematoxylin for 3 min. The excess hematoxylin was removed with several washes in tap water and with a final wash into 1% acidified alcohol for 3 min. The sections were submersed into Scott's tap water for 3 min followed with washing with tap water. Finally, the sections were dehydrated with incubation in 50% EtOH, 70% EtOH, 90% EtOH, 100% EtOH and HistoChoice clearing agent and mounted with a glass coverslip using one drop of DPX mountant.

Table 2.6: List of antibodies used for IHC

Antibody/Reagent	Host	Dilution	Supplier	Cat. number
anti-c-MYC	Mouse	1:50	Santa Cruz	sc-40
anti-MYCN	Mouse	1:100	Calbiochem	OP13
anti-phospho-AKT (Ser473)	Rabbit	1:200	LifeSpan Biosciences	LS-B1183
Mouse on Mouse (M.O.M.) basic kit	-	-	Vector Laboratories	BMK-2202
ImmPRESS HRP anti-rabbit IgG (Peroxidase)	-	-	Vector Laboratories	MP-7401
ImmPACT DAB peroxidase substrate	-	-	Vector Laboratories	SK-4105

2.17. siRNA mediated knock down

Table 2.7: List of siRNAs

siRNA	Supplier	Cat. number	Oligo or cDNA target sequence
PKM 1	Sigma Aldrich	-	CGUGGAUGAUGGGCUUAUU[dT][dT] AAUAAGCCCAUCAUCCACG[dT][dT]
PKM 2	Sigma Aldrich	EHU147561	CATTGATTCACCACCCATCACAGCCCGGAACACTGGCATCATC TGTACCATTGGCCCAGCTTCCCGATCAGTGGAGACGTTGAAGG AGATGATTAAGTCTGGAATGAATGTGGCTCGTCTGAACTTCTC TCATGGAACTCATGAGTACCATGCGGAGACCATCAAGAATGTG CGCACAGCCACGGAAAGCTTTGCTTCTGACCCCATCCTCTACC GGCCCGTTGCTGTGGCTCTAGACACTAAAGGACCTGAGATCCG AACTGGGCTCATCAAGGGCAGCGGCACTGCAGAGGTGGAGCTG AAGAAGGGAGCCACTCTCAAAATCACGCTGGATAACGCCTACA TGGAAAAGTGTGACGAGAACATCCTGTGGCTGGACTACAAGAA CATCTGCAAGGTGGTGGAAGTGGGCAGCAAGATCTACG
rLuc	Sigma Aldrich	EHURLUC	GATAACTGGTCCGCAGTGGTGGGCCAGATGTAAACAAATGAAT GTTCTTGATTCATTTATTAATTATTATGATTCAGAAAAACATG CAGAAAATGCTGTTATTTTTTTACATGGTAACGCGGCCTCTTC TTATTTATGGCGACATGTTGTGCCACATATTGAGCCAGTAGCG CGGTGTATTATACCAGACCTTATTGGTATGGGCAAATCAGGCA AATCTGGTAATGGTTCTTATAGGTTACTTGATCATTACAAATA TCTTACTGCATGGTTTGAACTTCTTAATTTACCAAAGAAGATC ATTTTTGTCGGCCATGATTGGGGTGCTTGTTTGGCATTTCATT ATAGCTATGAGCATCAAGATAAGATCAAAGCAATAGTTCACGC TGAAAGTGTAGTAGATGTGATTGAATCATGGGATGAATGG

TET21-N cells were transfected using the transfection reagent jetPRIME with 50 μM siRNAs targeting the gene of interest or rLuc as a control. 48 h after the transfections, the cells were collected and equal numbers of cells were seeded on tissue culture inserts with 0.4 μm pores

for co-culture with SH-EP cells. The remaining cells were used for protein analysis to confirm the downregulation of the gene targeted by the siRNA.

2.18. CD63 and PKM2 overexpression

The CD63-pEGFP C2 and pEGFP-C1-PKM2 plasmids were purchased from Addgene and transfected in TET21-N cells with the jetPRIME transfection reagent.

Table 2.8: List of plasmids

Plasmid	Supplier	Cat. Number
CD63-pEGFP C2	Addgene	62964
pEGFP-C1-PKM2	Addgene	64698

2.19. RNA isolation

Total RNA was extracted from the cells using the GenElute™ Mammalian Total RNA Miniprep Kit according to the manufacturer's guidelines. Briefly, the cells were collected, washed with PBS 1X and centrifuged at 1,500 rpm for 5 min. The cell pellets were resuspended in Lysis buffer with β-merhaptoethanol and loaded onto a blue filter column to remove cellular debris and shear DNA. The samples were centrifuged at 12,000 x g for 2 min and the column was discarded. 250 μl ethanol 70% was added in the flow through and the lysate/ethanol mixture was loaded onto a red binding column and centrifuged at maximum speed for 15 sec. The flow through was discarded and 500 μl of Wash Solution 1 were added on the column and centrifuged at maximum speed for 15 sec. The column was transferred into a fresh collection tube. 500 μl of Wash Solution 2 were added on the column and centrifuged at maximum speed for 15 sec. The flow through was discarded. 500 μl of Wash Solution 2 were added on the column and centrifuged at maximum speed for 2min. The flow through was discarded and the column was centrifuged once more at maximum speed for 1 min to dry. The column was transferred in a fresh tube. 50 μl of Elute Solution were added on each column and the columns were centrifuged at max speed for 1 min. The RNAs were collected and stored at -80^{o}C.

2.20. DNase treatment of total RNA extracts

To eliminate possible contamination of genomic DNA in the RNA extracts, the RNAs were treated with RNase-free DNase I. The reaction was set as follows:

RNA:	1 μg
10X DNase Buffer:	1 μl
DNase (1 u/μl):	1 μl
RNase/DNase-free H_2O:	To a final volume of 10 μl

The reaction was incubated at 37°C for 30 min. To deactivate the enzyme, 1 μl of EDTA 50 mM was added and the RNAs were incubated at 65°C for 10 min.

2.21. Reverse transcription

RNA was reverse transcribed into cDNA using the SuperScript™ II Reverse Transcriptase (RT). The reaction was set as follows:

Random primers (10 mM):	1 μl
DNase treated RNA:	0.5 μg
dNTPs (10 mM each):	1 μl
H_2O:	To a final volume of 12 μl

The reaction was incubated at 65°C for 5 min and the tubes were immediately transferred on ice. In each tube we added:

5X First-Strand Buffer:	4 μl
0.1 M DTT:	2 μl

The reaction was incubated at 25°C for 2 min. After that, 1 μl (200 units) of SuperScript™ II RT was added to each tube and pipetted well. The reaction was incubated at 25°C for 10 min and then 42°C for 50 min. To inactivate the reaction, the samples were heated at 70°C for 15 min.

As a negative control for contamination with genomic DNA, equal amounts of DNase treated RNA were processed in the same way but in the absence of RT.

2.22. Quantitative polymerase chain reaction (qPCR)

The cDNA products from the RT reaction were diluted 1:10 in DNase/RNase-free H_2O. 4 μl of the diluted cDNA were used as a template for the qPCR. The reaction was set as follows:

5X PowerUp™ SYBR™ Green Master Mix:	5 μl
Forward primer (10 mM):	0.375 μl
Reverse primer (10 mM):	0.375 μl
H_2O:	0.25 μl
cDNA:	4 μl

Each sample was run in triplicate in a 96 well microtiter plate. The qPCR was carried out by pre-incubating the samples for 2 min at 50°C and at 95°C for 10 min. The samples were then subjected to 40 cycles of amplification, constituted of a first step of incubation at 95°C for 15 sec, followed by a second step of incubation at 62°C for 1 min. Actin was used as a housekeeping gene. Relative quantities were calculated using the comparative Ct method (ΔΔCt).

Table 2.9: List of primers

Target	Primer	Sequence	Reference
c-MYC	Forward	5′ TCTTGACATTCTCCTCGGTG 3′	(Liu, et al., 2013)
	Reverse	5′ TACCCTCTCAACGACAGCAG 3′	
Cyclin D1	Forward	5′ CTTCCTCTCCAAAATGCCAG 3′	(Pavithra, et al., 2007)
	Reverse	5′ AGAGATGGAAGGGGGAAAGA 3′	
Actin	Forward	5′ CACACTGTGCCCATCTAC 3′	Designed previously in the laboratory
	Reverse	5′ CAGCGGAACCGCTCATTG 3′	

2.23. Statistical analysis using the IBM SPSS software

All experiments were carried out in at least three independent biological replicates. Independent or paired t test was used to test foe equal means of two samples. T test was selected due to normally distributed data across treatments. The null hypothesis of t test asserts that the means of two samples are equal. If the test for equality of means reports a significant difference (p <0.05) between the two samples means, then the null hypothesis could be rejected. Differences were considered significant when the p values obtained were ≤ 0.05. The statistical analysis was performed using the IBM SPSS software.

3. Results I: MYCN regulates the protein cargo of exosomes in neuroblastoma

3.1. Introduction

Preliminary data generated previously in our lab in collaboration with the lab of Prof. Giuseppe Palmisano in the University of Sao Paulo demonstrate that exosomes produced by neuroblastoma cells artificially overexpressing MYCN are enriched for distinct classes of proteins. More specifically, mass spectrometry analysis of exosomes isolated from neuroblastoma cells artificially overexpressing MYCN reveals that 111 proteins are upregulated and 41 proteins are downregulated compared with the exosomes of the same cell line when MYCN is not overexpressed (Fig. 3.1A, Appendix). The bioinformatics pathway analysis suggests that glycolytic enzymes, ribosomal proteins and extracellular matrix (ECM) interaction proteins are the functional groups of exosomal proteins that are mostly enriched in the exosomes of MYCN expressing neuroblastoma cells (Fig. 3.1B).

The results of this screening suggest that MYCN may play a role in regulating the protein cargo of exosomes in neuroblastoma. That is not surprising, as MYC proteins are known to modify the tumour microenvironment via the regulation of growth factors, cytokines and immune checkpoints regulators (Kang, et al., 2008; Song, et al., 2007; Casey, et al., 2018). The ability of MYC oncoproteins to act in a non-cell autonomous way might be critical for aggressive neuroblastomas, as 40% of the neuroblastoma tumours with *MYCN* amplification show heterogeneous (focal) amplification of the gene. These tumours have a negative prognosis and their behaviour is different from the uniformly amplified tumours. Therefore, it seems that MYCN promotes a crosstalk between parts of a neuroblastoma tumour with different amplification status (Marrano, et al., 2017), an effect that could be mediated by extracellular vesicles.

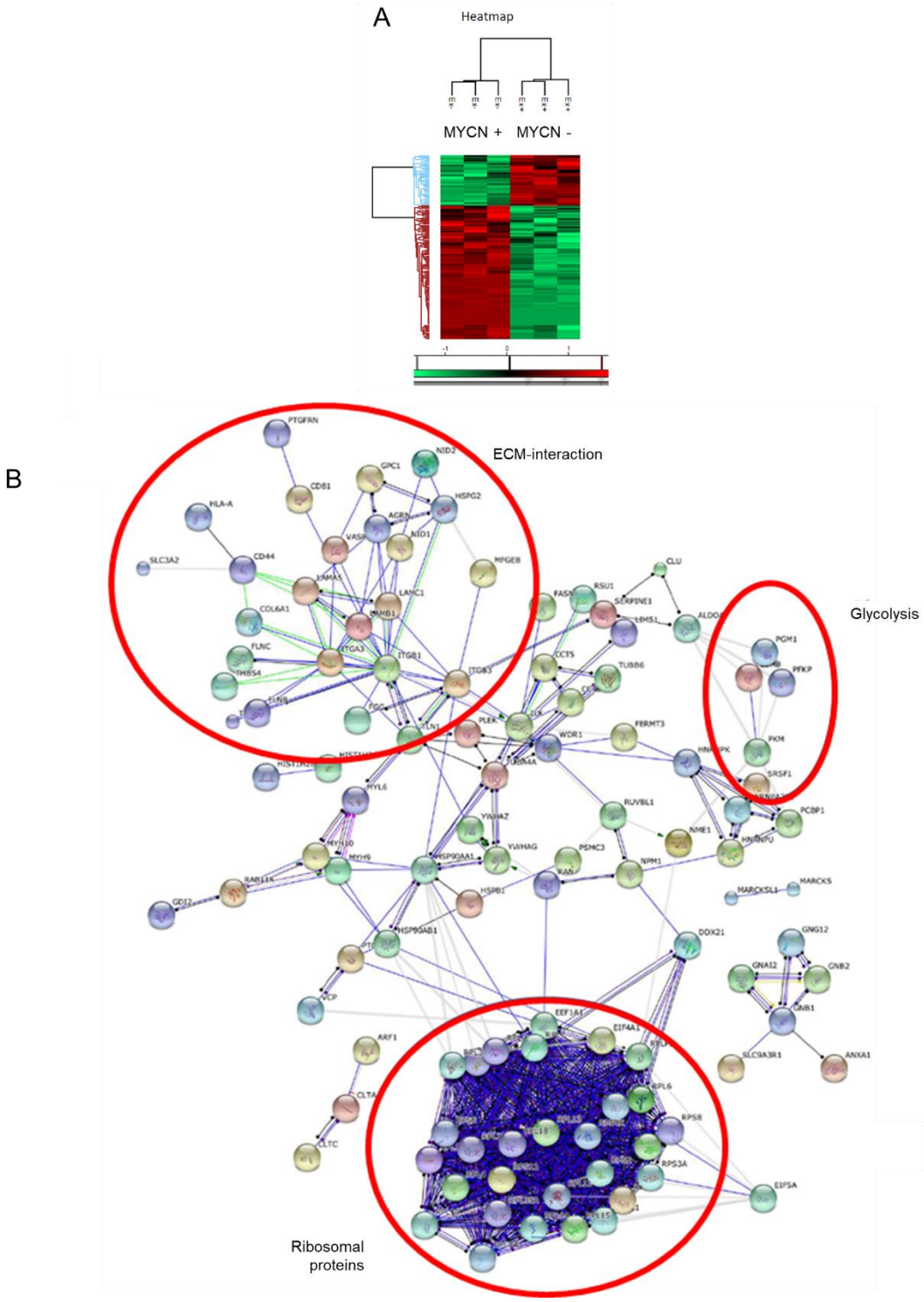

Figure 3.1: Mass spectrometry analysis of exosomes purified from cells with or without expression of MYCN. **A.** Heat map representation of the different proteins expressed in exosomes from MYCN positive or negative neuroblastoma cells. Using a switchable MYCN system coupled to mass spectrometry analysis, we have verified that MYCN specifically regulates 152 proteins in the exosomes secreted by neuroblastoma cells. **B.** Pathway analysis suggests that the MYCN-regulated proteins belong to 3 main functional groups: i) extracellular matrix-cells interactions, ii) glycolysis and iii) ribosome biogenesis.

3.1.1. Aims

Taking into consideration the results obtained with the mass spectrometry analysis, the aim of this chapter is to establish a protocol for the isolation of exosomes from cell culture supernatant media in order to validate the proteins that are differentially expressed in the exosomes secreted by MYCN positive and negative neuroblastoma cells with Western blot analysis. In addition, we are aiming to analyse exosomes circulating in the plasma of neuroblastoma patients and compare our findings with our *in vitro* system in order to investigate the hypothesis that MYCN can regulate the protein cargo of exosomes secreted by neuroblastoma cells.

3.2. Results

3.2.1. The TET21-N cell line can be used as a model for the overexpression of MYCN in neuroblastoma cells

The TET21-N neuroblastoma cell line derives from the parental neuroblastoma line SH-EP. SH-EP cells are an isogenic model of human neuroblastoma cells that are *MYCN* non amplified. They have been transfected with a MYCN tetracycline-repressible expression vector.

In the absence of doxycycline, a tetracycline derivative, the *MYCN* expression vector is activated and the expression of MYCN increases significantly. The cells express minimal amounts of MYCN in the presence of doxycycline (Fig. 3.2).

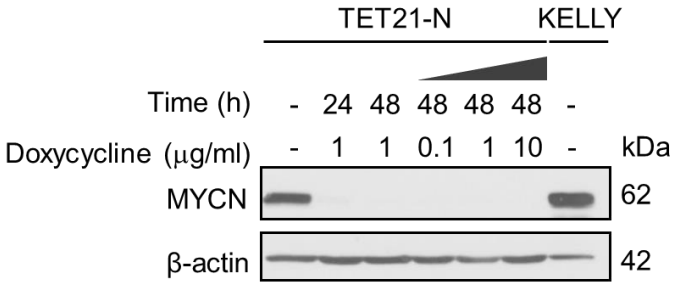

Figure 3.2: TET21-N cells overexpress MYCN and the expression is inhibited by treatment of cells with doxycycline. TET21-N cells were cultured in the presence or not of different concentrations of doxycycline for 24 and 48 h. The levels of MYCN were validated with western blot against the protein. Protein cell lysates from KELLY cells were used as a positive control for the expression of MYCN. β-actin was used as a loading control.

With the use of this isogenic cell line in our study, we minimize any cell type specific differences in our experiments. Therefore, we can use it to isolate exosomes the molecular content of which is mainly influenced by the presence of absence of MYCN.

3.2.2. Isolation and characterisation of exosomes from cell culture supernatant media

The exosomes that are produced by TET21-N cells cultured in the presence or absence of doxycycline were isolated from the cell culture supernatant with a series of centrifugation steps (Fig. 3.3).

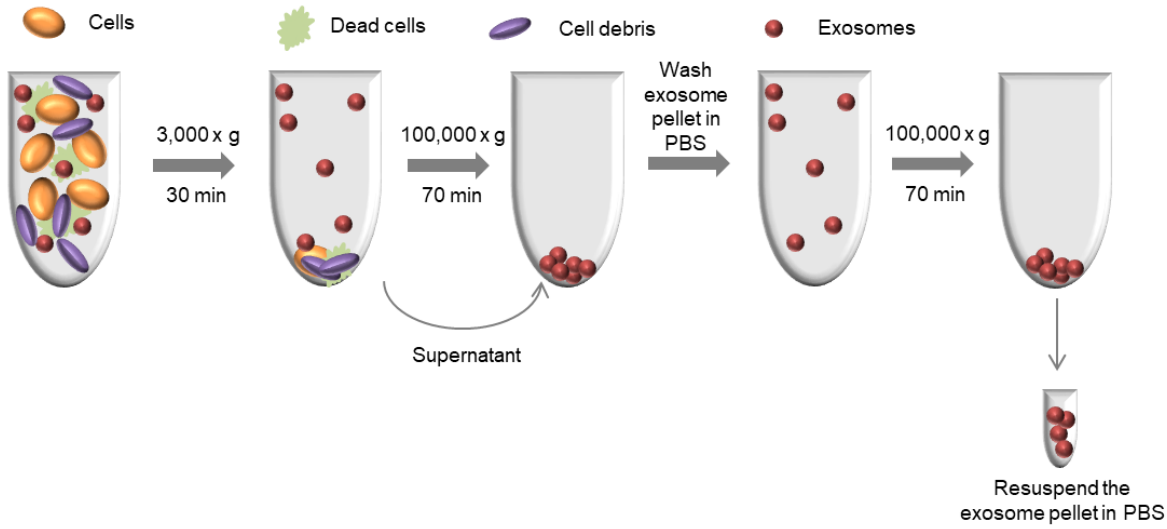

Figure 3.3: Schematic representation of the steps followed for the isolation of exosomes from cell culture supernatant media.

To validate the vesicles isolated with our protocol and characterise them as exosomes, a set of standards set by the literature must be met. The vesicles should be on average 100 nm large, enclosed by a lipid bilayer and their protein content should be enriched in exosomal markers that prove their endocytic origin.

To check the average size of the vesicles we isolate with the protocol described above, we used NTA and TEM. Our results obtained with both approaches prove that the population of vesicles isolated from cell culture supernatant is enriched in vesicles of average size 100 nm (Fig 3.4A, B).

Exosomes are vesicles that are enclosed by a lipid bilayer. To validate the membrane integrity of the exosomes in our preparations as well as their shape and morphology, we stained them with the membrane specific dye PKH67 and visualised them with ImageStream flow

cytometry. The positive staining proves that the exosomes in our preparations are intact (Fig. 3.4C).

Finally, as exosomes are produced through the endocytic pathway, they are enriched in endocytic markers such as the tetraspanin CD63. Indeed, when analysed with Western blot and compared with equal amounts of whole cell protein lysates, the protein extracts from the exosomes in our preparations are enriched for the exosomal marker CD63 (Fig. 3.4D).

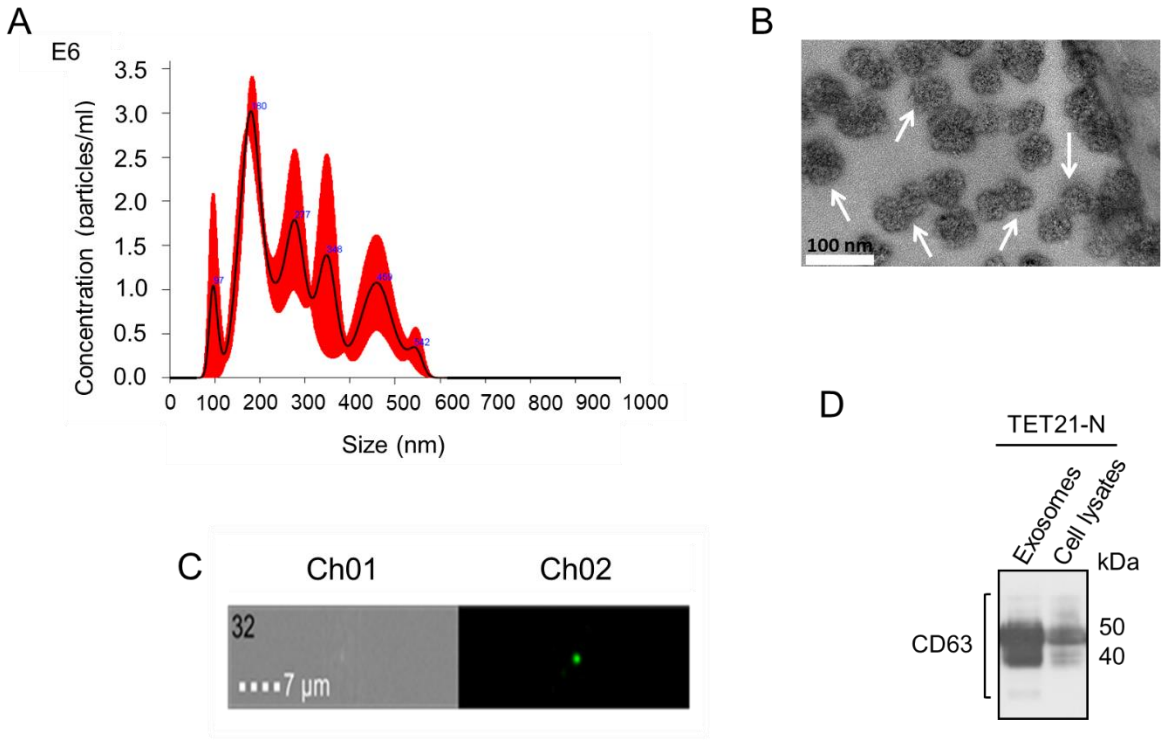

Figure 3.4: Exosome isolation from cell culture supernatant media. A. Exosomes were analysed with NTA to quantify the total number of particles/ml and their overall composition. **B.** Exosomes isolated by differential centrifugation were placed on carbon grids, stained with K-PTA and examined with transmission electron microscopy at 80 kV. **C**. The isolated exosomes were stained with the membrane specific dye PKH67 and visualised using ImageStream flow cytometry. **D.** 10 µg of proteins from exosomes and whole cell protein lysates of the donor cells were separated in an SDS-PAGE gel and immunoblotted against CD63.

Taking into consideration the size, morphology, shape, membrane integrity and the enrichment in exosomal markers proving the endocytic origin of exosomes, we showed that the protocol we follow for the isolation of exosomes from cell culture supernatant media is successful.

3.2.3. Validation of the mass spectrometry results with Western blot analysis

The mass spectrometry analysis of the exosomes from MYCN positive and negative neuroblastoma cells suggested a list of proteins that their expression is altered within the exosomes secreted by the cells. We therefore wanted to validate some of the proteins firstly identified in the mass spectrometry screening with Western blot analysis.

Since the mass spectrometry experiments were performed with exosomes produced by neuroblastoma cells artificially overexpressing MYCN, it was important to verify that these proteins are expressed in neuroblastoma cells containing naturally amplified *MYCN*. It is expected that this will be the case, since several of these proteins have been previously validated as important MYC targets and they predict poor survival. Therefore, we carried out protein profiling of a panel of *MYCN* amplified (KELLY) and non-amplified (SK-N-AS, SH-EP) cell lines, using antibodies against proteins identified in the pilot screen in the exosomes (Fig. 3.5).

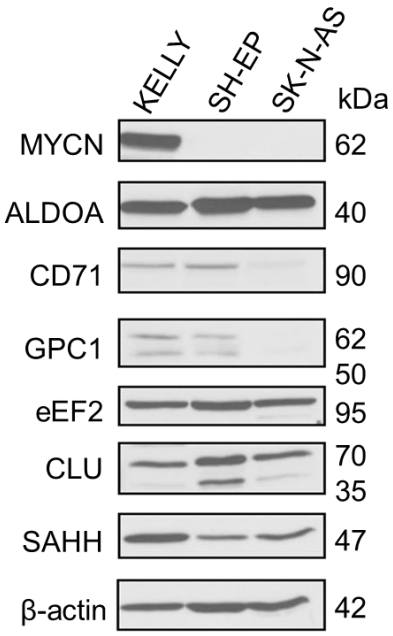

Figure 3.5: Western blot analysis of proteins firstly identified with the mass spec analysis. Proteins from naturally *MYCN* amplified (KELLY) or non-amplified (SH-EP, SK-N-AS) neuroblastoma cell lines were immunoblotted with antibodies against MYCN, aldolase a (ALDOA), tranferrin 1 (CD71), glypican 1 (GPC1), eEF2, clusterin (CLU) and SAHH. β-actin was used as a loading control.

As expected and consistent with the mass spectrometry data for the MYCN positive cells, KELLY express relatively more aldolase A (ALDOA), transferrin 1 (CD71), glypican 1 (GPC1) and elongation factor 2 (eEF2). At the same time, KELLY express less clusterin (CLU).

To further investigate the regulation of the proteins of our interest under the control of MYCN, we used the switchable MYCN system (Fig. 3.2) and we isolated exosomes and whole cell lysates from TET21-N cells to compare the levels of the proteins.

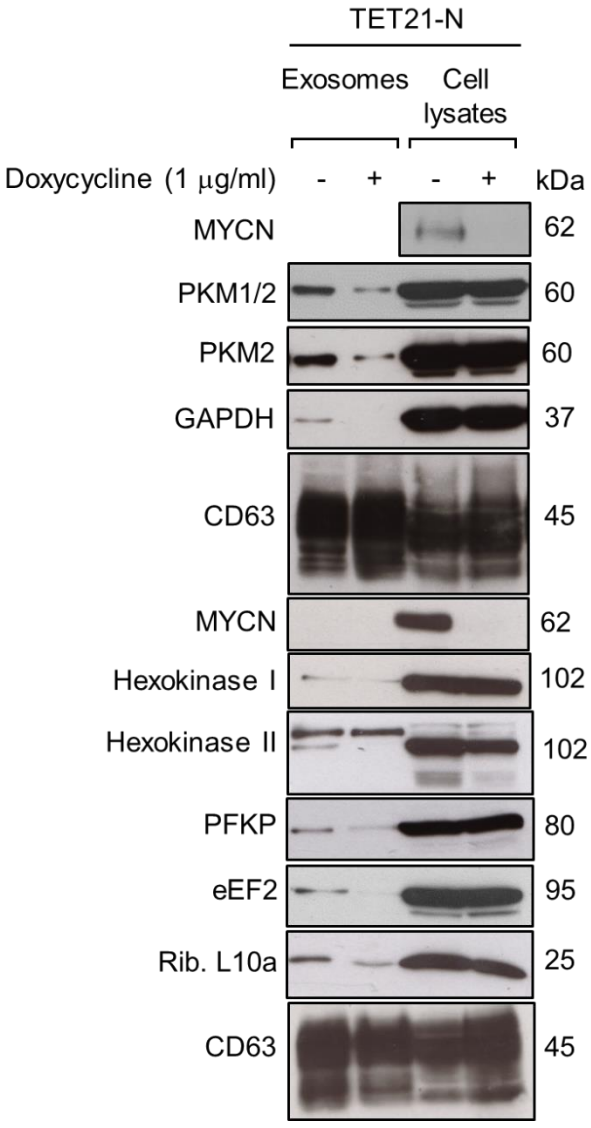

Figure 3.6: Western blot of exosomes and total cell lysates from TET21-N cells with or without MYCN confirms the MYCN-related differential loading of proteins within the exosomes. Western Blot analysis of the exosomes secreted by TET21-N cells in the presence or absence of doxycycline confirms that glycolytic enzymes, eukaryotic

elongation factor 2 (eEF2) and ribosomal protein L10a are among the proteins overexpressed in the exosomes secreted by MYCN positive cells. CD63 was used as a loading control.

Consistent with the mass spectrometry data, most of the proteins checked are upregulated in the exosomes from MYCN positive cells. Protein levels were generally unchanged in total cell lysates (Fig. 3.6). This observation implies that neuroblastoma exosome protein cargo does not merely reflect cellular content, suggesting that MYCN actively regulates exosome loading.

Some of the proteins validated as overexpressed in the exosomes of MYCN positive cells are of particular interest due to their importance in neuroblastoma biology. For example, overexpression of *eEF2* and the gene coding for the ribosomal protein L10a (rib. L10a) is predictive of poor outcome for neuroblastoma patients in a similar way that *MYCN* amplification is (Fig. 3.7).

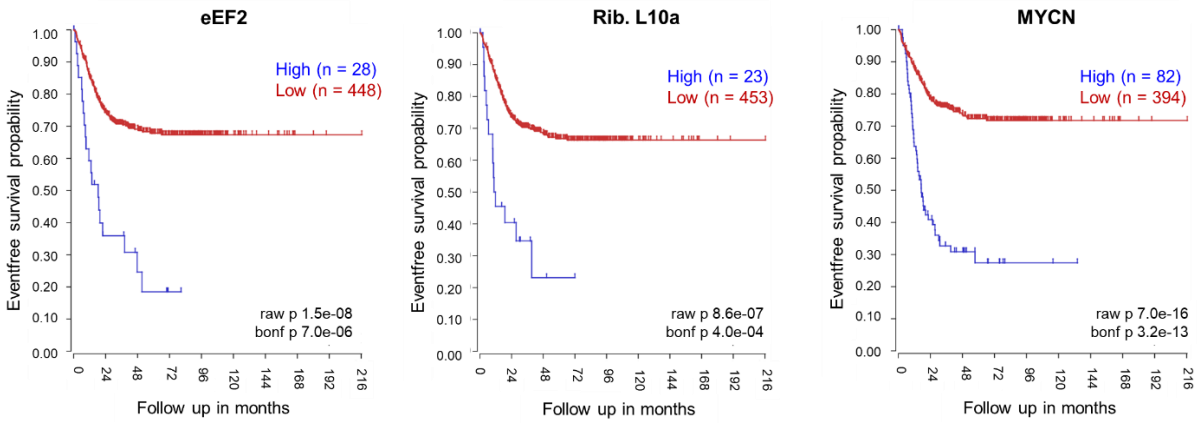

Figure 3.7: Kaplan-Meier curve for the event-free survival probability of neuroblastoma patients with *eEF2*, *rib. L10a* or *MYCN* expression. The red line indicates patients with low level of the genes while the blue line is indicating patients expressing high levels of the genes. All three genes are predictive of poor outcome for the neuroblastoma patients, while eEF2 and rib. L10a are transferred within the exosomes of MYCN positive neuroblastoma cells. The Kocak cohort was used for the generation of the curves (Kocak, et al., 2013).

Similarly, the identification of glycolytic kinases as one of the groups that is enriched in the exosomes secreted by MYCN positive cells is of particular interest. Two of these proteins,

PKM2 and hexokinase II correlate with poor survival probability for the neuroblastoma patients (Fig. 3.8).

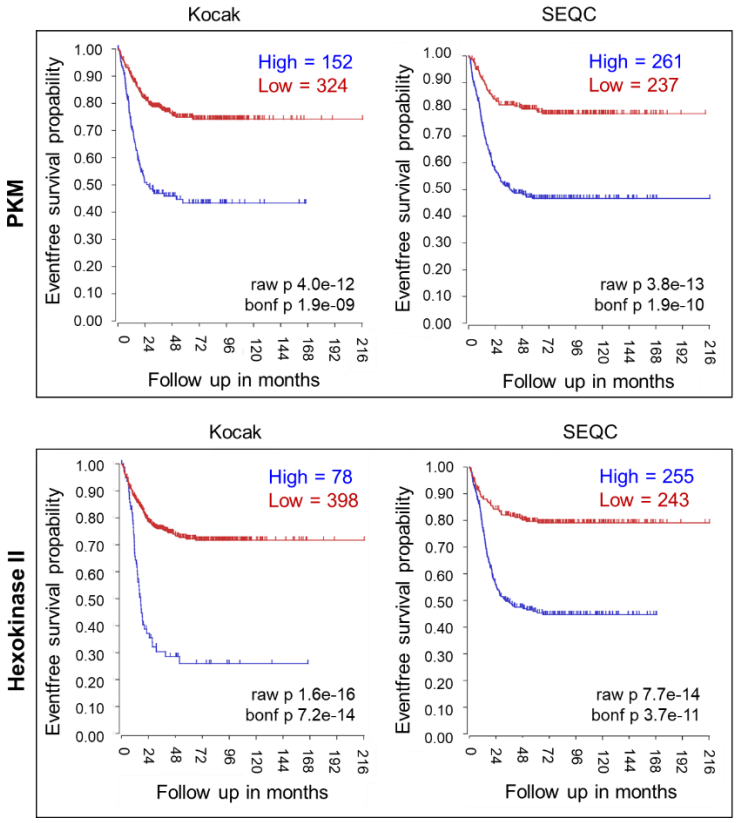

Figure 3.8: Kaplan-Meier curve for the event-free survival probability of neuroblastoma patients with *PKM* or *HK2* expression. The red line indicates patients with low level of the genes while the blue line is indicating patients expressing high levels of the genes. Both genes are predictive of poor outcome for the neuroblastoma patients and are identified within the exosomes of MYCN positive neuroblastoma cells. The Kocak and SEQC cohorts were used for the generation of the curves.

3.2.4. Isolation and characterisation of exosomes isolated from plasma samples of neuroblastoma patients

Extracellular vesicles secreted by different types of cells, both normal and cancer cells, can enter the blood stream and reach distant locations. This makes exosome secretion an important tool for tumours that prepare their metastatic niche in order to successfully disseminate, as they can condition and prepare the metastatic sites from distance (Ombrato,

et al., 2019). Since we have validated some of the exosomal proteins regulated by MYCN in our *in vitro* system, we were interested in investigating whether these proteins can be identified in exosomes circulating in the blood of neuroblastoma patients.

For that purpose, we isolated exosomes from plasma samples of patients with *MYCN* amplified or non-amplified neuroblastoma tumours and we tried to analyse their protein cargo with Western blot.

The preparations we obtained from the patient samples were successfully enriched in extracellular vesicles positive for the exosomal marker CD63 (Fig. 3.9B). To validate the plasma vesicles preparations we used an antibody against Galectin-3 binding protein (Gal-3BP) (Fig. 3.9C), which is a marker of exosomes, including those produced by neuroblastoma cells (Silverman, et al., 2012).

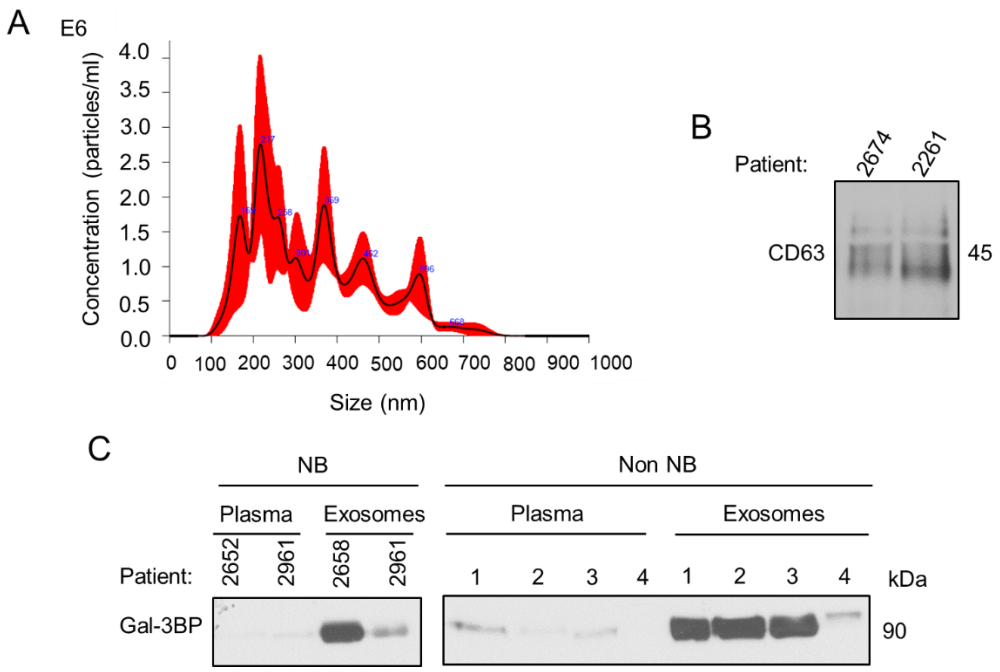

Figure 3.9: Exosome isolation from plasma samples of neuroblastoma patients. Exosomes were analysed with NTA to quantify the total number of particles/ml and their overall composition. **B.** 10 μg of proteins from exosomes isolated from two different plasma samples were separated in an SDS-PAGE gel and immunoblotted against CD63 protein. **C.** Equal amounts of proteins from unprocessed plasma and exosomes isolated from plasma of neuroblastoma and control patients were immunoblotted against Gal-3BP.

Since PKM2 and hexokinase II are differentially expressed in the exosomes of neuroblastoma cells secreted by MYCN positive or negative cells and predictive of poor outcome for the neuroblastoma patients, we wondered whether we could detect them in exosomes circulating in the plasma of patients bearing neuroblastomas with or without *MYCN* amplification. Interestingly, expression of PKM1/2 and hexokinase II was detected in the exosomes isolated from plasma samples of neuroblastoma patients, but was completely absent from the samples of non-cancer patients. Furthermore, the staining was more prominent in the exosomes circulating in the blood of patients with MYCN amplified tumours (Fig. 3.10).

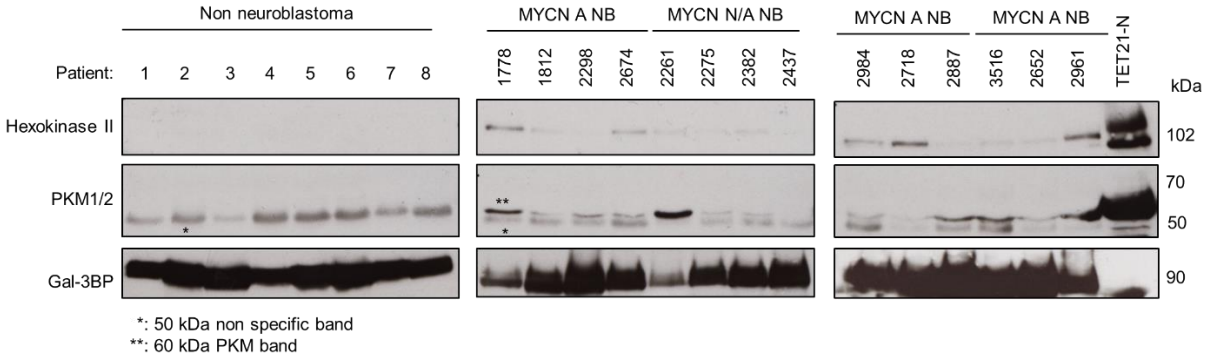

Figure 3.10: Exosomes in the plasma of neuroblastoma patients carry PKM. Exosomes were isolated from plasma samples of neuroblastoma patients with MYCN amplified or non-amplified neuroblastoma and non-neuroblastoma patients and their protein content was analysed with Western blot with antibodies against PKM1/2 and Hexokinase II. Gal-3BP was used as a loading control and total cell lysates from TET21-N cells were used as a positive control for PKM and hexokinase II.

3.3. Discussion

Exosomes are small extracellular vesicles of endocytic origin. They are biologically active and their function depends on the molecules that they are delivering in the cells that they are targeting.

In our model, we used neuroblastoma cells that can be manipulated in order to overexpress or not express MYCN and we isolated exosomes from the cell culture supernatant media in order to validate the proteins that are differentially expressed in these exosomes. The physicochemical properties of extracellular vesicles allow them to be isolated from cell culture supernatant media with high speed ultracentrifugation. To make sure that our preparations were enriched in the exosome population, we tested our exosome preparations for their size, membrane integrity and endocytic origin. Overall, the observational data collected with TEM, the positive staining for membrane specific dyes, the behaviour of the preparations under light scattering and their enrichment in the exosomal marker CD63 prove that out preparations are enriched in exosomes that are secreted by our donor cells.

The original analysis of the protein cargo of MYCN positive and negative neuroblastoma cells with mass spectrometry suggested that the proteins that are transferred within the exosomes can depend on the expression of MYCN in the donor cells. To validate that, we analysed a panel of proteins firstly identified with the mass spectrometry analysis with Western blot. We managed to identify eEF2, rib. L10a and a panel of glycolytic kinases among other proteins that are overexpressed in the exosomes secreted by MYCN positive neuroblastoma cells. Intriguingly, the levels of those proteins in the total cell lysates of the MYCN positive and negative TET21-N cells seem to remain stable, indicating a mechanism through which MYCN manages to sort and regulate the loading of those molecules in these vesicles for targeted extracellular secretion.

To validate our *in vitro* observations for the protein cargo of exosomes in neuroblastoma, we used exosomes isolated from plasma samples of patients bearing neuroblastoma and compared them with non-cancer patients samples. Interestingly, the glycolytic kinases pyruvate kinase and hexokinase II were identified as present in the exosomes circulating in the plasma of neuroblastoma patients. Taking into consideration the fact that these two glycolytic enzymes circulate in the blood of the patients and that the expression of the *PKM*

and *HK2* genes strongly correlates with poor patient prognosis (Fig. 3.8), our results suggest that these two glycolytic kinases might confer a growth/survival advantage to neuroblastoma cells.

In summary, the results presented in this part suggest that MYCN can regulate the loading of proteins within the exosomes secreted by neuroblastoma cells, a process that seems to be regulated and related with the expression of MYCN in the donor cells. Due to their roles in cell metabolism, the proteins that are delivered by the exosomes of MYCN positive neuroblastoma cells could potentially transfer the oncogenic activity of MYCN in the non *MYCN* amplified recipient cells. This regulation of the proteins that are delivered in the cells surrounding a MYCN amplified neuroblastoma tumour, could mediate the conditioning of the tumour microenvironment and support tumour growth. Since 40% of the tumours with *MYCN* amplification express MYCN focally, this mechanism could be of tremendous importance for the establishment of an aggressive behaviour and the support of tumour growth in a non-cell autonomous way with the participation of the MYCN negative cells of the neuroblastoma tumour.

4. Results II: MYCN positive neuroblastoma cells secrete exosomes that induce proliferation and glycolysis upon uptake

4.1. Introduction

4.1.1. Tumour cell metabolism

The proteins that regulate the metabolic activity of the cells and in particular glycolytic kinases are especially relevant in cancer. All cellular processes depend on the regulation of the metabolism and aggressive cancer cells have developed mechanisms in order to manipulate the metabolism and achieve tumour growth and metastatic dissemination. Mitochondrial oxidative phosphorylation is used by the majority of differentiated mammalian cells as their main source of energy production. However, cancer cells are able to increase their glucose uptake and metabolise it to lactate in aerobic conditions, thus shifting towards aerobic glycolysis, a process known as the Warburg effect (Warburg, 1956; Vander Heiden, et al., 2009).

In cancer, a number of enzymes that regulate the glycolytic pathway has been shown to be overexpressed (Altenberg & Greulich, 2004). A protein of particular interest is the pyruvate kinase. This enzyme is critical for the catalysis of the transfer of a phosphate group from phosphoenolpyruvate (PEP) to adenosine diphosphate (ADP) that results in the production of pyruvate and adenosine triphosphate (ATP) (Altenberg & Greulich, 2004). Pyruvate kinase has four isoforms. The gene *PKLR* encodes for the isoforms PKL and PKR that are expressed in the liver and erythrocytes, respectively. The M1 and M2 splice isoforms are the result of the alternative splicing of *PKM* pre-mRNA. Inclusion of exon 10 and exclusion of exon 9 produces PKM2, while the opposite results in PKM1 (Yang & Lu, 2015).

PKM2 has many roles in regulating the metabolic activity of the cells and it has been shown to be important for the shift in cellular metabolism observed in the Warburg effect. In addition, it is increased in many cancers with respect to the M1 variant, that is mainly found in normal tissues (Christofk, et al., 2008; Desai, et al., 2014).

Interestingly, PKM2 was one of the enzymes we have identified as overexpressed in the exosomes secreted by MYCN positive cells and was also identified in the exosomes circulating in the plasma of neuroblastoma, but not non-cancer patients.

4.1.2. The PI3K/AKT pathway in neuroblastoma tumours

Besides metabolism, tumour cells use other mechanisms and pathways of the cell to their advantage and one of those is protein synthesis. Abnormal protein synthesis has been linked with many kinds of cancer and the interference of tumour biology in the translational machinery can be in either of the initiation, elongation or termination steps of mRNA translation. One of the proteins that we identified in our proteomic screening as overexpressed in the exosomes secreted from MYCN positive neuroblastoma cells is eEF2, one of the regulators of the elongation step in translation (Lamberti, et al., 2004). eEF2 is overexpressed in hepatocellular carcinoma (Pott, et al., 2017), prostate cancer (Zhang, et al., 2018) and ovarian cancer, where it regulates tumour cell proliferation by regulating the PI3K/Akt pathway (Shi, et al., 2018). In neuroblastoma, eEF2 kinase regulates tumour cell metabolism by regulating the Warburg effect (Cheng, et al., 2016).

The PI3K/Akt pathway is frequently activated in neuroblastoma and this activation is significantly correlated with MYCN amplification or 1p36 aberrations. Importantly, phosphorylation of Akt on either the Ser473 or Thr308 is predictive of poor outcome for neuroblastoma patients (Cheng, et al., 2016).

4.1.3. Aims

The aim of this chapter is to explore the potential of exosomes secreted by MYCN positive neuroblastoma cells to alter the behaviour of the cells that uptake them. Based on our proteomic studies, our strongest molecular candidates are the proteins implicated in glycolysis and in particular the glycolytic kinases, and eEF2. Therefore, we decided to focus on functional assays that describe proliferation, metabolism and Akt activation and compare the behaviour of the recipient cells after treatment with exosomes from MYCN positive or negative TET21-N cells.

4.2. Results

4.2.1. Exosomes isolated from cell culture supernatant media are uptaken by cells in culture

To assess the biological function of exosomes in recipient cells we used the neuroblastoma cell line SH-EP, which is a stromal type neuroblastoma cell line, therefore simulating the Schwann stroma surrounding the nests of highly proliferating, MYCN or c-MYC activated neuroblasts in tumours. SH-EP cells were used as recipients of exosomes isolated from TET21-N expressing or not expressing MYCN.

To test whether the exosomes that we isolate from cell culture supernatant media are being uptaken by the recipient cells in culture, we treated SH-EP cells with PKH67-stained exosomes from TET21-N cells for 24 h (Fig. 4.1).

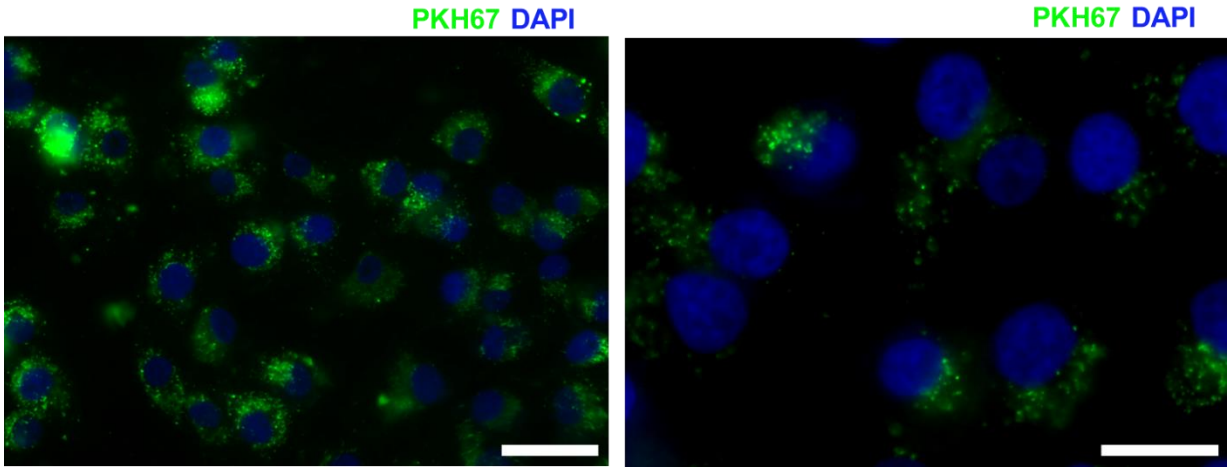

Figure 4.1: Uptake of exosomes secreted by TET21-N cells by SH-EP cells. Fluorescence microscopy of SH-EP cells after 24 h incubation in the presence of PKH67-labelled exosomes isolated from TET21-N cells culture media. Scale bar (from left to right), 50 μm, 25 μm.

As shown above, the exosomes are uptaken by the recipient cells and they are located around the cell membrane and into the cytoplasm. We, therefore, expect that the exosomes that we isolate from cell culture supernatant media can successfully target the recipient cells and deliver the proteins that they are carrying.

4.2.2. Exosomes secreted by MYCN positive neuroblastoma cells induce proliferation of non MYCN amplified neuroblastoma cells

One of the key characteristics of tumour cells is their ability to proliferate in higher rates. That would mean that external signals that are promoting tumourigenesis would interfere with the proliferation status of a cell in order for it to start grow and proliferate faster. If the exosomes from aggressive, MYCN positive neuroblastoma cells deliver proteins that can promote tumourigenesis, one of the events that we would expect to observe is induced proliferation of the recipient cells.

To test that, we treated SH-EP cells with exosomes isolated from TET21-N cells positive or negative for MYCN and we counted the total cell numbers for 3 consecutive days (Fig. 4.2A). When the cells received exosomes from the MYCN negative cells, their growth curve was not affected. However, when the cells received exosomes from MYCN positive cells, they increased their number faster and they reached confluency on the second day.

In addition, we performed the MTS proliferation assay with SH-EP cells treated with exosomes from MYCN positive or negative TET21N cells for 24 or 48 h. Similarly, the cells that received MYCN-induced exosomes showed induced proliferation (Fig. 4.2B).

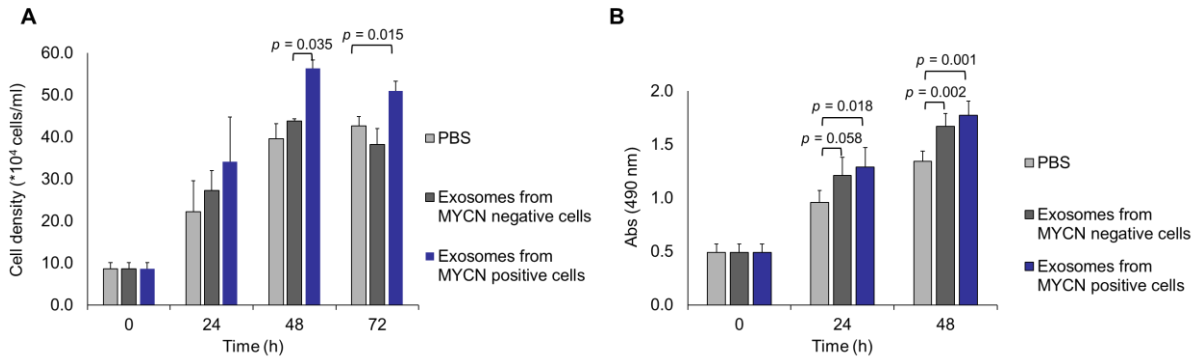

Figure 4.2: Exosomes secreted by MYCN positive neuroblastoma cells induce proliferation of non MYCN amplified recipient cells. **A.** Cell density of SH-EP cells after receiving the exosomes from MYCN positive or negative neuroblastoma cells. (n = 3). **B.** MTS proliferation assay with cells receiving exosomes from MYCN positive or negative TET21-N cells (n = 5). PBS was used as a control. Error bars represent SEM.

4.2.3. Exosomes secreted by MYCN positive neuroblastoma cells induce glycolysis in non MYCN amplified neuroblastoma cells

Glycolytic kinases are one of the most interesting groups identified with our proteomic screening, as two of them were also validated to be present in the exosomes isolated from plasma samples of neuroblastoma patients. Therefore, we measured the glycolytic activity of recipient cells after treatment with exosomes from MYCN positive or negative TET21-N cells.

The ability of the exosomes to induce glycolysis in the recipient cells was determined by measuring the production of L-lactate after the treatment of SH-EP cells with exosomes from MYCN positive or negative cells (Fig. 4.3). Indeed, after treatment with the exosomes for 24 h, the cells that received the exosomes from the MYCN positive neuroblastoma cells produced significantly more L-lactate than the cells that received the exosomes from the MYCN negative cells.

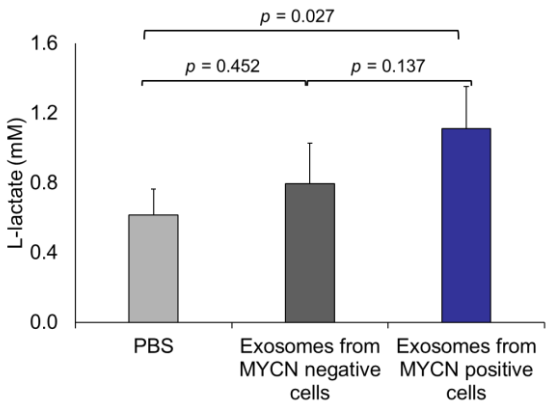

Figure 4.3: Exosomes secreted from MYCN positive TET21-N cells activate the metabolic activity of non MYCN amplified recipient cells. SH-EP cells (non MYCN amplified) secrete more L-lactate upon uptake of exosomes from MYCN positive cells (n = 4). PBS was used as a negative control. Error bars represent SEM.

Therefore, it seems that the exosomes secreted by MYCN positive neuroblastoma cells deliver proteins of the glycolytic pathway to their recipient cells, thus inducing glycolysis upon uptake.

4.2.4. Akt phosphorylation of the serine 473 residue is induced in SH-EP cells after treatment with exosomes from MYCN positive neuroblastoma cells

As mentioned before, the activation of the Akt pathway is highly relevant to neuroblastoma biology. Akt can be activated via phosphorylation regulated by a number of upstream events. Therefore, we decided to test whether the exosomes secreted by MYCN positive neuroblastoma cells have the potential to activate Akt. To do that, we treated FBS-deprived SH-EP cells with exosomes isolated from MYCN positive or negative TET21-N cells for a short period of time and stained them with an antibody recognising phospho-Akt (Ser473) (Fig. 4.4).

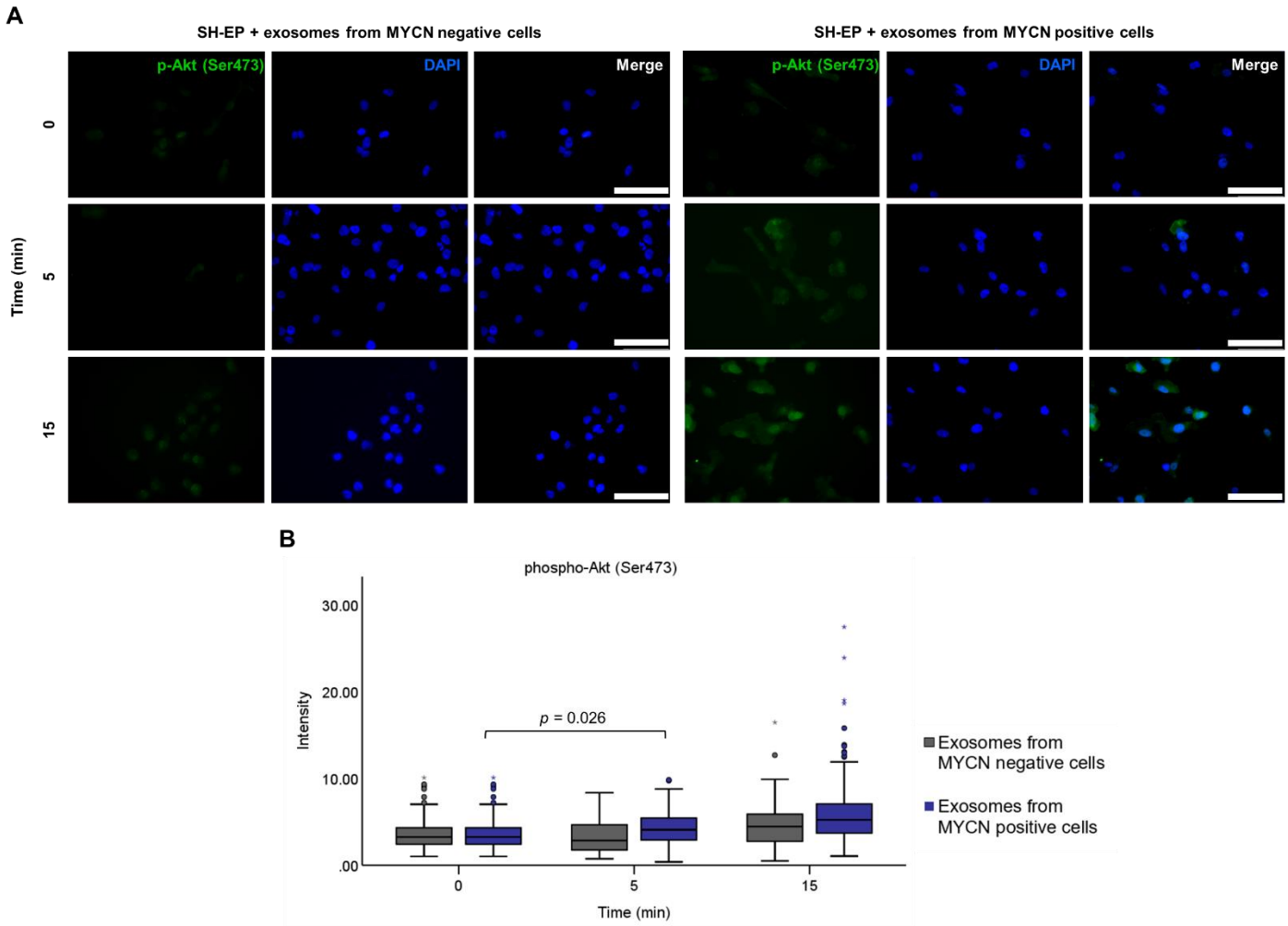

Figure 4.4: MYCN-induced exosomes activate Akt. A. Immunofluorescence analysis. SH-EP cells were exposed to exosomes from MYCN positive or negative cells and Akt phosphorylation was detected using a phospho-serine 473 antibody. Scale bar, 0.75 μm. **B.** The intensity of phospho-Akt staining against the background was quantified using ImageJ (n = 3).

These data suggest that exosomes secreted by MYCN positive neuroblastoma cells can induce Akt phosphorylation in SH-EP cells that have been FBS-deprived. The activation of the pathway is really quick, as it can be observed at just 5 min. The rapidity of the effect is consistent with our hypothesis that the biological function of the exosomes is at least partially mediated by the proteins that they are carrying, as a microRNA-mediated phenotype would take much longer to develop.

To further establish the relationship between MYCN expression and Akt phosphorylation in neuroblastoma, we wondered whether Akt is activated in neuroblastoma tumours with focal *MYCN* amplification. If MYCN positive neuroblastoma cells secrete factors, such as extracellular vesicles, that are able to phosphorylate Akt in the nearby recipient cells, then we should be able to observe homogeneous Akt phosphorylation in non-homogeneously MYCN positive tumours.

To test that, we used tumour sections from the TH-MYCN transgenic mouse model for neuroblastoma that were kindly provided to us by the laboratory of Prof. Louis Chesler in the Institute of Cancer Research. We stained serial sections of the same tumour for MYCN and phospho-Akt (Ser473) and compared the staining patterns (Fig. 4.5).

This experiment shows that in a neuroblastoma tumour that only some of the cells are expressing MYCN, Akt is homogeneously phosphorylated throughout the section. This is not proving that the pathway is regulated by exosomes secreted by the MYCN positive cells of the tumour, however it supports the idea that the aggressiveness of MYCN positive neuroblastoma tumours can be “expanded” beyond the MYCN positive cells. Exosome secretion is one of the mechanisms that the MYCN positive cells could employ in order to interact with distal parts of the tumour and change the behaviour of the nearby cells that receive the secreted vesicles.

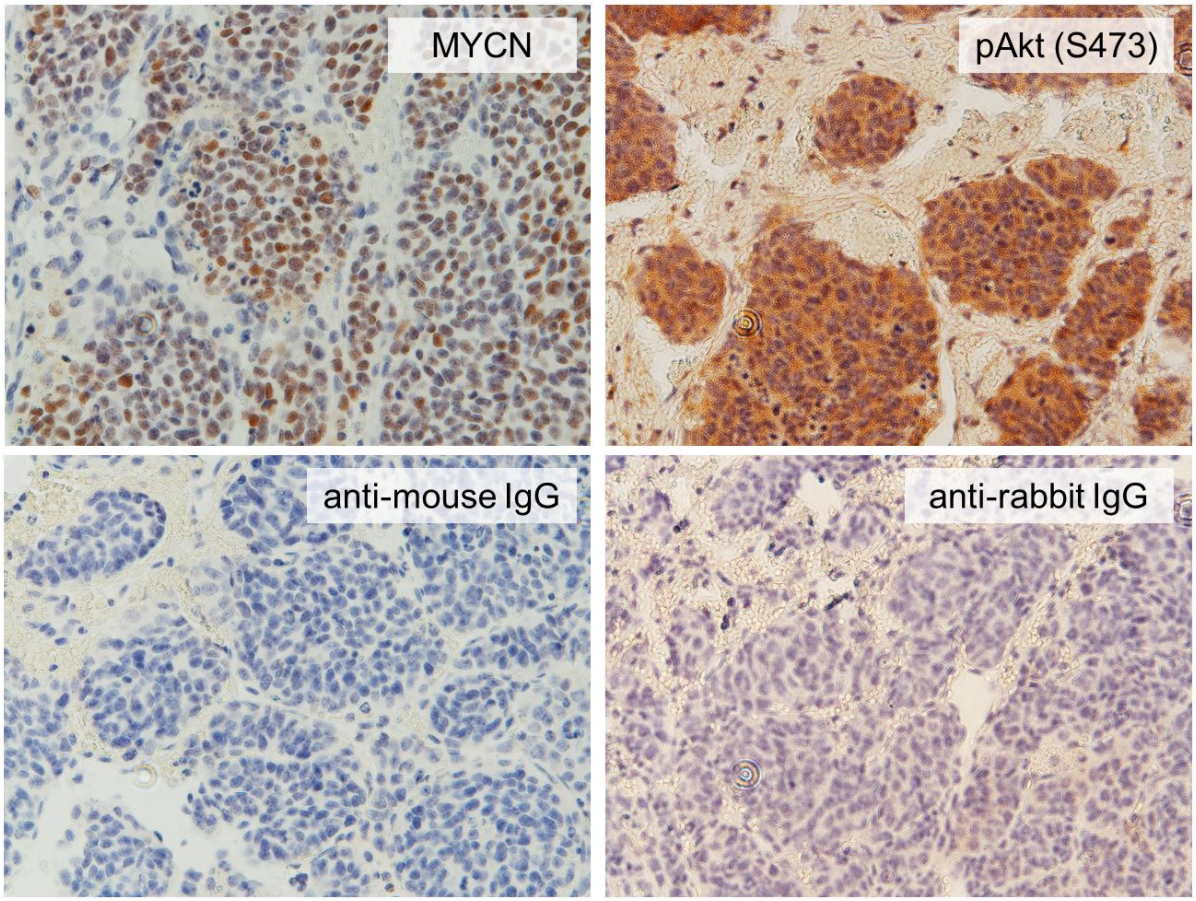

Figure 4.5: IHC of tumour sections from the TH-MYCN transgenic mouse model reveals the homogeneous expression of phospho-Akt (Ser473). Neuroblastoma tumours were resected from TH-MYCN transgenic mice and stained with antibodies against MYCN or phospho-Akt (Ser473) by immunohistochemistry. Expression of nuclear MYCN was heterogeneous whereas phospho-Akt expression was uniformly present in the cytoplasms of neuroblasts in the tumour nests.

4.3. Discussion

Exosomes are powerful mediators of intercellular communication, since they carry within them the signalling molecules and the machinery to induce behavioural changes in the cells that receive them. In our model of studying neuroblastoma, we identified proteins that are differentially expressed in the exosomes secreted by MYCN positive and negative neuroblastoma cells and knowing that the activity of the exosomes and their impact in the recipient cells will depend on their molecular cargo, we hypothesised that neuroblastoma secreted exosomes will have a MYCN-dependent phenotype on the cells that receive them. Therefore, we carried out a series of functional experiments to try to understand the effect of the uptake of exosomes secreted by MYCN positive and negative neuroblastoma cells.

In our system, we treated SH-EP cells, a *MYCN* non amplified cell line, with exosomes isolated from MYCN positive or negative TET21-N cells. With this setup, we attempt to simulate the interaction of exosomes from MYCN positive neuroblastoma cells with cells of the stromal component around the tumour that consist the tumour microenvironment and whose behaviour is critical for the support of tumour growth.

After confirming the successful delivery of the exosomes we isolate from cell culture supernatant into the recipient cells, we studied a set of phenotypes that could be altered based on whether the cells receive exosomes from MYCN positive or negative TET21-N cells. The first characteristic that we tested is cell proliferation, a basic oncogenic phenotype. As we hypothesised, exosomes from MYCN positive TET21-N cells promoted proliferation as measured by cell density and MTS assay in SH-EP cells, with respect to the treatments with exosomes from MYCN negative TET21-N cells or PBS.

The validation of the glycolytic enzymes as a group of proteins enriched in the exosomes secreted by the MYCN positive cells, led us to hypothesise that glycolysis could be affected as a result of the uptake of exosomes in the recipient cells. Indeed, the secretion of L-lactate was significantly higher in SH-EP cells after the treatment with exosomes from MYCN positive cells compared with the exosomes from MYCN negative cells.

Taken together, these experiments suggest that exosomes secreted by MYCN positive cells increase the proliferation rates and metabolic activity of recipient cells by inducing a Warburg switch.

Finally, another protein identified with our proteomic screening that draw our interest was eEF2. The fact that eEF2 is delivered in the recipient cells within the exosomes secreted by MYCN positive cells, made us consider Akt activation as a potential downstream pathway triggered by the uptake of the exosomes. Indeed, treatment of SH-EP cells with exosomes from MYCN positive neuroblastoma cells resulted in phosphorylation of Akt on Ser473. Akt is also phosphorylated in neuroblastoma tumours of mice with focal amplification of MYCN. Although this doesn't prove that the pathway is activated due to exosome secretion, it supports our hypothesis that even in tumours that MYCN is not homogeneously expressed, some pathways that are linked to MYCN activation do not follow the MYCN pattern and manage to be active even in parts of the tumour that are MYCN negative.

Overall, the data presented in this chapter indicate that MYCN can act in a non-cell autonomous manner to control the behaviour of a neuroblastoma tumour as a whole. The regulation of the molecular cargo of the exosomes secreted by the neuroblastoma cells results in different phenotypes of the cells targeted by these exosomes. This provides insights in a novel mechanism of MYCN-mediated intercellular communication in neuroblastoma.

5. Results III: Exosomes secreted by MYCN positive cells induce histone H3 T11 phosphorylation in a PKM2-dependent manner

5.1. Introduction

5.1.1. Non-metabolic functions of PKM2

As mentioned before, the M2 isoform of pyruvate kinase has been reported to be induced in many types of cancer compared to the M1 isoform of the enzyme. Interestingly, in addition to its role in glycolysis, PKM2 can also localise into the nucleus where it has non-metabolic functions (Lv, et al., 2013; Desai, et al., 2014). Acetylation of PKM2 by p300 transforms it from a cytoplasmic metabolic kinase to a nuclear protein kinase (Lv, et al., 2013). More specifically, in glioma, PKM2 localises in the nucleus where it directly binds on histone H3 and phosphorylates in on threonine 11. PKM2-mediated histone H3 phosphorylation results in c-MYC and cyclin D1 activation, increased cell cycle and tumour progression (Yang, et al., 2012). In addition, PKM2 regulates chromosome segregation and mitosis in cancer by interacting with the spindle checkpoint protein Bub3 to control cell cycle progression (Jiang, et al., 2014).

5.1.2. Aims

The aim of this chapter is to explore the possibility that PKM2 is delivered in cells that receive exosomes secreted by MYCN positive neuroblastoma cells and that this uptake can trigger PKM2-dependent phenotypes in the recipient cells related with our observations on increased metabolism and proliferation. If this is the case, our hypothesis that the effects we observe after the treatment with exosomes are a results of the proteins that are differentially expressed in the exosomes of MYCN positive and negative neuroblastoma cells will be supported.

5.2. Results

5.2.1. Use of the tissue culture insert co-culture method for the study of exosomes

To study the role of the proteins transferred in the purified exosomes secreted by the MYCN positive or negative TET21-N cells in a more physiologically relevant setting, we used a co-culture system. In this setup, induced or un-induced TET21-N cells were co-cultured with SH-EP cells while being separated by 0.4 μm pores tissue culture (TC) inserts (Fig. 5.1). The size of the pores allows EVs with a diameter smaller than 0.4 μm to go through from the donor cells site to the recipient cells, while the two different cell lines don not come in touch.

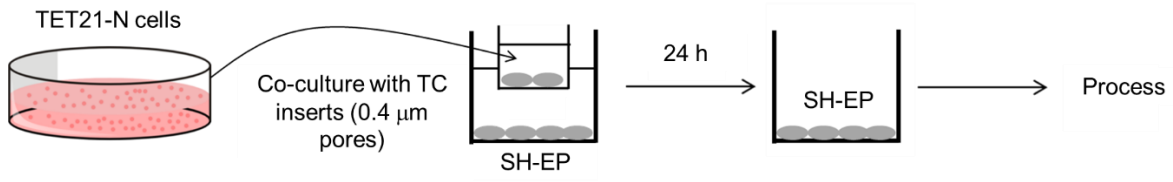

Figure 5.1: Schematic representation of the workflow followed for the experiments with the TC inserts.

The transfer of exosomes from donor to recipient cells was confirmed by transfecting TET21-N cells with a construct causing the overexpression of a CD63-GFP fusion protein (Fig. 5.2A) and observing the GFP signal in the SH-EP recipient cells after 24 hours (Fig. 5.2B).

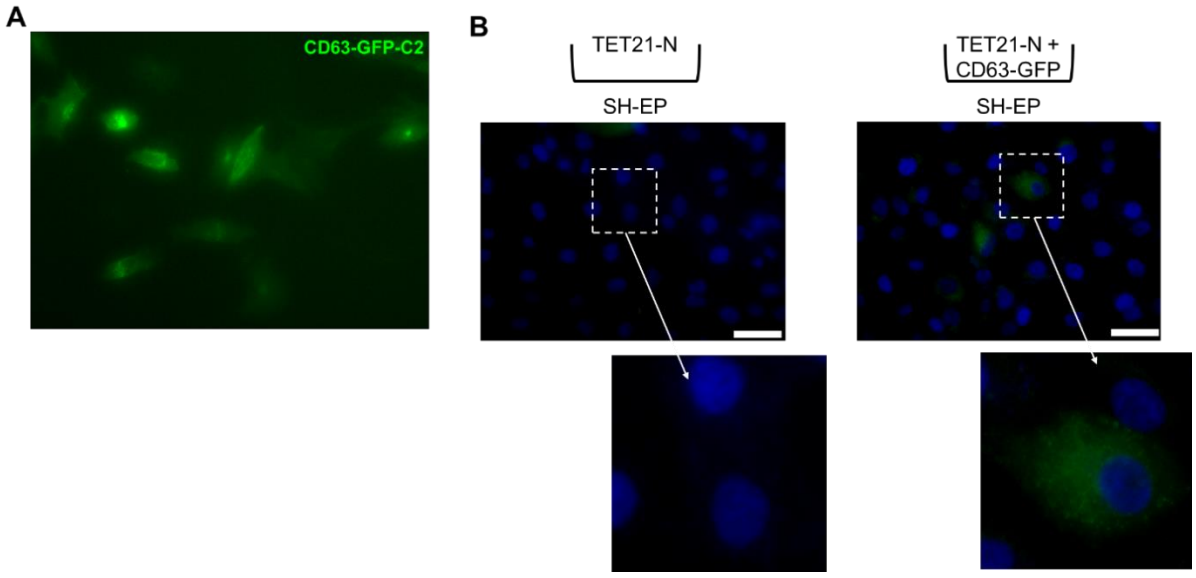

Figure 5.2: Exosomes from cells cultured on the TC insert are delivered to the cells cultured on the bottom of the plate. A. TET21-N cells 24 h post-transfection with the CD63-GFP-C2 plasmid. CD63-GFP is expressed and localised in the cytoplasm. **B.** SH-EP cells after 24 h co-culture with TET21-N cells transfected or not with CD63-GFP on the TC insert. SH-EP are receiving CD63-GFP through the TC inserts indicating the transfer and delivery of exosomes secreted by TET21-N cells. Scale bar, 50 μm.

The detection of an exosomal marker in the recipient cells transferred through the co-culture system confirms the successful delivery of exosomes from one side to the other. Therefore, we can use the co-culture method in order to study the role of exosomes secreted by TET21-N cells expressing or not expressing MYCN.

5.2.2. Neuroblastoma exosomes induce increased mitotic index and histone H3 (T11) phosphorylation in a PKM2-dependent manner

Taking into consideration the ability of nuclear PKM2 to phosphorylate histone H3, we hypothesised that exosomes enriched in PKM2 would be able to induce phosphorylation of histone H3 in recipient cells.

To test that, we treated SH-EP cells with exosomes purified from the cell culture supernatant media of TET21-N cells expressing or not expressing MYCN and we stained them for histone

H3 phosphorylation on threonine 11, the histone H3 modification that has been shown to be mediated by PKM2 (Fig. 5.3).

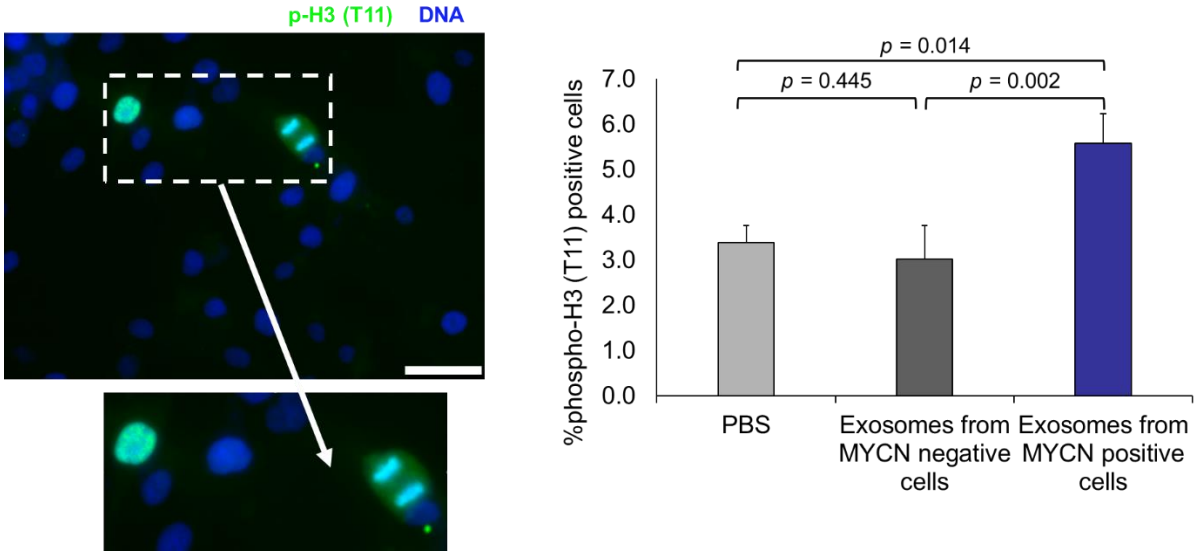

Figure 5.3: Exosomes secreted by MYCN positive neuroblastoma cells induce phosphorylation of histone H3 on threonine 11. SH-EP cells were treated with exosomes from MYCN positive or negative TET21-N cells for 24 h and stained for phospho-histone H3 (T11). The number of hyperphosphorylated cells was counted in each condition (n=4). Error bars represent SEM. Scale bar, 50 μm.

The data above show that purified exosomes form MYCN positive neuroblastoma cells can indeed induce the phosphorylation of histone H3.

To investigate this mechanism a little further, we used the same co-culture system described in the first section. First, as with CD63, we confirmed that PKM2 can be delivered in the recipient cells via exosomes by co-culturing PKM2-GFP overexpressing cells with SH-EP cells and observing the GFP signal in the SH-EP cells after 24 h (Fig. 5.4).

To link the biological effects observed in recipient SH-EP cells to the transfer of exosomal PKM2, we used two independent siRNAs that caused a reduction of PKM2 expression in the donor TET21N cells (Fig. 5.5A). Consequently, we used the PKM2-depleted MYCN positive TET21-N cells as donor cells in the co-culture system. As a control, we used MYCN positive TET21-N cells transfected with an siRNA that doesn't target any mammalian proteins (rLuc siRNA).

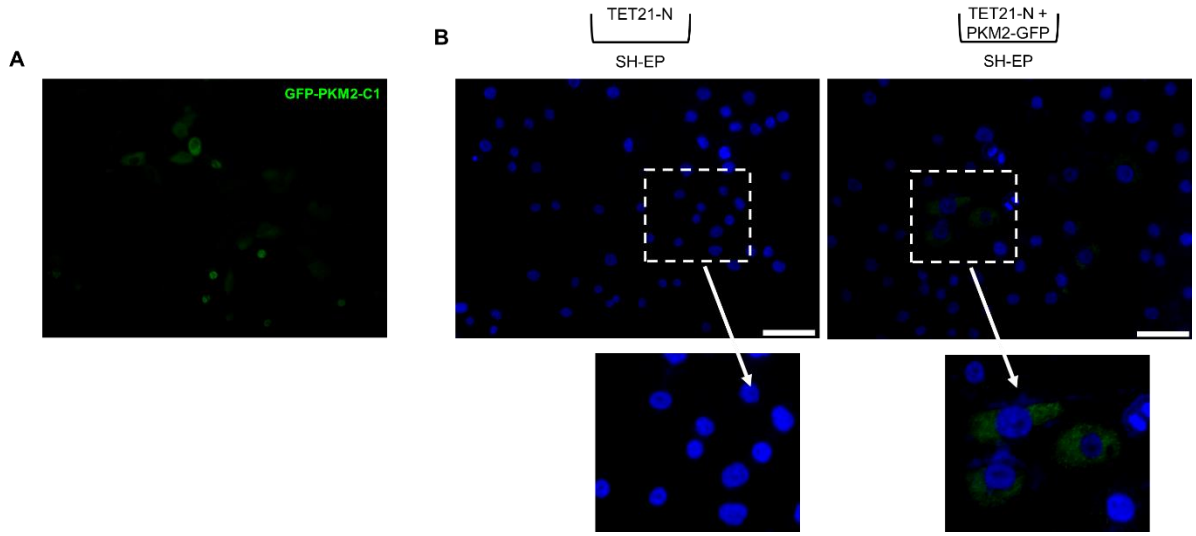

Figure 5.4: PKM2 is delivered via exosomes. A. TET21-N cells 24 h post-transfection with the GFP-PKM2-C1 plasmid. PKM2-GFP is expressed and localised in the cytoplasm and the nucleus. **B.** SH-EP cells after 24 h co-culture with TET21-N cells transfected or not with PKM2-GFP on the TC insert. SH-EP cells are receiving PKM2-GFP through the TC inserts indicating the transfer and delivery of PKM2 via exosomes secreted by TET21-N cells. Scale bar, 75 μm.

Histone H3 phosphorylation in SH-EP cells was significantly downregulated in the presence of the PKM2 siRNAs or when the expression of MYCN was turned off in donor cells, strongly suggesting that the transfer of PKM2 is essential to induce histone H3 phosphorylation in recipient cells (Fig. 5.5B).

Since histone H3 phosphorylation is tightly linked to mitosis, we calculated the mitotic index of SH-EP cells cultured in the different conditions and verified that the mitotic index was high when MYCN was activated, but reduced to baseline levels when MYCN was switched off or PKM2 was inhibited by siRNAs in the donor cells (Fig. 5.5C).

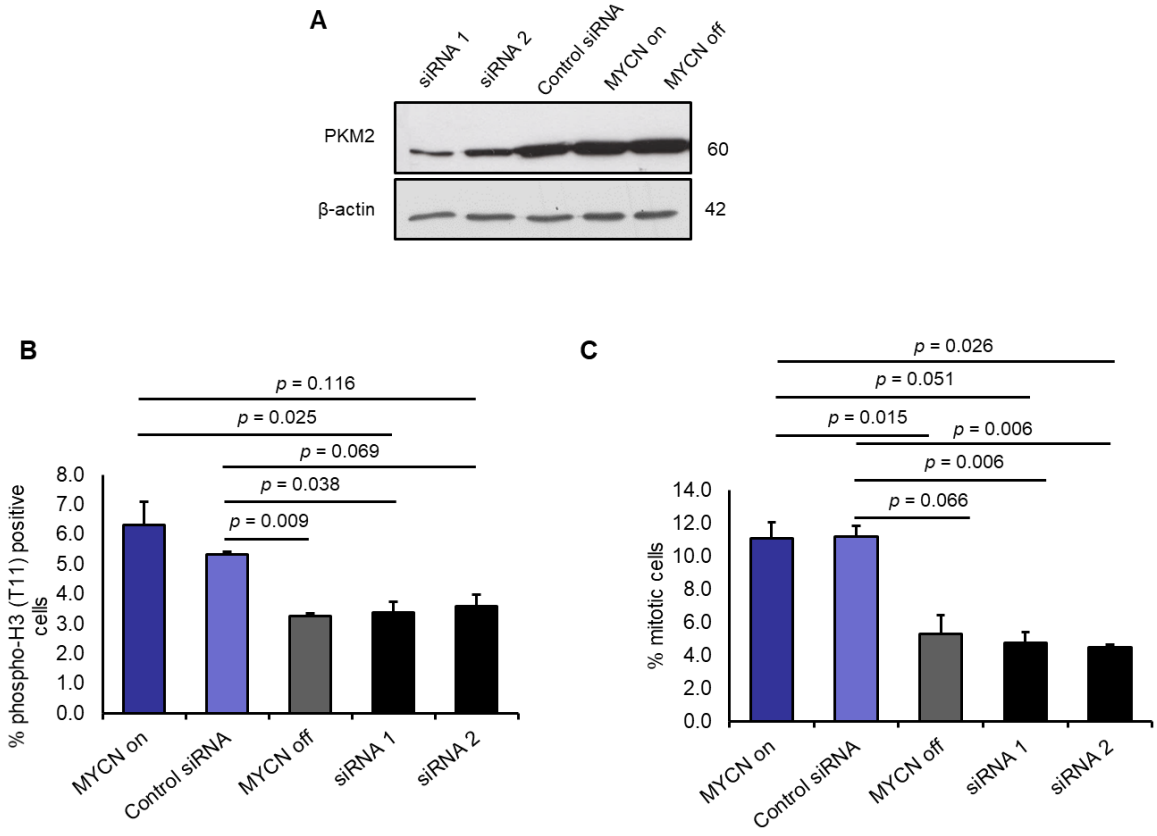

Figure 5.5: siRNA mediated knock-down of PKM2 in the donor cells inhibits the increase of histone H3 phosphorylation. A. Western blot analysis demonstrating siRNA mediated knock down of PKM2 by two different siRNAs in TET21-N cells. β-actin was used as a loading control. **B.** siRNA mediated knock down of PKM2 in TET21-N donor cells inhibits histone H3 phosphorylation (n = 3). **C.** Mitotic index. The mitotic index is expressed as the percentage of cells in mitosis (prophase, metaphase, anaphase, telophase) over the total number of cells (n=3). Error bars represent SEM.

To further test that the increase of histone H3 T11 phosphorylation was a result of the transfer of PKM2 in the recipient cells, we transfected SH-EP cells with plasmids encoding GFP or PKM2-GFP and we stained them for phospho-histone H3 (T11) 48 hours later. We confirmed that the ratio of phospho-histone positive cells to transfected cells was higher when the cells were transfected with PKM2-GFP (Fig. 5.6).

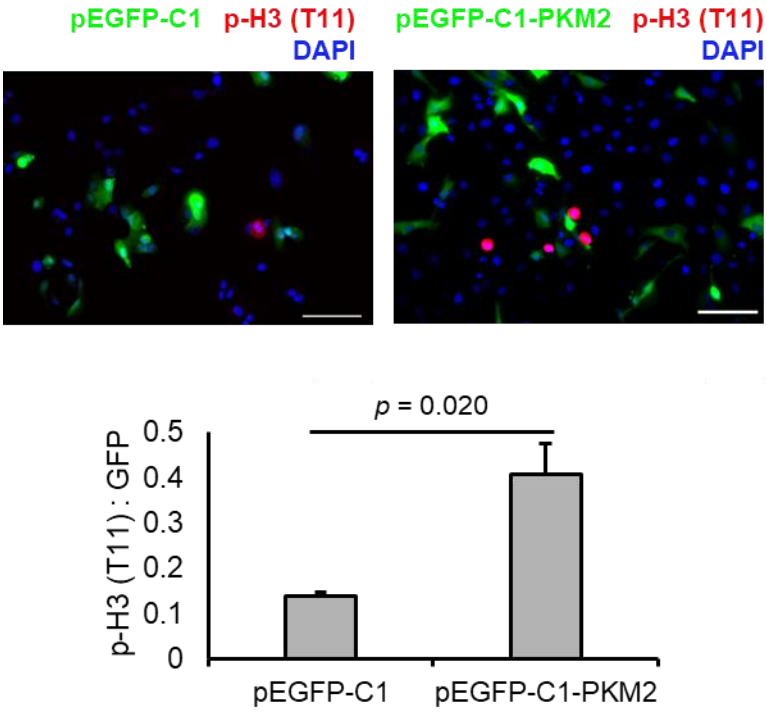

Figure 5.6: PKM2 overexpression leads to increased number of histone H3 T11 phosphorylated cells. SH-EP cells were transfected with vectors encoding GFP or PKM2-GFP and the ratio of p-H3 (T11) positive cells to transfected cells was quantified (n=3). Scale bar, 100 µm. Error bars represent SEM.

To increase the clinical relevance of these results, we investigated whether exosomes isolated from the plasmas of neuroblastoma patients could also induce phosphorylation of histone H3 on threonine 11, focusing on interphase cells. The intensity of histone H3 (T11) phosphorylation in interphase SH-EP cells was statistically significantly increased after incubation with exosomes purified from patients with MYCN amplified neuroblastomas, compared to patients with non-MYCN amplified tumours or children without cancer, supporting the results obtained with the cell line systems (Fig. 5.7).

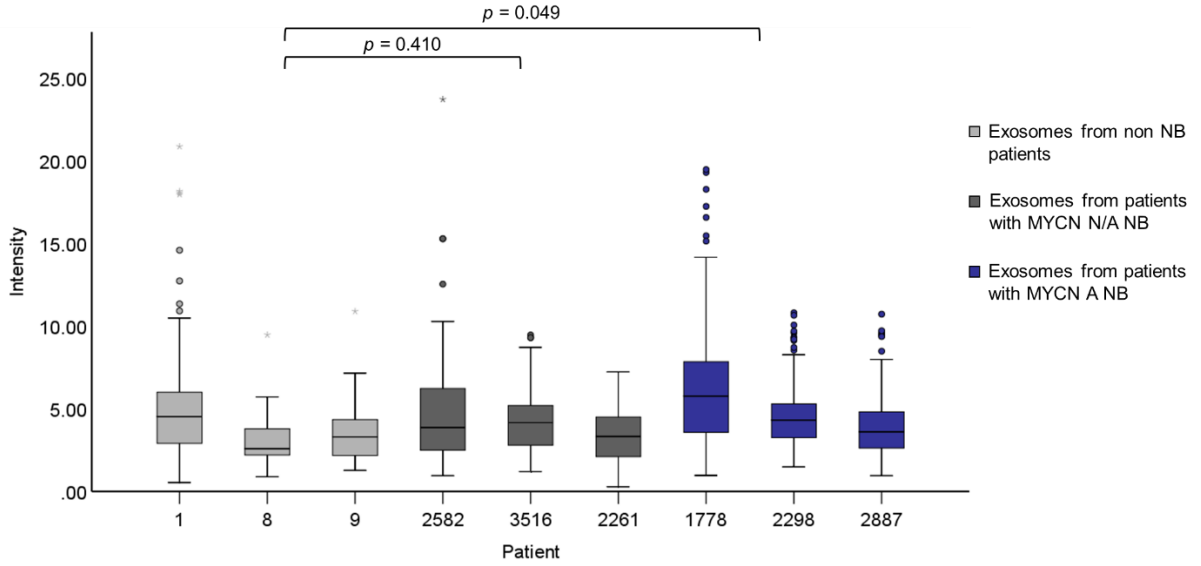

Figure 5.7: Exosomes circulating in the blood of neuroblastoma patients induce histone H3 phosphorylation (T11) in SH-EP cells. SH-EP cells were treated with exosomes isolated form plasma samples of neuroblastoma or non-cancer patients and stained with an antibody against phospho-H3 (T11). The intensity of the staining was compared with an independent-samples t test. Lavene's test was used to check the assumption of equal variances.

5.2.3. Exosome uptake leads to c-MYC activation in c-MYC non-expressing cells

A consequence of epigenetic modification of histones induced by nuclear PKM2 is the activation of c-MYC (Yang, et al., 2012). We therefore quantified c-MYC expression by immunofluorescence analysis in SH-EP cells, a c-MYC negative cell line, exposed to purified exosomes or co-cultured in transwell chambers with TET21-N cells in MYCN induced or un-induced conditions.

Exosomes purified from TET21-N cells with activated MYCN induced a higher expression of c-MYC than exosomes purified from cells in which MYCN expression has been switched off (Fig. 5.8A and B). Similarly, c-MYC expression was significantly increased in SH-EP cells co-cultured with TET21-N cells with MYCN switched on, compared to the condition in which MYCN was switched off (Fig. 5.8C).

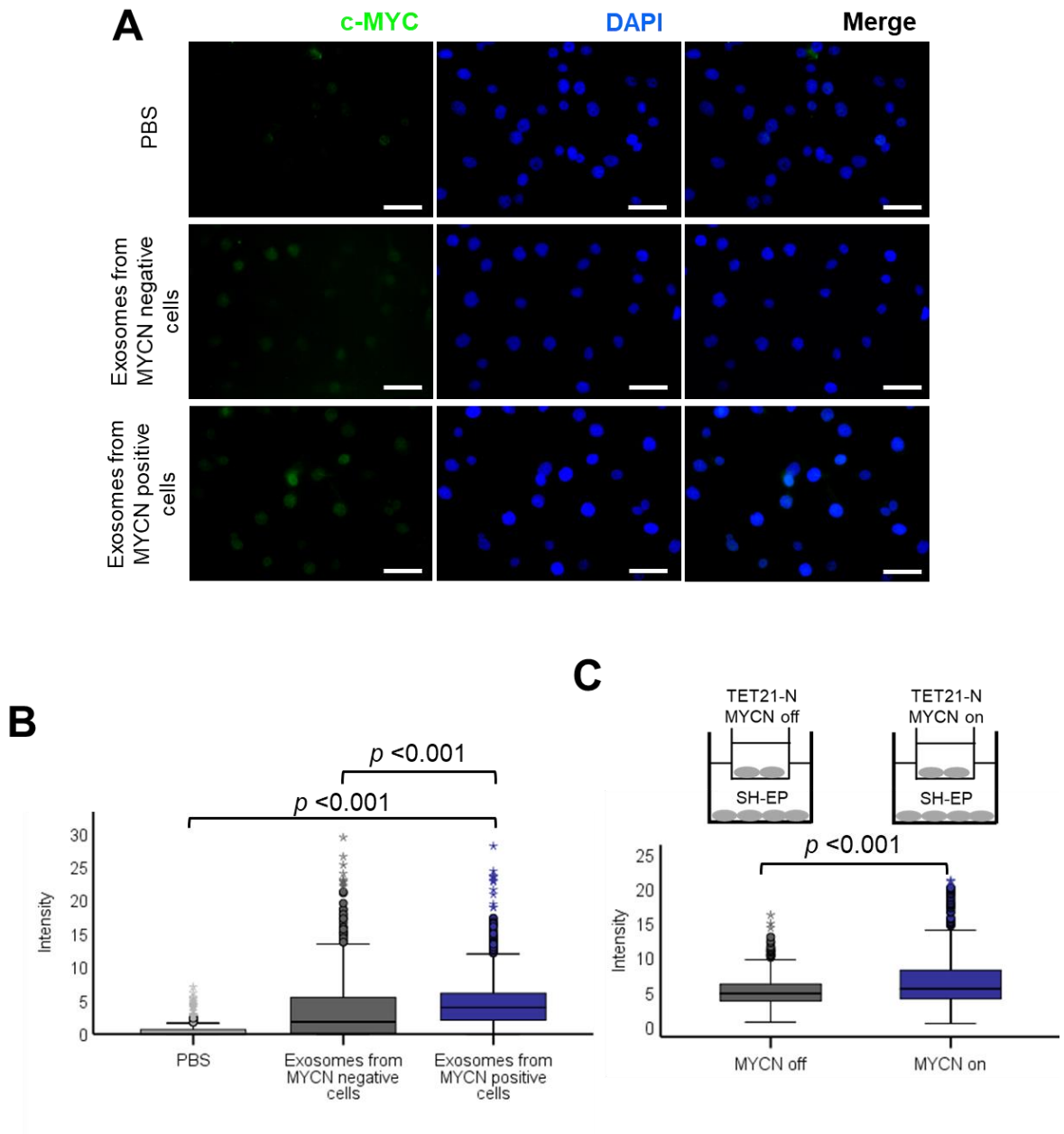

Figure 5.8: Exosomes from MYCN positive cells induce c-MYC expression in neuroblastoma cells that do not express c-MYC. **A.** SH-EP cells were treated with exosomes from MYCN positive or negative cells for 24 h and stained with an antibody against c-MYC. PBS was used as a control. Scale bar, 50 μm. **B.** Quantification of the intensity of the c-MYC staining (n=3). **C.** Quantification of c-MYC immunofluorescence staining in SH-EP cells after 24 h co-culture with TET21-N cells expressing or non-expressing MYCN (n=3).

To test if the interplay between MYCN positive neuroblastoma cells and c-MYC activation is relevant in the environment of a neuroblastoma tumour we used the syngeneic mouse model

of neuroblastoma (TH-MYCN) and we stained serial sections of the same tumour for MYCN or c-MYC. Intriguingly, c-MYC expression is detected in stromal cells surrounding nests of MYCN positive neuroblastomas (Fig. 5.9).

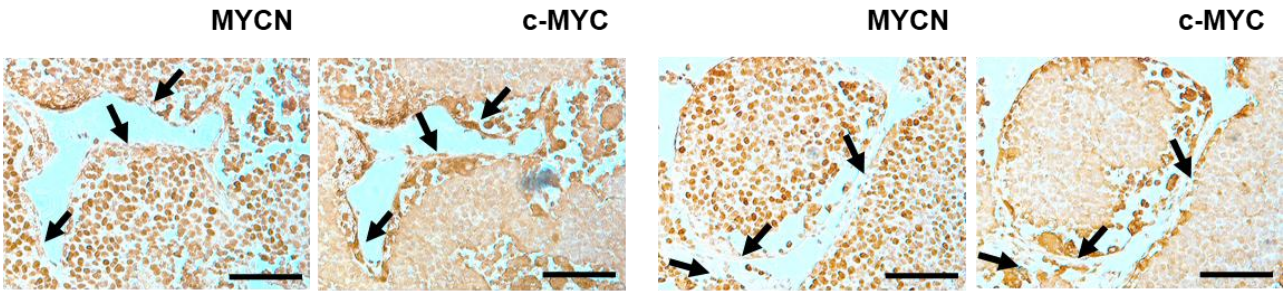

Figure 5.9: c-MYC is expressed in around MYCN positive neuroblastoma nests of neuroblastoma tumours. Stromal cells surrounding MYCN positive tumour nests express c-MYC. Neuroblastoma tumours developing in TH-MYCN mice were fixed, embedded in paraffin and serial sections stained with MYCN or c-MYC antibodies. Arrows indicate stromal cells negative for MYCN but expressing c-MYC. Scale bar, 75 μm.

This does not prove that c-MYC is activated in the stromal cells upon the uptake of neuroblastoma secreted exosomes, but it gives us an insight of the potential biological significance of this pathway. An *in vivo* model for the inhibition of exosome secretion should be developed in order to address whether c-MYC is activated in the stromal cells around neuroblastoma tumours only when the neuroblastoma cells are able to secrete exosomes towards the extracellular space.

Finally, after we established the induction of the protein levels of c-MYC following the treatment of cells with exosomes from MYCN positive neuroblastoma cells, we wondered whether we could detect a similar induction on the transcriptional level for *cMYC* and *cyclinD1*, a direct link between PKM2-mediated histone H3 (Thr11) phosphorylation and gene expression. To check that, we used the TC inserts system to co-cultured SH-EP cells with MYCN positive or negative TET21-N cells and we isolated RNA from the SH-EP cells 24 h after the co-culture to use for RT-qPCR (Fig. 5.10).

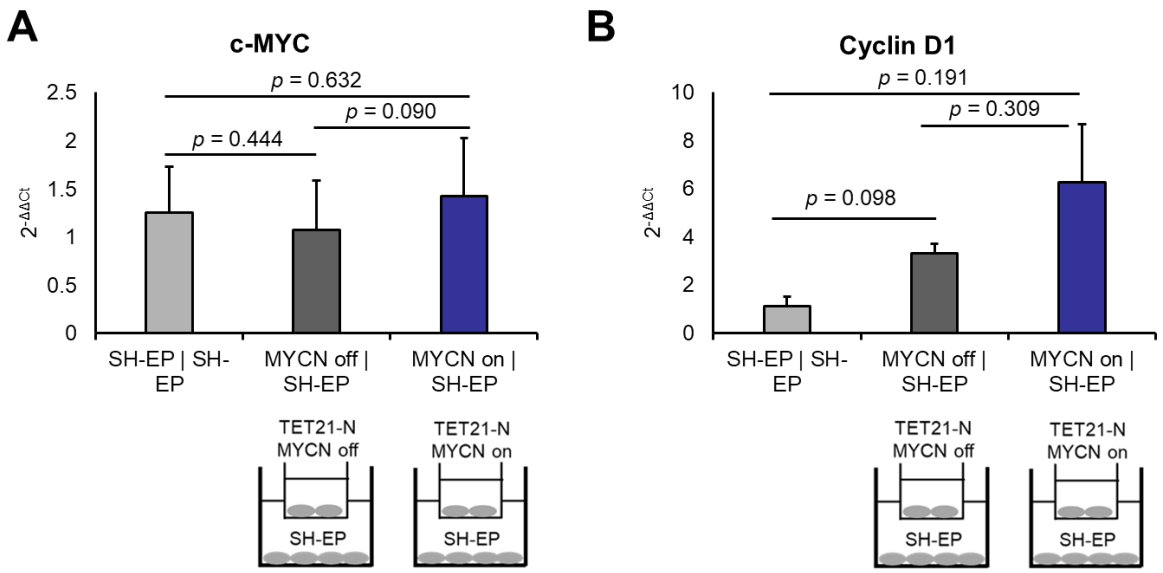

Figure 5.10: The mRNA levels of c-MYC and cyclin D1 could be altered when SH-EP cells are co-cultured with TET21-N cells. qPCR with cDNA from SH-EP cells after 24 h co-culture with TET21-N cells with or without MYCN expression for c-MYC (**A**) and cyclin D1 (**B**). Actin was used as a housekeeping gene. The graphs are representing the value of $2^{-\Delta\Delta Ct}$ (n = 3). Error bars represent SEM.

The qPCR for c-MYC and cyclin D1 did not reveal the transcriptional induction of the genes as we expected. Since these results are preliminary, we cannot be sure of whether the genes are indeed not induced or if the induction we see for c-MYC on the protein level is a result of translational modification and stabilisation of the c-MYC transcript without the increase of the mRNA levels of the gene. This potential should be exploited further with more experimental replicates and also with the use of purified exosomes.

5.3. Discussion

In summary, in this part we have shown that PKM2 is delivered via exosomes in the recipient cells. Neuroblastoma cells secreted exosomes enriched in PKM2 are able to induce the phosphorylation of histone H3 on the threonine 11 residue and increase the mitotic index of the recipient cells. Both these effects are inhibited by depleting the expression of PKM2 in the donor cells, indicating the major role of the kinases in the function and biological activity of the exosomes secreted by MYCN positive neuroblastoma cells. Finally, exosomes isolated from plasma samples of neuroblastoma patients with MYCN amplified neuroblastoma induce the levels of histone H3 (T11) phosphorylation in SH-EP cells in the interphase, indicating the clinical relevance of our findings.

To better understand the role of exosomal PKM2 and hexokinase II in regulating gene expression and cancer cell behaviour in the context of MYCN amplified neuroblastoma, we could generate MYCN amplified neuroblastoma cell lines with genetically inactivated PKM2 and hexokinase II. Short term inhibition of PKM2 expression using siRNAs did not result in overt loss of cell viability (Fig. 5.5A and data not shown). We could therefore employ the CRISPR/Cas9 technology, which allows precision DNA editing, to generate stable neuroblastoma cell lines depleted of the glycolytic enzymes. For this purpose, the classic MYCN amplified cell lines KELLY and IMR-32 could be used, since these have been found to be susceptible to CRISPR/Cas9 manipulations in our laboratory. Subsequently, the exosomes secreted by cells with edited PKM2 or hexokinase II could be purified by ultracentrifugation and subjected to Western blot analysis to confirm that the kinases have been depleted in the microvescicles.

PKM2 and hexokinase II activities are linked to AKT function in tumours (Nogueira, et al., 2018; Tao, et al., 2019). This is intriguing in the light of our observation that exosomes from MYCN positive cells rapidly induce AKT activity in neuroblastoma SH-EP cells (Fig. 4.4). An interesting approach would be to detect AKT activity in SH-EP cells exposed to exosomes with or without the glycolytic kinases. One could hypothesise that focal expression of MYCN in a heterogeneous neuroblastoma tumour will, by releasing exosomes containing glycolytic enzymes, promote AKT activity in the surrounding tumour cells and stroma. This hypothesis

is corroborated by our preliminary data indicating that focal expression of the human MYCN transgene in TH-MYCN mice is accompanied by homogeneously high expression of activated AKT (Fig. 4.5).

Finally, the potential role of exosomes in inducing epigenetic modifications in the recipient cells is of high interest, since it would reveal a mechanism through which the exosomes would induce permanent changes in the gene expression profile of the recipient cells. Although our results on the protein levels of c-MYC are intriguing, we should further investigate and understand what is happening on the transcriptional level.

6. Results IV: MYCN regulates histidine phosphorylation via exosome secretion

6.1. Introduction

Cells regulate the activity of proteins by adding or removing a phosphate group, i.e. a molecule containing phosphorus, a chemical reaction called phosphorylation. The main function of phosphorylation is to turn on or off protein activity, resulting in the normal operation of different cell systems. The addition or removal of phosphate groups from proteins is under the control of enzymes called kinases and phosphatases, respectively. In cancer, the modification of proteins by phosphorylation is often aberrant, causing increased cancer growth and metastasis (Lu & Hunter, 2018).

In the preliminary mass spectrometry screening of the exosomes secreted by neuroblastoma cells, we found that neuroblastoma cells with high levels of MYCN can transfer a specific class of kinases to other cells using these small vesicles, the histidine kinases NME1 and NME2.

NME1 and *NME2* (also known as *nm23-H1/H2*), encoding the nucleotide diphosphate kinases NME1 and NME2 (also known as NDPKA and NDPKB, respectively), have been previously identified as cancer-related genes that can suppress or promote tumour growth in a context-dependent manner. *Nm23* has been originally described as a gene with high expression in cancer cells with low metastatic potential (Steeg, et al., 1988) and has been believed to be a tumour suppressor since after, with evidence of its tumour supressing role in breast cancer (Heimann, et al., 1998), melanoma (Flørenes, et al., 1992) and colon and gastric cancers (Han, et al., 2016). However, other reports show overexpression of the gene and correlation with poor prognosis for the patient in haematological malignancies (Yokoyama, et al., 1998) and most recently in hepatocellular carcinoma, where the histidine phosphatase LHPP is inactivated and acts as a tumour suppressor (Hindupur, et al., 2018).

In neuroblastoma, NME1 has been shown to play a pro-tumourigenic and pro-metastatic role, and its mRNA expression is increased by the key neuroblastoma oncoprotein MYCN (Hailat, et al., 1991). Intriguingly, in non-Hodgkin's lymphoma, acute myelogenous leukaemia and also neuroblastoma the serum levels of NME1/2 are clinically significant and can be used as prognostic factors (Niitsu, et al., 2000; Okabe-Kado, 2002; Okabe-Kado, et al., 2005). Although

a tumour-promoting role of extracellular NME1/2 has been emerged in the last years in a number of tumour cohorts, no secretory mechanism has been described explaining how histidine kinases are found circulating in the plasma of cancer patients.

6.1.1. Aims

In the final results chapter, our aim is to explore the relationship between MYCN and histidine phosphorylation. Taking into consideration the clinical significance of serum NME1 in neuroblastoma and the fact that NME1 and NME2 were identified in the mass spectrometry screening of the exosomes secreted by neuroblastoma cells, we aim to investigate whether MYCN can regulate the levels of histidine phosphorylation and whether that ability can be transferred to distant cells via the exosomes secreted by MYCN positive neuroblastoma cells. Our goal is to understand whether MYCN promotes neuroblastoma growth and survival via secretion of NME1/2 kinases and concurrent inactivation of the histidine phosphatase LHPP.

6.2. Results

6.2.1. Expression of the histidine kinases NME1/2 is predictive of poor outcome in neuroblastoma

As mentioned above, it has been shown that the mRNA levels of *NME1* are increased in *MYCN* amplified neuroblastoma (Hailat, et al., 1991). Therefore, we were interested in the relationship between the expression of the histidine kinases NME1/2 and the histidine phosphatase LHPP and the prognosis of neuroblastoma patients.

To test that, we used gene expression data available on the R2: Genomics Analysis and Visualization Platform and two different cohorts of neuroblastoma patients, Kocak and SEQC. We plotted the patient's event free survival probability against high or low expression of the genes of interest and we also compared the expression of *NME1*, *NME2* and *LHPP* in patients with *MYCN* amplified or non-amplified neuroblastomas. Not to our surprise and as suggested by the literature on NME1, both kinases are predictive of poor outcome for the neuroblastoma patients when expressed in high levels, while the opposite happens with the histidine phosphatase LHPP (Fig. 6.1A). More importantly, the kinases are expressed in higher levels when *MYCN* is amplified and, again, the opposite happens with LHPP, which seems downregulated in *MYCN* amplified neuroblastomas (Fig. 6.2B).

These observations suggest that histidine phosphorylation plays a critical role in neuroblastoma biology and may facilitate in some way the aggressiveness of *MYCN* amplified tumours. Therefore, it seems important to further investigate the interplay between MYCN and the molecules regulating histidine phosphorylation in neuroblastoma.

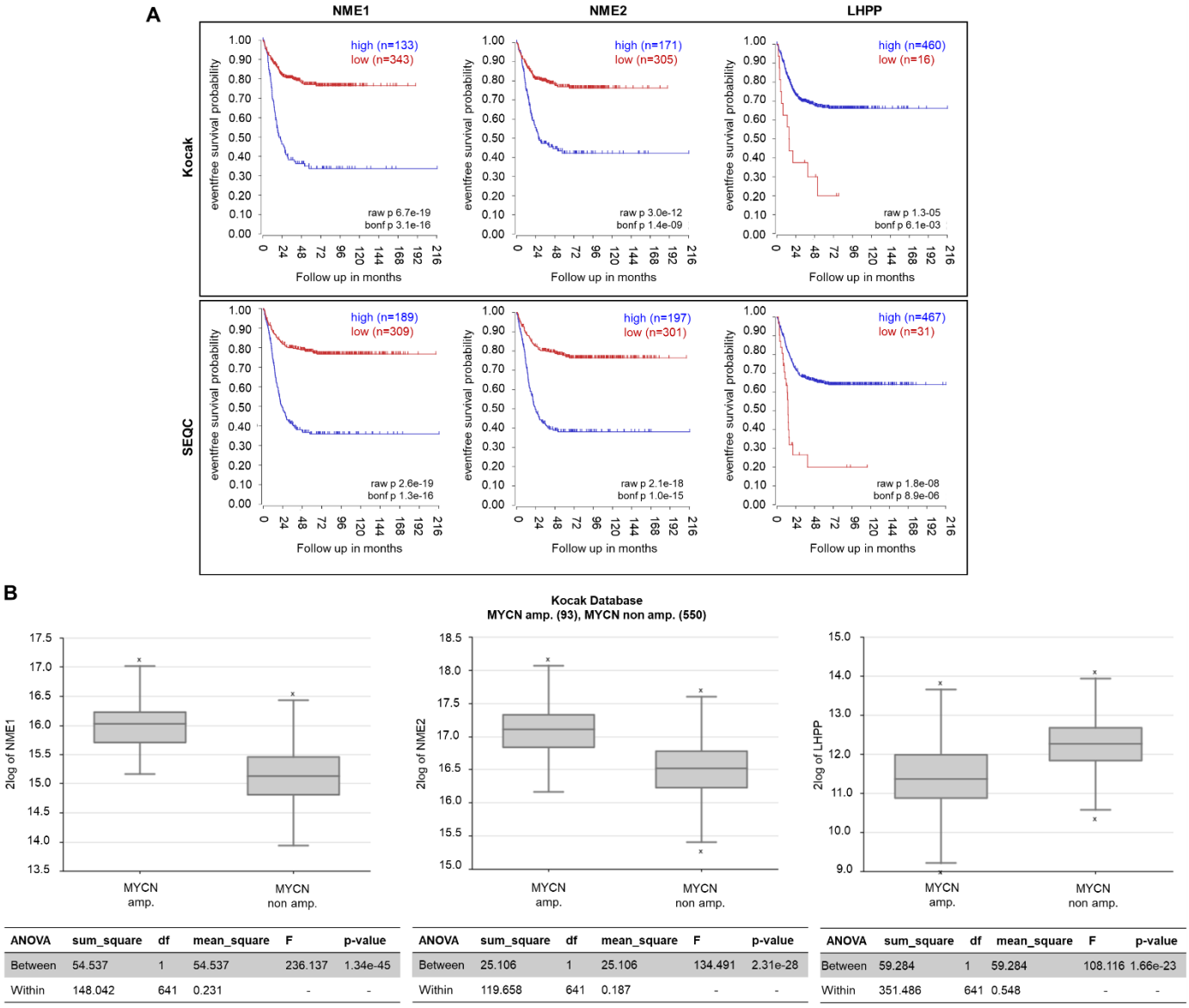

ANOVA	sum_square	df	mean_square	F	p-value
Between	54.537	1	54.537	236.137	1.34e-45
Within	148.042	641	0.231	-	-

ANOVA	sum_square	df	mean_square	F	p-value
Between	25.106	1	25.106	134.491	2.31e-28
Within	119.658	641	0.187	-	-

ANOVA	sum_square	df	mean_square	F	p-value
Between	59.284	1	59.284	108.116	1.66e-23
Within	351.486	641	0.548	-	-

Figure 6.1: mRNA expression of the histidine kinases NME1/2 and the histidine phosphatase LHPP correlates with patient outcome in neuroblastoma. **A.** Kaplan-Meier survival curves showing the correlation of gene expression for *NME1*, *NME2* and *LHPP* and neuroblastoma patients outcome. **B.** *NME1, NME2* and *LHPP* gene expression in *MYCN* amplified and non-amplified tumours.

6.2.2. MYCN induces the expression of NME1/2 in neuroblastoma cells

MYCN has been shown to be a transcriptional regulator of NME1 in neuroblastoma and the gene expression data suggest that this is the case for NME2 and LHPP as well. Therefore, we wanted to check the protein levels of NME1/2 and LHPP in the TET21-N cells with or without MYCN expression. Not surprisingly, TET21-N cells expressing MYCN have higher levels of both

NME1 and NME2 and lower levels of LHPP compared with TET21-N cells that have been treated with doxycycline for 48 h in order to turn off MYCN expression (Fig. 6.2A and B).

To further validate the role of MYCN in the regulation of the proteins of the histidine phosphorylation pathway, we checked the protein levels of NME1, NME2 and LHPP in neuroblastoma cell lines with naturally amplified (KELLY, IMR-32) or non-amplified (SH-EP, SK-N-AS) *MYCN.* Once again, NME1 protein levels were higher in the MYCN positive neuroblastoma cell lines. NME2 was low in both the MYCN negative cells lines, but KELLY cells didn't have very high levels either. Finally, the histidine phosphatase LHPP was absent from KELLY and expressed in relatively low levels in the IMR-32 cells (Fig. 6.2C).

These results indicate the role of MYCN in regulating the total levels of the proteins directly implicated in the histidine phosphorylation status of the cells.

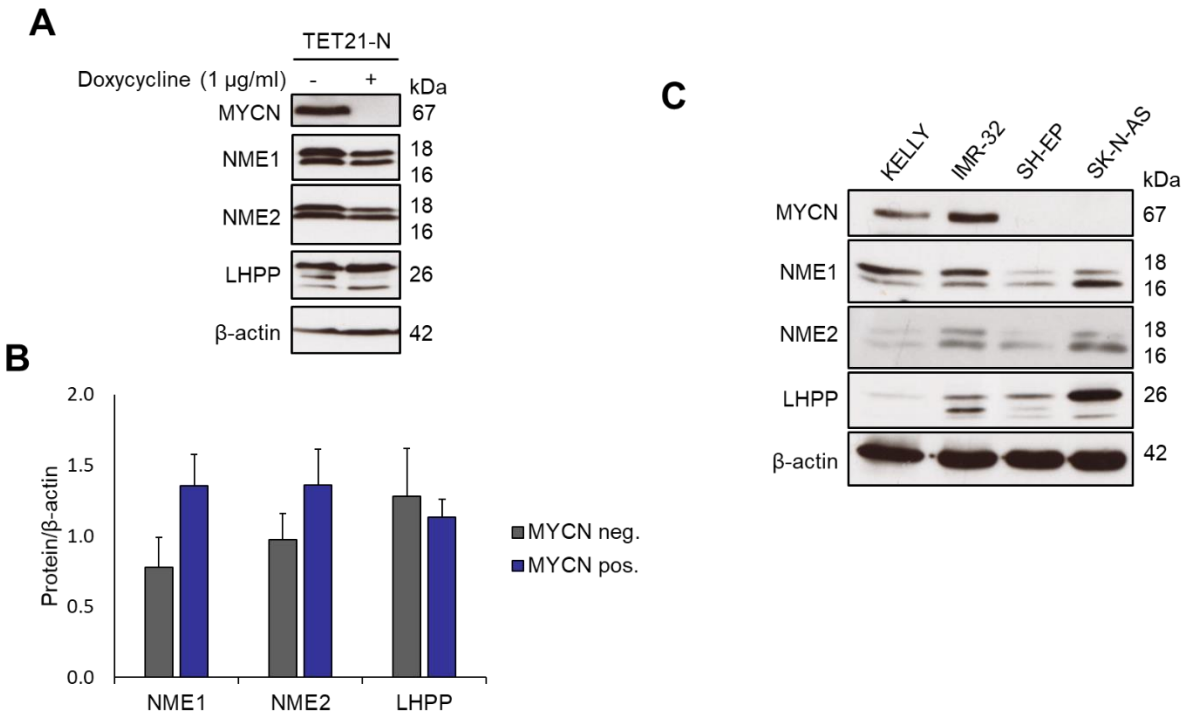

Figure 6.2: MYCN upregulates the histidine kinases NME1 and NME2 and the total levels of histidine phosphorylation in neuroblastoma cells. A. Western blot analysis of the total cell lysates of TET21-N cells in the presence or not of doxycycline reveals that MYCN positive cells have higher levels of the histidine kinases NME1 and NME2 and less LHPP. β-actin was used as a loading control. **B.** The intensity of the bands of independent experiments was quantified using ImageJ and normalised with the loading control's intensity (n=3). Error bars represent SEM. **C.** Western blot analysis of cell lines with naturally amplified (KELLY, IMR32) or non-amplified (SH-EP, SK-N-AS) MYCN for NME1/2 and LHPP. β-actin was used as a loading control.

6.2.3. Exosomes secreted by neuroblastoma cells contain the histidine kinases NME1 and NME2

The histidine kinases NME1 and NME2 were among the proteins identified with the mass spectrometry analysis to be differentially expressed in the exosomes of MYCN positive and negative TET21-N cells (Fig. 3.1). Therefore, we analysed exosomes from MYCN positive and negative neuroblastoma cells with Western blot to validate the presence of the two proteins in the exosomes isolated from cell culture supernatant media (Fig. 6.3).

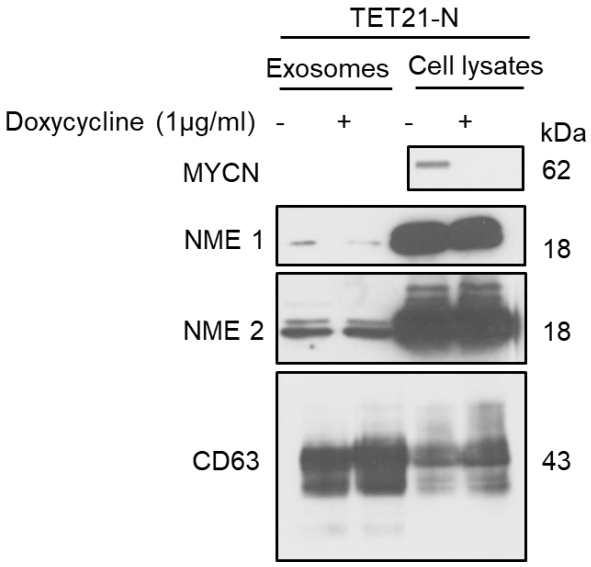

Figure 6.3: NME1 and NME2 are transferred within the exosomes of neuroblastoma cells. Western blot analysis of exosomes and total cell lysates of TET21-N cells in the presence or not of doxycycline reveals that MYCN-induced exosomes contain the histidine kinases NME1 and NME2. CD63 was used as a loading control.

As expected and consistent with the mass spectrometry data, NME1 and NME2 are present in the exosomes secreted by neuroblastoma cells. Their levels seem to be slightly higher in the exosomes secreted by MYCN positive neuroblastoma cells.

6.2.4. Exosomes secreted by MYCN positive neuroblastoma cells upregulate the total levels of histidine phosphorylation in recipient cells

Since the histidine kinases NME1 and NME2 are transferred via the exosomes isolated from the cell culture supernatant media of neuroblastoma cells, we wondered whether the exosomes are capable of inducing the levels of histidine phosphorylation in the recipient cells.

To test that, we isolated exosomes from MYCN positive or negative TET21-N cells and we used them to treat SH-EP cells for 15, 60 or 360 minutes. Immediately after the treatment, the SH-EP cells were directly lysed and the protein lysates from equal numbers of cells were immunoblotted with a modified Western blot protocol (see section 2.9.1) for N1 or N3 phospho-histidine (Fig. 6.4).

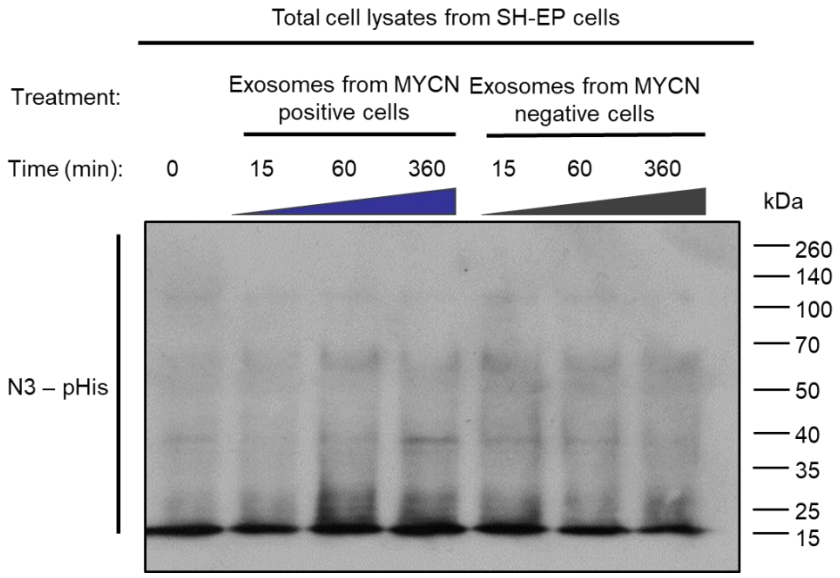

Figure 6.4: MYCN-induced exosomes upregulate the total levels of histidine phosphorylation in MYCN non-amplified cells. Western blot analysis of total cell lysates obtained by SH-EP cells after treatment with exosomes from MYCN positive or negative TET21N cells against N3-phosphohistidine.

Although we weren't able to detect N1 phospho-histidine, the results obtained with the antibody against the N3 type of histidine phosphorylation suggest that the exosomes isolated from MYCN positive TET21-N cells are more competent in inducing histidine phosphorylation in the recipient cells. This result indicates that the kinases transferred within the exosomes can be delivered successfully in the target cells and remain biologically active.

6.3. Discussion

In this chapter we presented preliminary data about the role of MYCN in the regulation of histidine phosphorylation in neuroblastoma cells and the potential transfer of this activity to distant cells via the delivery of exosomes containing the histidine kinases NME1 and NME2.

NME1 belongs to a family of enzymes initially classified as nucleotide diphosphate kinases. More recently, it has been shown that NME1 and NME2 are also histidine protein kinases, responsible for almost the totality of this protein modification in mammalian cells (Adam & Hunter, 2018). NME1/2 activity and histidine phosphorylation have been recently linked to liver tumourigenesis (Hindupur, et al., 2018) and although they have been suggested as tumour and metastasis suppressors, the role of histidine kinases in many tumours is controversial, with neuroblastoma being an example of a cancer in which histidine kinases act in a tumour-promoting manner.

NME1 is known to be a transcriptional target of MYCN and is suspected to be involved in neuroblastoma aggressiveness, since its gene expression strongly correlates with poor survival (Fig. 6.1) (Almgren, et al., 2004; Godfried, et al., 2002). In further support of this hypothesis, we have observed that the expression of the histidine phosphatase and tumour suppressor gene *LHPP* is inversely correlated with MYCN amplification in neuroblastomas and its low expression predicts poor patient survival (Fig. 6.1).

It has been known for many years that the product of the *NME1* gene can be secreted by cancer cells and the presence of NME1 protein in the sera of patients with neuroblastoma significantly correlates with clinical outcome (Okabe-Kado, et al., 2005). However, there is no known mechanism describing the secretion of NME1 or NME2 into the extracellular space. We showed that exosomes secreted by MYCN positive cells induce rapid histidine phosphorylation of specific proteins in target cells (Fig. 6.4), suggesting that MYCN could promote the aggressive behaviour of recipient cells via this protein modification. Our results indicate that NME1/2 can be localised into the exosomes that are secreted by neuroblastoma cells and the fact that the treatment of cells with these exosomes leads to increased histidine phosphorylation suggests that the kinases maintain their enzymatic activity and can induce histidine phosphorylation in the cells targeted by the exosomes. Intriguingly, exosomes produced by MYCN positive neuroblastoma cells, which correlate with enhanced growth and

metabolic activity, as discussed in the previous chapters, induce histidine phosphorylation in recipient cells more efficiently than exosomes produced by MYCN negative cells.

Collectively, these observations prompt us to form the hypothesis that aggressive neuroblastoma cells expressing MYCN produce and send to recipient cells little packages containing enzymatically active kinases.

The results of this chapter are preliminary and further experiments should be performed in order to validate the data and help us come to solid conclusions about the interplay between MYCN and histidine phosphorylation in neuroblastoma. The clinical significance of serum circulating NME1/2 strongly supports our hypothesis that the histidine kinases can be secreted and transferred within exosomes. We tried to validate the presence of NME1 and NME2 in the plasma samples of neuroblastoma patients, but we weren't able to detect them. The process of isolation and handling of these proteins and the really sensitive nature of histidine phosphorylation makes these experiments quite intricate, so the fact that we couldn't manage to detect the proteins implicated in histidine phosphorylation in the patients' samples could possibly be a result of technical failure.

Moreover, further experiments need to be performed in order to validate our *in vitro* findings about the ability of NME1/2-containing exosomes to induce histidine phosphorylation in the recipient cells. In order to identify the key protein substrates of NME1/2 phosphorylation in neuroblastoma cells, protein lysates from cells exposed to exosomes containing or not NME1/2 could be subjected to immunoprecipitation with antibodies targeting N1- or N3-phospho-histidine and analysed with mass spectrometry analysis. The most interesting candidates (e.g. proteins involved in cell division, regulation of DNA repair, cell signalling, cell survival) could be then subjected to functional validations and clinical correlations using *in silico* tools.

To further explore the interplay between neuroblastoma secreted exosomes end histidine phosphorylation, we could generate MYCN amplified neuroblastoma cell lines in which the expression of NME1 and NME2 or the histidine phosphatase LHPP is genetically inactivated. LHPP inhibits NME1/2 histidine auto-phosphorylation, a key step to activate the protein kinase activity. To this purpose, we could use the CRISPR/Cas9 technology that allows precision DNA editing. The exosomes secreted by cells with edited NME1, NME2 or LHPP

could then be purified by ultracentrifugation and subjected to Western blot assays to confirm that NME1/2 proteins have been depleted or activated, as expected. Secondly, the purified exosomes would be used in *in vitro* experiments to examine their biological effects. NME1/2 have been previously shown to promote neuroblastoma proliferation, migration and inhibit differentiation (Almgren, et al., 2004; Valentijn, et al., 2005). Thus, exosomes with low or high (by depletion of LHPP) NME1/2 protein levels/activity could be used to treat neuroblastoma cells that do not express MYCN.

Overall, we propose that there is the need for investigation of the role of exosome-mediated release of NME1/2 and histidine phosphorylation in the biology of neuroblastoma. By assessing whether phosphorylation induced by histidine kinases enriched in exosomes secreted by neuroblastoma cells can regulate the aggressiveness of the disease and unveiling new signalling pathways, novel diagnostic and therapeutic approaches could be exploited.

7. General discussion

7.1. Overview and significance of the study

The central hypothesis of this study is that tumours with focal amplification of *MYCN* have the potential to "condition" a) non-amplified cells of the tumour cells and b) cells of the tumour microenvironment by releasing exosomes packed with signalling proteins that induce behavioural changes (Fig.7.1).

MYC is a master gene required for the growth and development of stem cells and tissues. MYC family members are often activated in cancer and it is of vital importance to understand the mechanisms by which their alterations promote aggressive tumour growth. A full understanding of the function of MYC could potentially lead to the development of a cure for different types of human malignancies.

The role of MYC as a regulator of the tumour microenvironment, in addition to its intrinsic effects on cancer cells, is emerging. For example, c-MYC has been shown to alter immune cells metabolism and the cancer microenvironment by supporting the expression of HIF-1 and secretion of VEGF in tumour cells (Baudino, et al., 2002; Kim, et al., 2007; Podar & Anderson, 2010). In neuroblastomas, *MYCN* amplification is conductive to reduced immune infiltration (Zhang, et al., 2017; Wei, et al., 2018) and neuroblastoma cells have been shown to secrete microvesicles able to stimulate the production of pro-tumourigenic signals by bone marrow stromal cells (Nakata, et al., 2017). These studies prompted us to investigate the hypothesis that MYCN could exert non-cell autonomous effects by regulating the molecular cargo of exosomes.

Based on a preliminary mass spectrometry analysis of the protein content of exosomes isolated from MYCN positive and negative TET21-N neuroblastoma cells, we have identified distinct classes of proteins in neuroblastoma exosomes that are regulated by MYCN. Since the screen was carried out in an isogenic system, using a switchable *MYCN* transgene, there is confidence that the differences in protein content were only dependent on MYCN levels. In a recently published study, Fonseka *et al* have compared the protein content of exosomes purified from a single *MYCN* amplified versus a single *MYCN* non-amplified cell line. Using this approach, it is difficult to establish whether differences in exosomal proteins were related to

the levels of MYCN or the cell's genetic background. Nevertheless, knock-down of MYCN did induce changes of the biological properties of neuroblastoma exosomes, corroborating the view that the oncogene regulates the activity and content of microvescicles (Fonseka, et al., 2019).

After the identification of exosomal proteins potentially involved in important signalling and metabolic pathways, we mainly focused our attention on glycolytic kinases, since it is well established that MYC proteins are regulators of cell metabolism and the Warburg effect. MYC has been shown to regulate lactate production, glutaminolysis, and increase protein translation by promoting ribosome biogenesis (Dang, et al., 2009). Among the glycolytic enzymes enriched in neuroblastoma exosomes we identified hexokinase II and PKM2. PKM2 is of particular interest since this enzyme is an oncogene that not only promotes the Warburg effect, but also induces epigenetic changes through its nuclear function (Amin, et al., 2019). Notably, we detected the presence of hexokinase II and PKM2 in exosomes circulating in the blood stream of neuroblastoma patients and more frequently in those bearing *MYCN* amplified tumours. The glycolytic enzymes were undetectable in the exosomes of non-cancer patients, supporting the hypothesis that they are of cancer origin. Given that the expression of *PKM* and *HK2* in neuroblastoma samples are strong predictors of negative clinical outcome, analysis of the protein content of circulating exosomes could be used as a prognostic indicator and a non-invasive method for stratification of neuroblastoma patients.

Moreover, we studied the biological activity of neuroblastoma exosomes and we found that exosomes produced by cells expressing MYCN have a more potent biological activity than exosomes deriving from MYCN negative cells. For example, exosomes secreted by MYCN positive cells are more efficient inducers of growth and glycolysis than exosomes deriving from cells in which MYCN has been switched off. Furthermore, exposure of target cells to exosomes from MYCN positive neuroblastoma cells resulted in induced activation of the AKT kinase within five minutes after exposure. The PI3K/AKT signalling pathway plays a crucial role in neuroblastoma cell survival through stabilisation of MYCN. Importantly, the very fast response indicates that proteins, rather than nucleic acids, are required for the signalling effect.

The fact that PKM2 was identified in exosomes circulating in the blood stream of neuroblastoma patients made it the main focus in our study. Since PKM2 can be localised in the nucleus where it can directly bind histone H3, triggering its phosphorylation on the threonine 11 residue (Yang, et al., 2012), we used this modification as a readout for neuroblastoma exosomes effects. We verified that histone H3 (T11) phosphorylation is induced in cells that are exposed to exosomes secreted by MYCN positive neuroblastoma cells and that this phenotype is reversed after siRNA-mediated depletion of PKM2 in the MYCN positive donor cells. Most importantly, we found that the exosomes isolated from the plasma of neuroblastoma patients can also increase histone H3 (T11) phosphorylation in recipient cells. MYCN amplified cells are more sensitive to depletion of PKM2 than MYCN non-amplified cells, suggesting oncogenic addiction (Zhang, et al., 2016). This is because the PKM2 isoform is enriched in MYCN amplified neuroblastoma cells due to the ability of the MYC transcription factors to transactivate genes involved in RNA splicing, such as *PTBP1* and *HNRNPA1* (Zhang, et al., 2016; Cobbold, et al., 2010). It is tempting to speculate that the transfer of oncogenic kinases via exosomes operated by MYC mutant cells could contribute to the aggressive behaviour of the overall tumour mass by promoting the metabolic activity of cancer or stromal cells that do not carry oncogenic mutations. PKM2 enriched neuroblastoma exosomes have the potential to modify epigenetically recipient cells by enhancing histone H3 phosphorylation. This would permanently fix transient oncogenic signals, perhaps explaining why MYCN amplified tumours can revert to focally amplified and focally amplified to non-amplified during the evolution of the disease (Marrano, et al., 2017).

In this context, perhaps our most interesting observation is that exosomes secreted by MYCN expressing cells activate c-MYC expression in recipient SH-EP cells. High risk cancers with focally amplified *MYCN* might spread oncogenic signaling to parts of the tumour that are MYC negative or in infiltrating immune/stromal cells. Although we cannot exclude the possibility that the increased phosphorylation of histone H3 after incorporation of PKM2-enriched exosomes is consequential of a higher mitotic index, the activation of c-MYC strongly suggests that epigenetic changes might indeed occur in recipient cells.

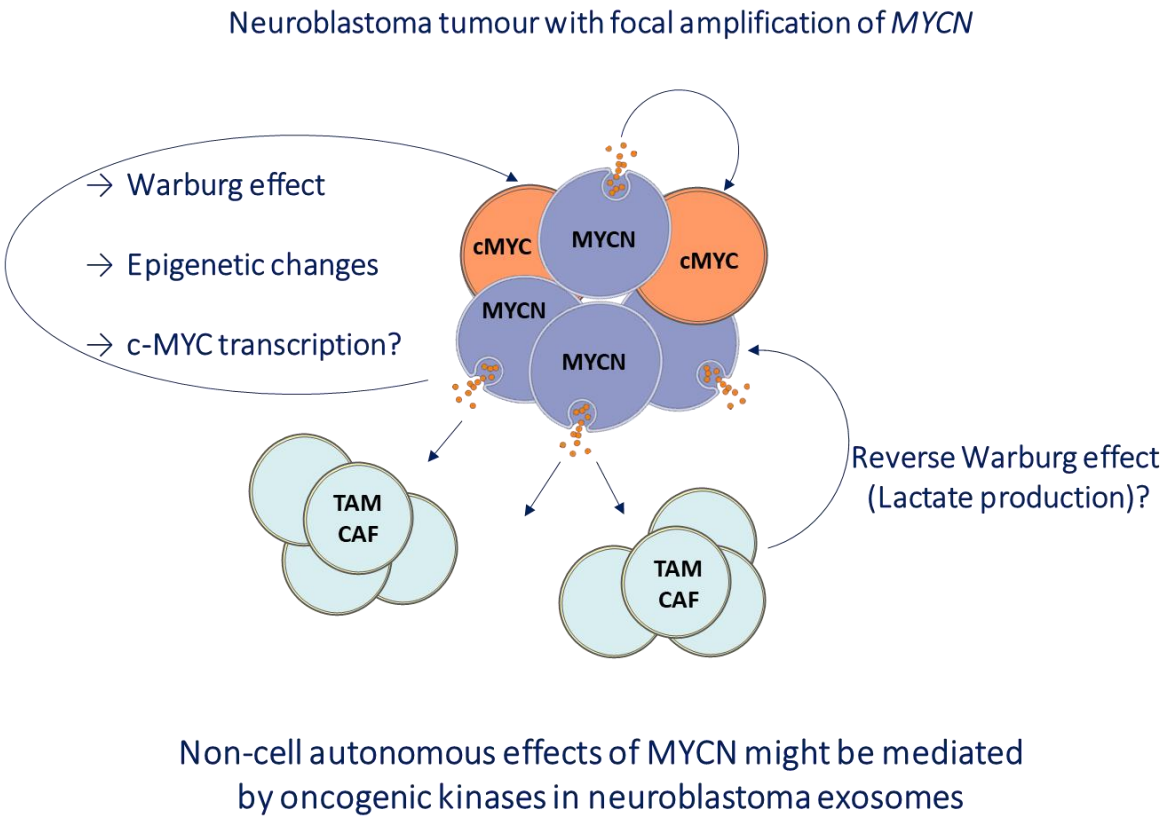

Figure 7.1: Proposed model. We suggest that MYCN positive neuroblastoma cells within a neuroblastoma tumour with focal amplification of *MYCN* communicate with the cells of the tumour and the tumour microenvironment by secreting exosomes containing kinases with oncogenic potential. The targeting of the recipient cells with these molecular active exosomes leads to behavioural changes that support tumour growth and metastasis of the aggressive neuroblastoma cells. Thus, MYCN acts in a non-cell autonomous manner in order to transfer its oncogenic action to distant locations.

A limitation of this study is that we have not examined the role of nucleic acids in neuroblastoma exosomes, although functional microRNAs have been previously detected in exosomes secreted by neuroblastoma cell lines or immune cells infiltrating neuroblastomas (Neviani, et al., 2019; Haug, et al., 2015). It is not possible to exclude that the transfer of MYCN-regulated microRNAs might have contributed to some of the biological effects observed in our study. However, siRNA-mediated inhibition of PKM2 in MYCN-expressing donor cells completely reversed the increase in histone H3 phosphorylation in recipient *MYCN* single copy cells, suggesting that this effect is at least partially regulated by protein transfer.

In conclusion, the results of our study suggest that *MYCN* amplified neuroblastomas might promote the spreading of oncogenic kinases and other biologically active proteins to the tumour microenvironment and remote body locations. Potentially, the proteins identified in our study could serve as biomarkers and targets for therapy in neuroblastoma and other cancers characterised by activation of MYC.

7.2. Future directions

In this study we tried to understand the role of exosomes in neuroblastoma biology. Importantly, we observed that these vesicles can change the behaviour of recipient neuroblastoma cells rendering them more aggressive. By understanding the mechanisms of vesicles secretion and potentially protein phosphorylation events following the uptake of neuroblastoma-secreted exosomes, it should be possible to develop drugs that interfere with these processes and, indirectly, mitigate the cancer-promoting activity of the key neuroblastoma oncogene MYCN.

Studies have shown that individual neuroblastoma tumours present a high degree of heterogeneity. Clonal species within the primary and metastatic sites are under constant selective pressure, promoting cancer aggressiveness and poor clinical outcome. One of the hypotheses that underpin this research is that these highly aggressive sub-clones, characterised by activation of the *MYCN* proto-oncogene, secrete vesicles containing molecules that condition the tumour microenvironment. Blocking this activity might thus result in the mitigation of the aggressive component of the cancer and a better patient outcome. Therefore, the understanding of the molecular mechanisms by which aggressive subtypes of tumour cells communicate oncogenic signals to other cells (either cancerous or normal) could be clinically exploited.

Specifically, dissecting the signalling pathways upstream and downstream of secreted exosomal proteins could lead to the development of small molecule inhibitors that could be used to target highly aggressive sub-clones of neuroblastoma cells, improving patient prognosis.

We have shown that exosomes released by MYCN-expressing neuroblastoma cells modify the behaviour of MYCN non-amplified recipient cells. Several proteins have been identified that could be required for this activity. The glycolytic kinases PKM2 and hexokinase II as well as the histidine kinases NME1 and NME2 are among the most interesting candidates. It seems that phosphorylation is one modification that is triggered by the uptake of exosomes secreted by MYCN positive neuroblastoma cells, therefore we could potentially take advantage of this mechanism and block it in order to validate its therapeutic value.

Collectively, our data highlight the need for the deeper study of the function of exosomes in neuroblastoma. The investigation of the role of exosome-mediated release of oncogenic kinases in neuroblastoma can help unveiling new modalities of cell to cell transmission of oncogenic signalling and could therefore prove useful for therapeutic purposes in cancers characterised by the activation of MYC oncoproteins.

7.2.1. Studying the role of neuroblastoma secreted exosomes *in vivo*

A very important point not addressed in this study is whether neuroblastoma exosomes regulate tumour growth *in vivo*. The design of an *in vivo* model for the study of the role of exosomes in neuroblastoma is crucial for the understanding of the therapeutic potentials that this pathway may hold for the disease.

To do that, we could grow neuroblastoma tumours in mice and use them as a model for the study of exosomes. To simulate tumour heterogeneity of *MYCN* amplification, we could inject the flanks of immunodeficient mice with a mixture of *MYCN* amplified (KELLY or IMR-32) and *MYC* single copy (SH-EP) neuroblastoma cells that are non tumourigenic and are representative of the Schwann stroma.

Our preliminary results suggest that exosomes secreted by high-risk neuroblastoma cells could transfer the oncogenic activity of MYCN to other cells. From a therapeutic perspective, blocking vesicles release could be a new and attractive modality of clinical intervention.

Well established chemical blockers of vesicle biogenesis and release, such as Rab27 inhibitors and the sphyngomyelinase inhibitor SW4869, are not clinically viable and relatively toxic to

cell lines *in vitro*. However, a recently published study has led to the identification of exosome inhibitors through a high throughput screen of clinically viable molecules. The antifungal molecule Ketoconazole and the farnesyltransferase inhibitor Tipifarnib were found to potently and specifically inhibit exosome biogenesis and release (Datta, et al., 2018). Both compounds are in clinical use and present favourable toxicity profiles. It could be really interesting, therefore, to validate the use of both drugs initially *in vitro* in order to verify that they are able to suppress the secretion of neuroblastoma vesicles and to antagonise the biological effects of exosomes.

Another approach to study the role of neuroblastoma-secreted exosomes in tumour growth could be to inject mice with *MYCN* amplified neuroblastoma cells unable to produce exosomes. It has been shown that Rab GTPases control the pathways that lead to exosome secretion and that silencing of Rab27a or Rab27b inhibits exosome secretion (Ostrowski, et al., 2010). That means that neuroblastoma cells engineered to stably express an shRNA vector targeting Rab27a or Rab27b should not be able to secrete exosomes. This is easy to follow, if the cells also carry a vector for the overexpression of a CD63-GFP fusion protein which will accumulate in the exosomes generated in the endosomal pathway and mark them green. So, in essence, neuroblastoma cells stably transfected with a CD63-GFP expression vector would secrete 'green' exosomes in the cell culture supernatant media, while cells an shRNA against Rab27a/Rab27b should not secret them. After an *in vitro* validation of this system, the two different stable cell lines could be injected into mice and the growth of neuroblastoma tumours generated from neuroblastoma cells able to secrete or not exosomes would be compared. Since exosomes are GFP positive, they could be traced *in vivo* for further characterization of their function.

7.2.2. Use of exosomes as a diagnostic tool for neuroblastoma

Finally, the presence of PKM2 and hexokinase II in exosomes circulating in the plasma of neuroblastoma patients could be of high clinical significance as it has the potential to be used to develop new non-invasive diagnostic approaches and improve risk stratification in neuroblastoma. Exosomes secreted by cancer cells can escape the tumour microenvironment and enter the blood stream from where they can be isolated. Circulating exosomes are being

assessed as a potential diagnostic tool in various diseases. Liquid biopsies could be used as an alternative to the conventional needle (tissue) biopsies and cancer exosomes are already being used as biomarkers in melanoma, pancreatic cancer, non-small cell lung cancer (NSCLC) and glioblastoma (table 7.1)

Table 7.1: Commercially available kits for the isolation of exosomes from cancer patients and correlation with detected molecular markers

Marker	Cancer	Body fluid	Correlation	Citation
GPC-1	Pancreatic	Serum	Early detection, progression	(Melo, et al., 2015)
TYRP2	Melanoma	Plasma	Tumour detection	(Peinado, et al., 2012)
VLA-4	Melanoma	Plasma	Tumour detection	(Peinado, et al., 2012)
HSP70	Melanoma	Plasma	Tumour detection	(Peinado, et al., 2012)
MET	Melanoma, NSCLC	Plasma	Tumour detection, progression	(Peinado, et al., 2012; Jakobsen, et al., 2015)
CD9	NSCLC	Plasma	Progression	(Jakobsen, et al., 2015)
CD81	NSCLC	Plasma	Progression	(Jakobsen, et al., 2015)
Tsg101	NSCLC	Plasma	Progression	(Jakobsen, et al., 2015)
EGFRvIII	NSCLC, Glioblastoma	Plasma, cerebrospinal fluid	Tumour detection, progression	(Jakobsen, et al., 2015; Skog, et al., 2008)
CD151	NSCLC	Plasma	Progression	(Jakobsen, et al., 2015)
miR-21	Glioblastoma	Cerebrospinal fluid	Tumour detection	(Akers, et al., 2013)

A limited number of studies have examined the diagnostic potential of exosomes in cancer but not in neuroblastoma. We hope that in the future, exosomal proteins could be used as biomarkers to predict prognosis and therapeutic response in neuroblastoma and, perhaps, other paediatric tumours.

8. References

Adam, K. & Hunter, T., 2018. Histidine kinases and the missing phosphoproteome from prokaryotes to eukaryotes. *Laboratory Investigation,* 98(2), p. 233.

Adhikary, S. et al., 2005. The ubiquitin ligase HectH9 regulates transcriptional activation by Myc and is essential for tumor cell proliferation. *Cell,* 123(3), pp. 409-421.

Admyre, C., Johansson, S., Paulie, S. & Gabrielsson, S., 2006. Direct exosome stimulation of peripheral humanT cells detected by ELISPOT. *European journal of immunology,* 36(7), pp. 1772-1781.

Akers, J. et al., 2013. MiR-21 in the extracellular vesicles (EVs) of cerebrospinal fluid (CSF): a platform for glioblastoma biomarker development. *PloS one,* 8(10), p. e78115.

Almgren, M., Henriksson, K., Fujimoto, J. & Chang, C., 2004. Nucleoside Diphosphate Kinase A/nm23-H1 Promotes Metastasis of NB69-Derived Human Neuroblastoma. *Molecular cancer research,* 2(7), pp. 87-394.

Altenberg, B. & Greulich, K., 2004. Genes of glycolysis are ubiquitously overexpressed in 24 cancer classes. *Genomics,* 84(6), pp. 1014-1020.

Amin, S., Yang, P. & Li, Z., 2019. Pyruvate kinase M2: A multifarious enzyme in non-canonical localization to promote cancer progression. *Biochimica et biophysica acta - reviews on cancer,* 1871(2), pp. 331-341.

Arabi, A. et al., 2005. c-Myc associates with ribosomal DNA and activates RNA polymerase I transcription. *Nature cell biology,* 7(3), p. 303.

Astuti, D. et al., 2001. RASSF1A promoter region CpG island hypermethylation in phaeochromocytomas and neuroblastoma tumours. *Oncogene,* 20(51), p. 7573.

Bader, S., Fasching, C., Brodeur, G. & Stanbridge, E., 1991. Dissociation of suppression of tumorigenicity and differentiation in vitro effected by transfer of single human chromosomes into human neuroblastoma cells. *Cell growth & differentiation: the molecular biology journal of the American Association for Cancer Research,* 2(5), pp. 245-255.

Bang, C. & Thum, T., 2012. Exosomes: new players in cell–cell communication. *The international journal of biochemistry & cell biology,* 44(11), pp. 2060-2064.

Barrès, C. et al., 2010. Galectin-5 is bound onto the surface of rat reticulocyte exosomes and modulates vesicle uptake by macrophages. *Blood,* 115(3), pp. 696-705.

Batagov, A., Kuznetsov, V. & Kurochkin, I., 2011. Identification of nucleotide patterns enriched in secreted RNAs as putative cis-acting elements targeting them to exosome nano-vesicles. *BMC genomics ,* Volume 12, p. S18.

Baudino, T. et al., 2002. c-Myc is essential for vasculogenesis and angiogenesis during development and tumor progression. *Genes & development,* 16(19), pp. 2530-2543.

Beierle, E. et al., 2007. N-MYC regulates focal adhesion kinase expression in human neuroblastoma. *Journal of Biological Chemistry,* 282(17), pp. 12503-12516.

Bell, E., Lunec, J. & Tweddle, D., 2007. Cell cycle regulation targets of MYCN identified by gene expression microarrays. *Cell cycle,* 6(10), pp. 1249-1256.

Bluhm, E., Daniels, J., Pollock, B. & Olshan, A., 2006. Maternal use of recreational drugs and neuroblastoma in offspring: a report from the Children's Oncology Group (United States). *Cancer Causes & Control,* 17(5), pp. 663-669.

Boeva, V. et al., 2017. Heterogeneity of neuroblastoma cell identity defined by transcriptional circuitries. *Nature genetics,* 49(9), p. 1408.

Bosse, K. et al., 2017. Identification of GPC2 as an oncoprotein and candidate immunotherapeutic target in high-risk neuroblastoma. *Cancer cell,* 32(3), pp. 295-309.

Bown, N. et al., 1999. Gain of chromosome arm 17q and adverse outcome in patients with neuroblastoma. *New England Journal of Medicine,* 340(25), pp. 1954-1961.

Bown, N. et al., 2001. 17q gain in neuroblastoma predicts adverse clinical outcome. *Medical and Pediatric Oncology: The Official Journal of SIOP—International Society of Pediatric Oncology (Societé Internationale d'Oncologie Pédiatrique),* 36(1), pp. 14-19.

Brodeur, G., 2003. Neuroblastoma: biological insights into a clinical enigma. *Nature reviews. Cancer,* 3(3), p. 203.

Brodeur, G. & Maris, J., 2002. In: P. Pizzo & D. Poplack, eds. *Principles and practice of pediatric oncology.* Philadelphia: Lippincott Williams & Williams, pp. 895-937.

Brodeur, G. et al., 1997. Biology and genetics of human neuroblastomas. *Journal of pediatric hematology/oncology,* 19(2), pp. 93-101.

Brodeur, G. et al., 1984. Amplification of N-myc in untreated human neuroblastomas correlates with advanced disease stage. *Science,* Issue 224, pp. 1121-1124.

Brodeur, G., Sekhon, G. & Goldstein, M., 1977. Chromosomal aberrations in human neuroblastomas. *Cancer,* 40(5), pp. 2256-2263.

Casey, S., Baylot, V. & Felsher, D., 2018. The MYC oncogene is a global regulator of the immune response. *Blood,* 113(18), pp. 2007-2015.

Chang, T. et al., 2008. Widespread microRNA repression by Myc contributes to tumorigenesis. *Nature genetics,* 40(1), p. 43.

Cheng, Y. et al., 2016. eEF-2 kinase is a critical regulator of Warburg effect through controlling PP2A-A synthesis. *Oncogene,* 35(49), p. 6293.

Chen, Y. et al., 2007. Integration of genome and chromatin structure with gene expression profiles to predict c-MYC recognition site binding and function. *PLoS computational biology,* 3(4), p. e63.

Chipumuro, E. et al., 2014. CDK7 inhibition suppresses super-enhancer-linked oncogenic transcription in MYCN-driven cancer. *Cell,* 159(5), pp. 1126-1139.

Christianson, H. et al., 2013. Cancer cell exosomes depend on cell-surface heparan sulfate proteoglycans for their internalization and functional activity. *Proceedings of the National Academy of Sciences,* 110(43), pp. 17380-17385.

Christofk, H. et al., 2008. The M2 splice isoform of pyruvate kinase is important for cancer metabolism and tumour growth. *Nature,* 452(7184), p. 230.

Clayton, A., 2012. Cancer cells use exosomes as tools to manipulate immunity and the microenvironment. *Oncoimmunology,* 1(1), pp. 78-80.

Cobbold, L. et al., 2010. Upregulated c-myc expression in multiple myeloma by internal ribosome entry results from increased interactions with and expression of PTB-1 and YB-1. *Oncogene,* 29(19), p. 2884.

Cohn, S. et al., 2009. The International Neuroblastoma Risk Group (INRG) classification system: an INRG task force report. *Journal of clinical oncology,* 27(2), pp. 289-297.

Cohn, S. et al., 1990. Analysis of DNA ploidy and proliferative activity in relation to histology and N-myc amplification in neuroblastoma. *The American journal of pathology,* 136(5), p. 1043.

Cole, K. et al., 2011. RNAi screen of the protein kinome identifies checkpoint kinase 1 (CHK1) as a therapeutic target in neuroblastoma. *Proceedings of the National Academy of Sciences,* 108(8), pp. 3336-3341.

Colletti, M. et al., 2017. Proteomic Analysis of Neuroblastoma-Derived Exosomes: New Insights into a Metastatic Signature. *Proteomics,* 17(23-24), p. 1600430.

Colombo, M., Raposo, G. & Théry, C., 2014. Biogenesis, secretion, and intercellular interactions of exosomes and other extracellular vesicles. *Annual review of cell and developmental biology,* Volume 30, pp. 255-289.

Cook, M. et al., 2004. Maternal medication use and neuroblastoma in offspring. *American journal of epidemiology,* 159(8), pp. 721-731.

Corvetta, D. et al., 2013. hysical interaction between MYCN oncogene and polycomb repressive complex 2 (PRC2) in neuroblastoma functional and therapeutic implications. *Journal of Biological Chemistry,* 288(12), pp. 8332-8341.

Dammann, R. et al., 2000. Epigenetic inactivation of a RAS association domain family protein from the lung tumour suppressor locus 3p21.3. *Nature genetics,* 25(3), p. 315.

Dang, C., Le, A. & Gao, P., 2009. MYC-induced cancer cell energy metabolism and therapeutic opportunities. *Clinical cancer research,* 15(21), pp. 6479-6483.

Datta, A. et al., 2018. High-throughput screening identified selective inhibitors of exosome biogenesis and secretion: A drug repurposing strategy for advanced cancer. *Scientific reports,* 8(1), p. Scientific reports.

De Bernardi, B., Pistoia, V., Gambini, C. & Granata, C., 2008. Peripheral neuroblastic tumors. In: I. D. Hay & J. A. Wass, eds. *Clinical Endocrine Oncology, Second Edition.* Oxford: Blackwell Publishing, Ltd, pp. 360-369.

De Roos, A. et al., 2001. Parental occupational exposures to chemicals and incidence of neuroblastoma in offspring. *American journal of epidemiology,* 154(2), pp. 106-114.

Denzer, K. et al., 2000. Follicular dendritic cells carry MHC class II-expressing microvesicles at their surface. *The Journal of Immunology,* 165(3), pp. 1259-1265.

Desai, S. et al., 2014. Tissue-specific isoform switch and DNA hypomethylation of the pyruvate kinase PKM gene in human cancers. *Oncotarget,* 5(18), p. 8202.

Dews, M. et al., 2006. Augmentation of tumor angiogenesis by a Myc-activated microRNA cluster. *Nature genetics,* 38(9), p. 1060.

Diskin, S. et al., 2012. Common variation at 6q16 within HACE1 and LIN28B influences susceptibility to neuroblastoma. *Nature genetics,* 44(10), pp. 1126-1130.

Dragovic, R. et al., 2011. Sizing and phenotyping of cellular vesicles using Nanoparticle Tracking Analysis. *Nanomedicine: Nanotechnology, Biology and Medicine,* 7(6), pp. 780-788.

Eilers, M. & Eisenman, R., 2008. Myc's broad reach. *Genes & development,* 22(20), pp. 2755-2766.

Eisenman, R., 2001. Deconstructing myc. *Genes & development,* 15(16), pp. 2023-2030.

Fauré, J. et al., 2006. Exosomes are released by cultured cortical neurones. *Molecular and Cellular Neuroscience,* 31(4), pp. 642-648.

Fernandez, P. et al., 2003. Genomic targets of the human c-Myc protein. *Genes & development,* 17(9), pp. 1115-1129.

Fevrier, B. et al., 2004. Cells release prions in association with exosomes. *Proceedings of the National Academy of Sciences of the United States of America,* 101(26), pp. 9683-9688.

Flørenes, V. et al., 1992. Levels of nm23 messenger RNA in metastatic malignant melanomas: inverse correlation to disease progression. *Cancer research,* 52(21), pp. 6088-6091.

Fonseka, P. et al., 2019. Exosomes from N-Myc amplified neuroblastoma cells induce migration and confer chemoresistance to non-N-Myc amplified cells: implications of intra-tumour heterogeneity. *Journal of extracellular vesicles,* 8(1), p. 1597614.

Fotsis, T. et al., 1999. Down-regulation of endothelial cell growth inhibitors by enhanced MYCN oncogene expression in human neuroblastoma cells. *The FEBS Journal,* 263(3), pp. 757-764.

Gajos-Michniewicz, A., Duechler, M. & Czyz, M., 2014. MiRNA in melanoma-derived exosomes. *Cancer letters,* 347(1), pp. 29-37.

Gansler, T. et al., 1986. Flow cytometric DNA analysis of neuroblastoma. Correlation with histology and clinical outcome. *Cancer ,* 58(11), pp. 2453-2458.

Gatta, G. et al., 2014. Childhood cancer survival in Europe 1999–2007: results of EUROCARE-5—a population-based study. *The lancet oncology,* 15(1), pp. 35-47.

George, R. et al., 2008. Activating mutations in ALK provide a therapeutic target in neuroblastoma. *Nature,* 455(7215), p. 975.

Gherardi, S., Valli, E., Erriquez, D. & Perini, G., 2013. MYCN-mediated transcriptional repression in neuroblastoma: the other side of the coin. *Frontiers in Oncology,* Issue 3, pp. 42-50.

Ghossoub, R. et al., 2014. Syntenin-ALIX exosome biogenesis and budding into multivesicular bodies are controlled by ARF6 and PLD2. *Nature communications,* Volume 5, p. 3477.

Godfried, M. et al., 2002. The N-myc and c-myc downstream pathways include the chromosome 17q genes nm23-H1 and nm23-H2. *Oncogene,* 21(13), p. 2097.

Gogolin, S. et al., 2013. CDK4 inhibition restores G_1-S arrest in MYCN-amplified neuroblastoma cells in the context of doxorubicin-induced DNA damage. *Cell cycle,* 12(7), pp. 1091-1104.

Gomez-Roman, N., Grandori, C., Eisenman, R. & White, R., 2003. Direct activation of RNA polymerase III transcription by c-Myc. *Nature,* 6920(421), p. 290.

Goodman, L. et al., 1997. Modulation of N-myc expression alters the invasiveness of neuroblastoma. *Clinical and Experimental Metastasis,* 15(2), pp. 130-139.

Grandori, C. et al., 2005. c-Myc binds to human ribosomal DNA and stimulates transcription of rRNA genes by RNA polymerase I. *Nature cell biology,* 7(3), p. 311.

Grinberg, A., Hu, C. & Kerppola, T., 2004. Visualization of Myc/Max/Mad family dimers and the competition for dimerization in living cells. *Molecular and cellular biology,* 24(10), pp. 4294-4308.

Grivennikov, S., Greten, F. & Karin, M., 2010. Immunity, inflammation, and cancer. *Cell,* 140(6), pp. 883-899.

Gualdrini, F. et al., 2010. Addiction of MYCN amplified tumours to B-MYB underscores a reciprocal regulatory loop. *Oncotarget,* 1(4), p. 278.

Guccione, E. et al., 2006. Myc-binding-site recognition in the human genome is determined by chromatin context. *Nature cell biology,* 8(7), p. 764.

Hailat, N. et al., 1991. High levels of p19/nm23 protein in neuroblastoma are associated with advanced stage disease and with N-myc gene amplification. *The Journal of clinical investigation,* 88(1), pp. 341-345.

Hanahan, D. & Weinberg, R., 2011. Hallmarks of cancer: the next generation. *Cell,* 144(5), pp. 646-674.

Hanson, P. & Cashikar, A., 2012. Multivesicular body morphogenesis. *Annual review of cell and developmental biology,* Volume 28, pp. 337-362.

Han, W. et al., 2016. Prognostic Value of NME1 (NM23-H1) in Patients with Digestive System Neoplasms: A Systematic Review and Meta-Analysis. *PloS one,* 11(8), p. e0160547.

Harding, C., Heuser, J. & Stahl, P., 1983. Receptor-mediated endocytosis of transferrin and recycling of the transferrin receptor in rat reticulocytes. *The Journal of cell biology,* 97(2), pp. 329-339.

Haug, B. et al., 2015. Exosome-like extracellular vesicles from MYCN-amplified neuroblastoma cells contain oncogenic miRNAs. *Anticancer research,* 35(5), pp. 2521-2530.

Headland, S. et al., 2014. Cutting-edge analysis of extracellular microparticles using ImageStreamX imaging flow cytometry. *Scientific reports,* Volume 4.

Heck, J. et al., 2009. The epidemiology of neuroblastoma: a review. *Paediatric and perinatal epidemiology,* 23(2), pp. 125-143.

Heimann, R., Ferguson, D. & Hellman, S., 1998. The relationship between nm23, angiogenesis, and the metastatic proclivity of node-negative breast cancer. *Cancer research,* 58(13), pp. 2766-2771.

Hindupur, S. et al., 2018. The protein histidine phosphatase LHPP is a tumour suppressor. *Nature,* 555(7698), p. 678.

Hnisz, D. et al., 2013. Super-enhancers in the control of cell identity and disease. *Cell,* 155(4), pp. 934-947.

Hood, J., San, R. & Wickline, S., 2011. Exosomes released by melanoma cells prepare sentinel lymph nodes for tumor metastasis. *Cancer research,* 71(11), pp. 3792-3801.

Hossain, M. et al., 2008. N-MYC promotes cell proliferation through a direct transactivation of neuronal leucine-rich repeat protein-1 (NLRR1) gene in neuroblastoma. *Oncogene,* 27(46), p. 6075.

Hsu, C. et al., 2010. Regulation of exosome secretion by Rab35 and its GTPase-activating proteins TBC1D10A–C. *The Journal of cell biology,* 189(2), pp. 223-232.

Huang, M. & Weiss, W., 2013. Neuroblastoma and MYCN. *Cold Spring Harbor perspectives in medicine,* 3(10), p. a014415.

Huber, K., 2006. The sympathoadrenal cell lineage: specification, diversification, and new perspectives. *Developmental biology,* 298(2), pp. 335-343.

Iavarone, A. et al., 1994. he helix-loop-helix protein Id-2 enhances cell proliferation and binds to the retinoblastoma protein. *Genes & development,* 8(11), pp. 1270-1284.

Iritani, B. et al., 2002. Modulation of T-lymphocyte development, growth and cell size by the Myc antagonist and transcriptional repressor Mad1. *The EMBO journal,* 21(18), pp. 4820-4830.

Jaiswal, J., Andrews, N. & Simon, S., 2002. Membrane proximal lysosomes are the major vesicles responsible for calcium-dependent exocytosis in nonsecretory cells. *J Cell Biol,* 159(4), pp. 625-635.

Jakobsen, K. et al., 2015. Exosomal proteins as potential diagnostic markers in advanced non-small cell lung carcinoma. *Journal of extracellular vesicles,* 4(1), p. 26659.

Jeppesen, D. et al., 2014. Quantitative proteomics of fractionated membrane and lumen exosome proteins from isogenic metastatic and nonmetastatic bladder cancer cells reveal differential expression of EMT factors. *Proteomics,* 14(6), pp. 699-712.

Jiang, Y. et al., 2014. PKM2 regulates chromosome segregation and mitosis progression of tumor cells. *Molecular cell,* 53(1), pp. 75-87.

Johnstone, R. et al., 1987. Vesicle formation during reticulocyte maturation. Association of plasma membrane activities with released vesicles (exosomes).. *Journal of Biological Chemistry,* 262(19), pp. 9412-9420.

Kaneko, Y. et al., 1987. Different karyotypic patterns in early and advanced stage neuroblastomas. *Cancer research,* 47(1), pp. 311-318.

Kang, J. et al., 2008. N-myc is a novel regulator of PI3K-mediated VEGF expression in neuroblastoma. *Oncogene,* 27(28), p. 3999.

Keerthikumar, S. et al., 2015. Proteogenomic analysis reveals exosomes are more oncogenic than ectosomes. *Oncotarget,* 6(17), p. 15375.

Kim, J. et al., 2008. An extended transcriptional network for pluripotency of embryonic stem cells. *Cell,* 132(6), pp. 1049-1061.

Kim, J. et al., 2007. HIF-1 and dysregulated c-Myc cooperatively induces VEGF and metabolic switches, HK2 and PDK1. *Molecular and Cellular Biology,* 27(21), pp. 7381-7393.

Kim, S. et al., 2003. Skp2 regulates Myc protein stability and activity. *Molecular cell,* 11(5), pp. 1177-1188.

Kleijmeer, M. et al., 1998. Selective enrichment of tetraspan proteins on the internal vesicles of multivesicular endosomes and on exosomes secreted by human B-lymphocytes.. *Journal of Biological Chemistry,* 273(32), pp. 20121-20127.

Knudson Jr, A. & Strong, L., 1972. Mutation and cancer: neuroblastoma and pheochromocytoma. *American journal of human genetics,* 24(5), p. 514.

Kocak, H. et al., 2013. Hox-C9 activates the intrinsic pathway of apoptosis and is associated with spontaneous regression in neuroblastoma. *Cell death & disease,* 4(4), p. e586.

Koppen, A. et al., 2007. Direct regulation of the minichromosome maintenance complex by MYCN in neuroblastoma. *European journal of cancer,* 43(16), pp. 2413-2422.

Kowal, J., Tkach, M. & Théry, C., 2014. Biogenesis and secretion of exosomes. *Current opinion in cell biology,* Issue 29, pp. 116-125.

Kucharzewska, P. et al., 2013. Exosomes reflect the hypoxic status of glioma cells and mediate hypoxia-dependent activation of vascular cells during tumor development. *Proceedings of the National Academy of Sciences,* 110(18), pp. 7312-7317.

Lamberti, A. et al., 2004. The translation elongation factor 1A in tumorigenesis, signal transduction and apoptosis. *Amino acids,* 26(4), pp. 443-448.

Lamparski, H. et al., 2002. Production and characterization of clinical grade exosomes derived from dendritic cells. *Journal of immunological methods,* 270(2), pp. 211-226.

Lasorella, A., Iavarone, A. & Israel, M., 1996. Id2 specifically alters regulation of the cell cycle by tumor suppressor proteins. *Molecular and cellular biology,* 16(6), pp. 2570-2578.

Lastowska, M. et al., 1997. ain of chromosome arm 17q predicts unfavourable outcome in neuroblastoma patients. UK Children's Cancer Study Group and the UK Cancer Cytogenetics Group.. *European journal of cancer (Oxford, England: 1990),* 33(10), pp. 1627-1633.

Lawlor, E. et al., 2006. Reversible kinetic analysis of Myc targets in vivo provides novel insights into Myc-mediated tumorigenesis. *Cancer research,* 66(9), pp. 4591-4601.

Lin, C. et al., 2009. Myc-regulated microRNAs attenuate embryonic stem cell differentiation. *The EMBO journal,* 28(20), pp. 3157-3170.

Li, N. et al., 2017. Therapeutically targeting glypican-2 via single-domain antibody-based chimeric antigen receptors and immunotoxins in neuroblastoma. *Proceedings of the National Academy of Sciences,* 114(32), pp. E6623-E6631.

Liu, H. et al., 2013. Single-cell clones of liver cancer stem cells have the potential of differentiating into different types of tumor cells. *Cell death & disease,* 4(10), p. e857.

Liu, T. et al., 2007. Activation of tissue transglutaminase transcription by histone deacetylase inhibition as a therapeutic approach for Myc oncogenesis. *Proceedings of the National Academy of Sciences,* 104(47), pp. 18682-18687.

Li, Z. et al., 2003. A global transcriptional regulatory role for c-Myc in Burkitt's lymphoma cells. *Proceedings of the National Academy of Sciences,* 100(14), pp. 8164-8169.

Logan, M. et al., 2004. A critical role for vesicle-associated membrane protein-7 in exocytosis from human eosinophils and neutrophils. *Allergy,* 61(6), pp. 777-784.

Longo, L. et al., 2007. Genetic predisposition to familial neuroblastoma: identification of two novel genomic regions at 2p and 12p. *Human heredity,* 63(3-4), pp. 205-211.

Look, A. et al., 1984. Cellular DNA content as a predictor of response to chemotherapy in infants with unresectable neuroblastoma. *New England Journal of Medicine,* 311(4), pp. 231-235.

Look, A. et al., 1991. Clinical relevance of tumor cell ploidy and N-myc gene amplification in childhood neuroblastoma: a Pediatric Oncology Group study. *Journal of Clinical Oncology,* 9(4), pp. 581-591.

Lotterman, C., Kent, O. & Mendell, J., 2008. Functional integration of microRNAs into oncogenic and tumor suppressor pathways. *Cell Cycle,* 7(16), pp. 2493-2499.

Lovén, J. et al., 2013. Selective inhibition of tumor oncogenes by disruption of super-enhancers`. *Cell,* 153(2), pp. 320-334.

Luga, V. et al., 2012. Exosomes mediate stromal mobilization of autocrine Wnt-PCP signaling in breast cancer cell migration. *Cell,* 151(7), pp. 1542-1556.

Luksch, R. et al., 2016. Neuroblastoma (Peripheral neuroblastic tumours). *Critical reviews in oncology/hematology,* Issue 107, pp. 163-181.

Lu, Z. & Hunter, T., 2018. Metabolic kinases moonlighting as protein kinases. *Trends in biochemical sciences,* 43(4), pp. 301-310.

Lv, L. et al., 2013. Mitogenic and oncogenic stimulation of K433 acetylation promotes PKM2 protein kinase activity and nuclear localization. *Molecular cell,* 52(3), pp. 340-352.

Lv, L. et al., 2013. Mitogenic and oncogenic stimulation of K433 acetylation promotes PKM2 protein kinase activity and nuclear localization. *Molecular cell,* 52(3), pp. 340-352.

Malanchi, I. et al., 2012. Interactions between cancer stem cells and their niche govern metastatic colonization. *Nature,* 481(7379), p. 85.

Manolio, T. et al., 2009. Finding the missing heritability of complex diseases. *Nature,* 461(7265), p. 747.

Marimpietri, D. et al., 2013. Proteome profiling of neuroblastoma-derived exosomes reveal the expression of proteins potentially involved in tumor progression. *PloS one,* 8(9), p. e75054.

Marrano, P., Irwin, M. & Thorner, P., 2017. Heterogeneity of MYCN amplification in neuroblastoma at diagnosis, treatment, relapse, and metastasis. *Chromosomes and Cancer,* 56(1), pp. 28-41.

Marshall, G. et al., 2014. The prenatal origins of cancer. *Nature Reviews. Cancer,* 14(4), p. 277.

Matthay, K. et al., 2016. Neuroblastoma. *Nature reviews Disease primers,* Volume 2.

McArthur, G. et al., 2002. MAD1 and p27KIP1 cooperate to promote terminal differentiation of granulocytes and to inhibit Myc expression and cyclin E-CDK2 activity. *Molecular and cellular biology,* 22(9), pp. 3014-3023.

McCall, E., Olshan, A. & Daniels, J., 2005. Maternal hair dye use and risk of neuroblastoma in offspring. *Cancer Causes & Control,* 16(6), pp. 743-748.

Mears, R. et al., 2004. Proteomic analysis of melanoma-derived exosomes by two-dimensional polyacrylamide gel electrophoresis and mass spectrometry. *Proteomics,* 4(12), pp. 4019-4031.

Melo, S. et al., 2015. Glypican-1 identifies cancer exosomes and detects early pancreatic cancer. *Nature,* 523(7559), p. 177.

Mertens, F., Johansson, B., Höglund, M. & Mitelman, F., 1997. Chromosomal imbalance maps of malignant solid tumors: a cytogenetic survey of 3185 neoplasms. *Cancer research,* 57(13), pp. 2765-2780.

Mezquita, P., Parghi, S., Brandvold, K. & Ruddell, A., 2005. Myc regulates VEGF production in B cells by stimulating initiation of VEGF mRNA translation. *Oncogene,* 24(5), p. 889.

Michalek, A. et al., 1996. Gravid health status, medication use, and risk of neuroblastoma. *American journal of epidemiology,* 143(10), pp. 996-1001.

Minciacchi, V., Zijlstra, A., Rubin, M. & Di Vizio, D., 2017. Extracellular vesicles for liquid biopsy in prostate cancer: where are we and where are we headed?. *Prostate cancer and prostatic diseases,* 20(3), p. 251.

Molenaar, J. et al., 2012. LIN28B induces neuroblastoma and enhances MYCN levels via let-7 suppression. *Nature genetics,* 44(11), pp. 1199-1206.

Mossé, Y. et al., 2014. Neuroblastoma in older children, adolescents and young adults: a report from the International Neuroblastoma Risk Group project. *Pediatric blood & cancer,* 61(4), pp. 627-635.

Mossë, Y. et al., 2008. Identification of ALK as the major familial neuroblastoma predisposition gene. *Nature,* 455(7215), p. 930.

Murphy, D. et al., 2008. Distinct thresholds govern Myc's biological output in vivo. *Cancer cell,* 14(6), pp. 447-457.

Muth, D. et al., 2010. Transcriptional repression of SKP2 is impaired in MYCN-amplified neuroblastoma. *Cancer research,* 70(9), pp. 3791-3802.

Nakagawa, M. et al., 2008. Generation of induced pluripotent stem cells without Myc from mouse and human fibroblasts. *Nature biotechnology,* 26(1), p. 101.

Nakagawa, M. et al., 2010. Promotion of direct reprogramming by transformation-deficient Myc. *Proceedings of the National Academy of Sciences,* 107(32), pp. 14152-14157.

Nakata, R. et al., 2017. Contribution of neuroblastoma-derived exosomes to the production of pro-tumorigenic signals by bone marrow mesenchymal stromal cells. *Journal of extracellular vesicles,* 6(1), p. 1332941.

Neviani, P. et al., 2019. Natural Killer–Derived Exosomal miR-186 Inhibits Neuroblastoma Growth and Immune Escape Mechanisms. *Cancer research,* 79(6), pp. 1151-1164.

Newick, K., O'Brien, S., Moon, E. & Albelda, S. M., 2017. CAR T cell therapy for solid tumors. *Annual review of medicine,* Issue 68, pp. 139-152.

Ngo, C. et al., 2000. An in vivo function for the transforming Myc protein: elicitation of the angiogenic phenotype. *Cell growth & differentiation: the molecular biology journal of the American Association for Cancer Research,* 11(4), p. 201.

Niitsu, N. et al., 2000. Plasma levels of the differentiation inhibitory factor nm23-H1 protein and their clinical implications in acute myelogenous leukemia. *Blood,* 96(3), pp. 1080-1086.

Nogueira, V., Patra, K. & Hay, N., 2018. Selective eradication of cancer displaying hyperactive Akt by exploiting the metabolic consequences of Akt activation. *Elife,* Volume 7, p. e32213.

Nolte-'t Hoen, E. et al., 2012. Deep sequencing of RNA from immune cell-derived vesicles uncovers the selective incorporation of small non-coding RNA biotypes with potential regulatory functions. *Nucleic acids research,* 40(18), pp. 9272-9285.

O'Donnell, K. et al., 2005. c-Myc-regulated microRNAs modulate E2F1 expression. *Nature,* 435(7043), p. 839.

Okabe-Kado, J., 2002. Serum nm23-H1 protein as a prognostic factor in hematological malignancies. *Leukemia & lymphoma,* 43(4), pp. 859-867.

Okabe-Kado, J. et al., 2005. Clinical significance of serum NM23-H1 protein in neuroblastoma. *Cancer science,* 96(10), pp. 653-660.

Olshan, A. et al., 1999. Neuroblastoma and parental occupation. *Cancer Causes and Control,* 10(6), pp. 539-549.

Ombrato, L. et al., 2019. Metastatic-niche labelling reveals parenchymal cells with stem features. *Nature,* 572(7771), pp. 603-608.

Ostrowski, M. et al., 2010. Rab27a and Rab27b control different steps of the exosome secretion pathway. *Nature cell biology,* 12(1), p. 19.

Pan, B. et al., 1985. Electron microscopic evidence for externalization of the transferrin receptor in vesicular form in sheep reticulocytes. *The Journal of cell biology,* 101(3), pp. 942-948.

Park, J., Eggert, A. & Caron, H., 2008. Neuroblastoma: biology, prognosis, and treatment. *Pediatric clinics of North America,* 55(1), pp. 97-120.

Pavithra, L. et al., 2007. Stabilization of SMAR1 mRNA by PGA2 involves a stem–loop structure in the 5′ UTR. *Nucleic acids research,* 35(18), pp. 6004-6016.

Peinado, H. et al., 2012. Melanoma exosomes educate bone marrow progenitor cells toward a pro-metastatic phenotype through MET. *Nature medicine,* 18(6), pp. 883-891.

Pello, O. et al., 2012. Role of c-MYC in alternative activation of human macrophages and tumor-associated macrophage biology. *Blood,* 119(2), pp. 411-421.

Perini, G., Diolaiti, D., Porro, A. & Della Valle, G., 2005. In vivo transcriptional regulation of N-Myc target genes is controlled by E-box methylation. *Proceedings of the National Academy of Sciences,* 102(34), pp. 12117-12122.

Pisitkun, T., Shen, R. & Knepper, M., 2004. Identification and proteomic profiling of exosomes in human urine. *Proceedings of the national academy of sciences of the United States of America,* 101(36), pp. 13368-13373.

Podar, K. & Anderson, K., 2010. A therapeutic role for targeting c-Myc/Hif-1-dependent signaling pathways. *Cell Cycle,* 9(9), pp. 1722-1728.

Pott, L. et al., 2017. Eukaryotic elongation factor 2 is a prognostic marker and its kinase a potential therapeutic target in HCC. *Oncotarget,* 8(7), p. 11950.

Pott, S. & Lieb, J., 2015. What are super-enhancers?. *Nature genetics,* 47(1), p. 8.

Puri, N. & Roche, P., 2008. Mast cells possess distinct secretory granule subsets whose exocytosis is regulated by different SNARE isoforms. *Proceedings of the National Academy of Sciences,* 105(7), pp. 2580-2585.

Rakhra, K. et al., 2010. CD4+ T cells contribute to the remodeling of the microenvironment required for sustained tumor regression upon oncogene inactivation. *Cancer cell,* 18(5), pp. 485-498.

Ramteke, A. et al., 2015. Exosomes secreted under hypoxia enhance invasiveness and stemness of prostate cancer cells by targeting adherens junction molecules. *Molecular carcinogenesis,* 54(7), pp. 554-565.

Rao, S. et al., 2004. Identification of SNAREs involved in synaptotagmin VII-regulated lysosomal exocytosis. *Journal of Biological Chemistry,* 279(19), pp. 20471-20479.

Raposo, G. et al., 1996. B lymphocytes secrete antigen-presenting vesicles. *Journal of Experimental Medicine,* 183(3), pp. 1161-1172.

Raposo, G. & Stoorvogel, W., 2013. Extracellular vesicles: exosomes, microvesicles, and friends. *The journal of cell biology*.

Raschellà, G. et al., 1999. Expression of B-myb in neuroblastoma tumors is a poor prognostic factor independent from MYCN amplification. *Cancer research,* 59(14), pp. 3365-3368.

Raschell, G. et al., 1995. Requirement of b-myb function for survival and differentiative potential of human neuroblastoma cells. *Journal of Biological Chemistry,* 270(15), pp. 8540-8545.

Roma-Rodrigues, C., Fernandes, A. & Baptista, P., 2014. Exosome in tumour microenvironment: overview of the crosstalk between normal and cancer cells. *BioMed research international.*

Ronquist, G. & Brody, I., 1985. The prostasome: its secretion and function in man. *Biochimica et Biophysica Acta (BBA)-Reviews on Biomembranes,* 822(2), pp. 203-218.

Rybak, A. et al., 2008. A feedback loop comprising lin-28 and let-7 controls pre-let-7 maturation during neural stem-cell commitment. *Nature cell biology,* 10(8), p. 987.

Sala, A., 2015. Targeting MYCN in Pediatric Cancers. *Frontiers in Oncology,* Volume 4, p. 330.

Savina, A., Vidal, M. & Colombo, M., 2002. The exosome pathway in K562 cells is regulated by Rab11. *Journal of cell science,* 115(12), pp. 2505-2515.

Schulte, J. et al., 2008. MYCN regulates oncogenic MicroRNAs in neuroblastoma. *International journal of cancer,* 122(3), pp. 699-704.

Schüz, J. et al., 2001. Risk factors for pediatric tumors of the central nervous system: Results from a German population-based case-control study. *Pediatric Blood & Cancer,* 36(2), pp. 274-282.

Segura, E. et al., 2005. ICAM-1 on exosomes from mature dendritic cells is critical for efficient naive T-cell priming. *Blood,* 106(1), pp. 216-223.

Sharma, S., Gillespie, B., Palanisamy, V. & Gimzewski, J., 2011. Quantitative nanostructural and single-molecule force spectroscopy biomolecular analysis of human-saliva-derived exosomes. *Langmuir,* 27(23), pp. 14394-14400.

Shchors, K. et al., 2006. The Myc-dependent angiogenic switch in tumors is mediated by interleukin 1β. *Genes & development,* 20(18), pp. 2527-2538.

Shi, N. et al., 2018. Eukaryotic elongation factors 2 promotes tumor cell proliferation and correlates with poor prognosis in ovarian cancer. *Tissue and Cell,* Volume 53, pp. 53-60.

Silverman, A. et al., 2012. A Galectin-3–Dependent Pathway Upregulates Interleukin-6 in the Microenvironment of Human Neuroblastoma. *Cancer research,* 72(9), pp. 2228-2238.

Skog, J. et al., 2008. Glioblastoma microvesicles transport RNA and proteins that promote tumour growth and provide diagnostic biomarkers. *Nature cell biology,* 10(12), p. 1470.

Sodir, N. et al., 2011. Endogenous Myc maintains the tumor microenvironment. *Genes & development,* 25(9), pp. 907-916.

Song, L. et al., 2007. Oncogene MYCN regulates localization of NKT cells to the site of disease in neuroblastoma. *The Journal of clinical investigation,* 117(9), pp. 2702-2712.

Soucek, L. & Evan, G., 2010. The ups and downs of Myc biology. *Current opinion in genetics & development,* 20(1), pp. 91-95.

Soucek, L. et al., 2007. Mast cells are required for angiogenesis and macroscopic expansion of Myc-induced pancreatic islet tumors. *Nature medicine,* 13(10), p. 1211.

Spix, C. et al., 2006. Neuroblastoma incidence and survival in European children (1978–1997): report from the Automated Childhood Cancer Information System project. *European journal of cancer,* 42(13), pp. 2081-2091.

Staller, P. et al., 2001. Repression of p15 INK4b expression by Myc through association with Miz-1. *Nature cell biology,* 3(4), p. 392.

Steeg, P. et al., 1988. Evidence for a novel gene associated with low tumor metastatic potential. *JNCI: Journal of the National Cancer Institute,* 80(3), pp. 200-204.

Stenmark, H., 2009. Rab GTPases as coordinators of vesicle traffic. *Nature reviews Molecular cell biology,* 10(8), pp. 513-525.

Stuffers, S., Sem Wegner, C., Stenmark, H. & Brech, A., 2009. Multivesicular endosome biogenesis in the absence of ESCRTs. *Traffic,* 10(7), pp. 925-937.

Tanaka, N. & Fukuzawa, M., 2008. MYCN downregulates integrin α1 to promote invasion of human neuroblastoma cells. *International journal of oncology,* 33(4), pp. 815-821.

Tao, T. et al., 2019. Down-regulation of PKM2 decreases FASN expression in bladder cancer cells through AKT/mTOR/SREBP-1c axis. *Journal of cellular physiology,* 234(3), pp. 3088-3104.

Taylor, D. & Gercel-Taylor, C., 2013. The origin, function, and diagnostic potential of RNA within extracellular vesicles present in human biological fluids. *Frontiers in genetics,* Volume 4.

Teitz, T. et al., 2000. Caspase 8 is deleted or silenced preferentially in childhood neuroblastomas with amplification of MYCN. *Nature medicine,* 6(5), p. 529.

Théry, C., Amigorena, S., Raposo, G. & Clayton, A., 2006. Isolation and characterization of exosomes from cell culture supernatants and biological fluids. *Current protocols in cell biology,* pp. 3-22.

Théry, C. et al., 2001. Proteomic analysis of dendritic cell-derived exosomes: a secreted subcellular compartment distinct from apoptotic vesicles. *The Journal of Immunology,* 166(12), pp. 7309-7318.

Tolbert, V. & Matthay, K., 2018. Neuroblastoma: clinical and biological approach to risk stratification and treatment. *Cell and tissue research,* 372(2), pp. 195-209.

Trajkovic, K. et al., 2008. Ceramide triggers budding of exosome vesicles into multivesicular endosomes. *Science,* 319(5867), pp. 1244-1247.

Trams, E., Lauter, C., Salem, J. & Heine, U., 1981. Exfoliation of membrane ecto-enzymes in the form of micro-vesicles. *Biochimica et Biophysica Acta (BBA)-Biomembranes,* 645(1), pp. 63-70.

Trochet, D. et al., 2004. Germline mutations of the paired–like homeobox 2B (PHOX2B) gene in neuroblastoma. *The American Journal of Human Genetics,* 74(4), pp. 761-764.

Valadi, H. et al., 2017. Exosome-mediated transfer of mRNAs and microRNAs is a novel mechanism of genetic exchange between cells. *Nature cell biology,* 9(6), p. 654.

Valentijn, L. et al., 2005. Inhibition of a new differentiation pathway in neuroblastoma by copy number defects of N-myc, Cdc42, and nm23 gene. *Cancer research,* 65(8), pp. 3136-3145.

Valli, E. et al., 2012. CDKL5, a novel MYCN-repressed gene, blocks cell cycle and promotes differentiation of neuronal cells. *Biochimica et Biophysica Acta (BBA)-Gene Regulatory Mechanisms,* 1819(11-12), pp. 1173-1185.

van Groningen, T. et al., 2019. A NOTCH feed-forward loop drives reprogramming from adrenergic to mesenchymal state in neuroblastoma. *Nature communications,* 10(1), p. 1530.

van Groningen, T. et al., 2017. Neuroblastoma is composed of two super-enhancer-associated differentiation states. *Nature genetics,* 49(8), p. 1261.

van Niel, G., D'Angelo, G. & Raposo, G., 2018. Shedding light on the cell biology of extracellular vesicles. *Nature reviews Molecular cell biology,* 19(4), p. 213.

Van Niel, G. et al., 2001. Intestinal epithelial cells secrete exosome–like vesicles. *Gastroenterology,* 121(2), pp. 337-349.

Vander Heiden, M., Cantley, L. & Thompson, C., 2009. Understanding the Warburg effect: the metabolic requirements of cell proliferation. *Science,* 324(5930), pp. 1029-1033.

Vandesompele, J. et al., 2001. Multicentre analysis of patterns of DNA gains and losses in 204 neuroblastoma tumors: how many genetic subgroups are there?. *Medical and Pediatric Oncology: The Official Journal of SIOP—International Society of Pediatric Oncology (Societé Internationale d'Oncologie Pédiatrique),* 36(1), pp. 5-10.

Vanichapol, T., Chutipongtanate, S., Anurathapan, U. & Hongeng, S., 2018. Immune Escape Mechanisms and Future Prospects for Immunotherapy in Neuroblastoma. *BioMed research international.*

Vlassov, A., Magdaleno, S., Setterquist, R. & Conrad, R., 2012. Exosomes: current knowledge of their composition, biological functions, and diagnostic and therapeutic potentials. *Biochimica et Biophysica Acta (BBA)-General Subjects,* 1820(7), pp. 940-948.

Von Der Lehr, N. et al., 2003. The F-box protein Skp2 participates in c-Myc proteosomal degradation and acts as a cofactor for c-Myc-regulated transcription. *Molecular cell,* 11(5), pp. 1189-1200.

Warburg, O., 1956. On the origin of cancer cells. *Science,* 123(3191), pp. 309-314.

Wei, J. et al., 2018. Clinically relevant cytotoxic immune cell signatures and clonal expansion of T-cell receptors in high-risk MYCN-not-amplified human neuroblastoma. *Clinical Cancer Research,* 24(22), pp. 5673-5684.

Weiss, W. et al., 1997. Targeted expression of MYCN causes neuroblastoma in transgenic mice. *The EMBO journal,* 16(11), pp. 2985-2995.

Welcker, M. et al., 2004. A nucleolar isoform of the Fbw7 ubiquitin ligase regulates c-Myc and cell size. *Current Biology,* 14(20), pp. 1852-1857.

Whyte, W. et al., 2013. Master transcription factors and mediator establish super-enhancers at key cell identity genes. *Cell,* 153(2), pp. 307-319.

Witwer, K. et al., 2013. Standardization of sample collection, isolation and analysis methods in extracellular vesicle research. *Journal of extracellular vesicles,* 2(1), p. 20360.

Wolfers, J. et al., 2001. Tumor-derived exosomes are a source of shared tumor rejection antigens for CTL cross-priming. *Nature medicine,* 7(3), p. 297.

Wong, D. et al., 2008. Module map of stem cell genes guides creation of epithelial cancer stem cells. *Cell stem cell,* 2(4), pp. 333-344.

Wright, J., 1910. Neurocytoma or neuroblastoma, a kind of tumor not generally recognized. *The Journal of experimental medicine,* 12(4), p. 556.

Yada, M. et al., 2004. Phosphorylation-dependent degradation of c-Myc is mediated by the F-box protein Fbw7. *The EMBO journal,* 23(10), pp. 2116-2125.

Yang, W. & Lu, Z., 2015. Pyruvate kinase M2 at a glance. *Journal of cell science,* 128(9), pp. 1655-1660.

Yang, W. et al., 2012. PKM2 phosphorylates histone H3 and promotes gene transcription and tumorigenesis. *Cell,* 150(4), pp. 685-696.

Yokoyama, A. et al., 1998. Evaluation by multivariate analysis of the differentiation inhibitory factor nm23 as a prognostic factor in acute myelogenous leukemia and application to other hematologic malignancies. *Blood,* 91(6), pp. 1845-1851.

Yu, A. L. et al., 2010. Anti-GD2 antibody with GM-CSF, interleukin-2, and isotretinoin for neuroblastoma. *New England Journal of Medicine,* 363(14), pp. 1324-1334.

Zeller, K. et al., 2006. Global mapping of c-Myc binding sites and target gene networks in human B cells. *Proceedings of the National Academy of Sciences,* 103(47), pp. 17834-17839.

Zhang, H. & Grizzle, W., 2014. Exosomes: a novel pathway of local and distant intercellular communication that facilitates the growth and metastasis of neoplastic lesions. *The American journal of pathology,* 184(1), pp. 28-41.

Zhang, P. et al., 2017. MYCN amplification is associated with repressed cellular immunity in neuroblastoma: an In Silico immunological analysis of TARGET Database. *Frontiers in immunology,* Volume 8, p. 1473.

Zhang, S. et al., 2016. MYCN controls an alternative RNA splicing program in high-risk metastatic neuroblastoma. *Cancer letters,* 371(2), pp. 214-224.

Zhang, W. et al., 2015. Comparison of RNA-seq and microarray-based models for clinical endpoint prediction. *Genome biology,* 16(1), p. 133.

Zhang, X. et al., 2018. Eukaryotic elongation factor 2 (eEF2) is a potential biomarker of prostate cancer. *Pathology & Oncology Research,* 24(4), pp. 885-890.

Zhao, X. et al., 2008. The HECT-domain ubiquitin ligase Huwe1 controls neural differentiation and proliferation by destabilizing the N-Myc oncoprotein. *Nature cell biology,* 10(6), p. 643.

Zimmerman, K. et al., 1986. Differential expression of myc family genes during murine development. *Nature,* 319(6056), p. 780.

Zitvogel, L. et al., 1998. Eradication of established murine tumors using a novel cell-free vaccine: dendritic cell derived exosomes. *Nature medicine,* 4(5), pp. 594-600.

Zylbersztejn, K. & Galli, T., 2011. Vesicular traffic in cell navigation. *The FEBS journal,* 278(23), pp. 4497-4505.

9. Appendix

Table 9.1: Proteins identified by mass spectrometry as differentially regulated in the exosomes secreted by MYCN positive or negative TET21-N cells

Accession	Description	Score	Unique peptides	Sequence coverage [%]	MW [kDa]
O95834	Echinoderm microtubule-associated protein-like 2	11.128	6	11.9	70.678
O75083	WD repeat-containing protein 1	41.171	11	26.2	66.193
P62826	GTP-binding nuclear protein Ran	14.036	6	33.3	24.423
P14618	Pyruvate kinase PKM	200.54	32	71	57.936
P05121	Plasminogen activator inhibitor 1	15.368	6	21.1	45.059
Q86UX7	Fermitin family homolog 3	31.082	9	16.8	75.952
P12109	Collagen alpha-1(VI) chain	77.599	9	11.6	108.53
P07900	Heat shock protein HSP 90-alpha	59.801	15	32.4	84.659
P07195	L-lactate dehydrogenase B chain	35.663	5	23.1	36.638
Q9UBG0	C-type mannose receptor 2	62.354	11	8.5	166.67
Q15113	Procollagen C-endopeptidase enhancer 1	7.0803	1	2.9	47.972
Q9Y240	C-type lectin domain family 11 member A	10.896	3	12.4	35.694
P51570	Galactokinase	3.0411	2	5.6	42.272
P36871	Phosphoglucomutase-1	13.868	4	13.5	61.448
P48740	Mannan-binding lectin serine protease 1	7.5485	4	5.2	79.246
P10909	Clusterin	17.722	6	19.2	52.494
P31146	Coronin-1A	3.7805	2	3.9	51.026
Q9ULV4	Coronin-1C	34.565	7	19.6	53.248
Q15404	Ras suppressor protein 1	7.968	5	24.5	31.54
P50395	Rab GDP dissociation inhibitor beta	54.946	3	26.1	50.663
P21333	Filamin-A	225.49	51	30.7	280.74

Accession	Description	Score	Unique peptides	Sequence coverage [%]	MW [kDa]
P50552	Vasodilator-stimulated phosphoprotein	6.3269	3	10.3	39.829
P08567	Pleckstrin	5.1824	2	11.4	40.124
Q15555	Microtubule-associated protein RP/EB family member 2	32.895	5	19.3	37.031
P48059	LIM and senescent cell antigen-like-containing domain protein 1	28.598	7	27.4	37.251
P02794	Ferritin heavy chain	5.4839	2	10.9	21.225
P68366	Tubulin alpha-4A chain	195.37	5	67.4	49.924
Q9H6S1	5-azacytidine-induced protein 2	2.321	1	4.3	44.934
Q9BUF5	Tubulin beta-6 chain	53.738	4	40.4	49.857
P35579	Myosin-9	323.31	56	42.1	226.53
P02679	Fibrinogen gamma chain	20.991	2	6	51.511
P35443	Thrombospondin-4	32.84	4	12.5	105.87
Q9Y490	Talin-1	323.31	96	53.6	269.76
Q13418	Integrin-linked protein kinase	53.291	21	60.8	51.419
Q9NZN3	EH domain-containing protein 3	29.122	4	20.7	60.886
P23526	Adenosylhomocysteinase	31.68	11	28.7	47.716
P0DMV9	Heat shock 70 kDa protein 1B	81.723	14	35.6	70.051
P00966	Argininosuccinate synthase	18.863	5	15.8	46.53
P60660	Myosin light polypeptide 6	26.416	8	53	16.93
O43505	Beta-1,4-glucuronyltransferase 1	2.6341	3	10.1	47.119
P21399	Cytoplasmic aconitate hydratase	5.6885	2	4.6	98.398
P04264	Keratin, type II cytoskeletal 1	164.01	13	38.5	66.038
P02786	Transferrin receptor protein 1	34.432	2	3.4	84.87
P61981	14-3-3 protein gamma	51.537	5	38.9	28.302
P62491	Ras-related protein Rab-11A	6.1436	5	30.6	24.393
Q9Y4K0	Lysyl oxidase homolog 2	22.594	2	4.8	86.724
P26006	Integrin alpha-3	32.772	10	10.7	116.61
Q01813	ATP-dependent 6-phosphofructokinase, platelet type	70.555	9	22.3	85.595
Q9NQC3	Reticulon-4	5.7776	3	5.1	129.93

Accession	Description	Score	Unique peptides	Sequence coverage [%]	MW [kDa]
P22626	Heterogeneous nuclear ribonucleoproteins A2/B1	17.363	5	23.2	37.429
Q9Y265	RuvB-like 1	29.803	7	27	50.227
Q71DI3	Histone H3.2	2.9645	3	16.9	15.388
P15531	Nucleoside diphosphate kinase	19.141	2	46.7	17.149
P08195	4F2 cell-surface antigen heavy chain	97.382	14	27.8	67.993
P13639	Elongation factor 2	102.16	25	38.3	95.337
P62879	Guanine nucleotide-binding protein G(I)/G(S)/G(T) subunit beta-2	51.855	5	49.4	37.331
O14817	Tetraspanin-4	20.537	2	20.2	26.118
P08758	Annexin A5	25.974	7	28.4	35.936
P62158	Calmodulin	27.346	5	36.9	16.837
P18621	60S ribosomal protein L17	25.047	7	46.2	21.397
Q9P2B2	Prostaglandin F2 receptor negative regulator	14.085	7	10.8	98.555
P84077	ADP-ribosylation factor 1	16.007	3	38.1	20.697
P62280	40S ribosomal protein S11	8.8076	3	24.7	18.431
P48643	T-complex protein 1 subunit epsilon	27.936	6	23.7	59.67
P62873	Guanine nucleotide-binding protein G(I)/G(S)/G(T) subunit beta-1	94.563	8	60.3	37.377
P14543	Nidogen-1	33.252	12	14.8	136.38
Q15365	Poly(rC)-binding protein 1	34.265	4	29.5	37.497
P04083	Annexin A1	66.802	8	32.9	38.714
P61978	Heterogeneous nuclear ribonucleoprotein K	20.163	5	19.7	50.976
P63104	14-3-3 protein zeta/delta	149.71	11	60.4	27.745
O00560	Syntenin-1	93.19	10	59.4	32.444
Q14520	Hyaluronan-binding protein 2	14.97	4	6.2	62.671
P61247	40S ribosomal protein S3a	18.329	7	25.8	29.945
Q99878	Histone H2A type 1-J	56.311	0	61.7	13.936
P35580	Myosin-10	8.9457	3	9.9	229
P20645	Cation-dependent mannose-6-phosphate receptor	7.7714	4	19.9	30.993
P63241	Eukaryotic translation initiation factor 5A-1	47.079	7	74.7	16.832

Accession	Description	Score	Unique peptides	Sequence coverage [%]	MW [kDa]
P16401	Histone H1.5	31.926	7	26.5	22.58
P05106	Integrin beta-3	121.01	17	28.2	87.057
P04075	Fructose-bisphosphate aldolase A	65.803	14	51.1	39.42
P62753	40S ribosomal protein S6	22.971	7	26.5	28.68
Q15185	Prostaglandin E synthase 3	7.923	3	25	18.697
P29966	Myristoylated alanine-rich C-kinase substrate	49.761	8	47.9	31.554
Q14315	Filamin-C	19.791	7	6.6	291.02
P60842	Eukaryotic initiation factor 4A-I	58.867	10	34.5	46.153
Q9UBI6	Guanine nucleotide-binding protein G(I)/G(S)/G(O) subunit gamma-12	12.797	5	73.6	8.0061
P08238	Heat shock protein HSP 90-beta	248.04	15	35.5	83.263
P55072	Transitional endoplasmic reticulum ATPase	76.333	13	27.3	89.321
O15230	Laminin subunit alpha-5	19.6	7	2.9	399.73
P49368	T-complex protein 1 subunit gamma	19.721	6	15.6	60.533
Q02543	60S ribosomal protein L18a	10.641	5	26.1	20.762
Q15758	Neutral amino acid transporter B(0)	9.6988	3	5.9	56.598
P04899	Guanine nucleotide-binding protein G(i) subunit alpha-2	46.99	6	46.5	40.45
O75531	Barrier-to-autointegration factor	6.8268	1	27	10.058
P46781	40S ribosomal protein S9	21.805	4	21.1	22.591
P18077	60S ribosomal protein L35a	11.498	4	29.1	12.538
P16070	CD44 antigen	34.316	7	10.5	81.537
P68104	Elongation factor 1-alpha 1	51.657	14	53.5	50.14
P62701	40S ribosomal protein S4, X isoform	15.867	6	27.4	29.597
P16403	Histone H1.2	9.9311	5	23.5	21.364
P08133	Annexin A6	74.272	19	38.9	75.872
P62424	60S ribosomal protein L7a	60.576	12	47.4	29.995
Q06830	Peroxiredoxin-1	31.765	10	65.3	22.11
P62269	40S ribosomal protein S18	12.12	5	32.2	17.718
P61313	60S ribosomal protein L15	21.717	8	36.3	24.146

Accession	Description	Score	Unique peptides	Sequence coverage [%]	MW [kDa]
Q14764	Major vault protein	90.27	27	47	99.326
P62917	60S ribosomal protein L8	21.913	5	25.7	28.024
P27635	60S ribosomal protein L10	46.533	6	29.9	24.604
P07942	>splaminin subunit beta-1	77.852	18	14.5	198.04
P46777	60S ribosomal protein L5	13.45	5	19.9	34.362
P35052	Glypican-1	30.25	11	27.8	61.68
Q02878	60S ribosomal protein L6	41.349	10	37.8	32.728
P04792	Heat shock protein beta-1	27.352	6	56.1	22.782
P50914	60S ribosomal protein L14	34.487	6	29.8	23.432
Q00839	Heterogeneous nuclear ribonucleoprotein U	40.118	11	15.2	90.583
P18124	60S ribosomal protein L7	37.404	9	34.3	29.225
P62241	40S ribosomal protein S8	85.056	10	49	24.205
P39023	60S ribosomal protein L3	81.48	12	31.3	46.108
Q08431	Lactadherin	172.73	20	63.6	43.122
P07355	Annexin A2	147.52	18	52.2	38.604
P46779	60S ribosomal protein L28	9.0207	5	27	15.747
P26373	60S ribosomal protein L13	26.082	10	39.8	24.261
Q00610	Clathrin heavy chain 1	323.31	42	44.1	191.61
P36578	60S ribosomal protein L4	56.31	19	43.1	47.697
Q07020	60S ribosomal protein L18	41.146	5	30.9	21.634
P15880	40S ribosomal protein S2	23.415	7	25.3	31.324
P98160	Basement membrane-specific heparan sulfate proteoglycan core protein	323.31	75	27.2	468.83
Q9NR30	Nucleolar RNA helicase 2	14.319	4	7.3	87.343
P49006	MARCKS-related protein	8.1764	2	14.4	19.529
P62910	60S ribosomal protein L32	10.886	1	9.6	15.86
P46778	60S ribosomal protein L21	8.5082	2	20.6	18.565
P13746	HLA class I histocompatibility antigen, A-11 alpha chain	31.275	1	21.1	40.936
O43570	Carbonic anhydrase 12	20.686	4	21.8	39.45

Accession	Description	Score	Unique peptides	Sequence coverage [%]	MW [kDa]
Q07955	Serine/arginine-rich splicing factor 1	11.312	4	22.2	27.744
P09496	Clathrin light chain A	6.2018	5	16.9	27.076
P05387	60S acidic ribosomal protein P2	9.9143	2	39.1	11.665
O75369	Filamin-B	12.439	5	5.5	278.16
P06748	Nucleophosmin	44.562	7	34	32.575
O14745	Na(+)/H(+) exchange regulatory cofactor NHE-RF1	1.9544	2	10.3	38.868
P49327	Fatty acid synthase	168.54	33	21.3	273.42
Q16363	Laminin subunit alpha-4	31.176	6	5.2	202.52
P17980	26S protease regulatory subunit 6A	26.065	3	12.5	49.203
Q14112	Nidogen-2	69.253	10	11.7	151.25
P80723	Brain acid soluble protein 1	77.185	10	79.7	22.693
P60033	CD81 antigen	79.183	3	25	25.809
P62913	60S ribosomal protein L11	12.754	4	24.2	20.252
P11047	Laminin subunit gamma-1	235.49	27	25.7	177.6
P05556	Integrin beta-1	123.01	19	27.7	88.414
P35527	Keratin, type I cytoskeletal 9	119.94	15	39.2	62.064
Q99880	Histone H2B type 1-L	44.881	6	45.2	13.952
O00468	Agrin	118.06	16	13	217.23